TECHNISCHE
UNIVERSITÄT
WIEN

VIENNA
UNIVERSITY OF
TECHNOLOGY

WIEN

Institut für Strömungslehre
und Wärmeübertragung
Resselgasse 3
A-1040 Wien
http://www.fluid.tuwien.ac.at

**Dipl.-Ing. Dr.
Herbert Steinrück**
Tel +43.1.58801.32231
Fax +43.1.58801.32299
herbert.steinrueck@tuwien.ac.at

Gutachten über die Dissertation
"Mixed convection flow past a horizontal plate"
von Herrn Dipl.-Ing. Ljubomir Savić

In der vorliegenden Dissertation wird die zweidimensionale Strömung um eine horizontale beheizte Platte unter Berücksichtigung schwacher (hydrostatischer) Auftriebseffekte im Grenzfall großer Reynoldszahlen Re untersucht. Die Wirkung des hydrostatischen Auftriebs wird durch den Auftriebsparameter $K = Gr/Re^{5/2}$, wobei Gr die Grashofzahl bezeichnet, beschrieben. Weiters wird voraus gesetzt, dass die parallele Anströmng unter dem kleinen Winkel ϕ zur horizontalen x-Achse erfolgt.

Bisherige Untersuchungen von gemischten Konvektionsströmungen über horizontale Oberflächen behandelten vor allem die Grenzschichtströmung über eine halbunendliche Platte. Dabei stellte sich jedoch heraus, dass die Grenzschichtgleichungen, erweitert um die mittels Bousinessq Approximation berücksichtigten Auftriebskräfte, im Falle der Strömung über eine gekühlte Platte ihren parabolischen Charakter verlieren. Die Lösungen werden offensichtlich von stromabseitigen Bedingungen beeinflusst. Daher war es nahe liegend, die Strömung um eine endliche Platte zu untersuchen. Sowohl das globale als auch das lokale Strömungsfeld in der Nähe der Hinterkante sind dabei von Interesse. Dementsprechend besteht die Arbeit aus zwei Teilen.

Methodisch wird ein gekoppelter Grenzübergang Re $\to \infty$, K $\to 0$, $\phi \to 0$ durchgeführt, wobei zwei geeignete Kopplungsparamter $\kappa = K\,Re^{1/4}$ bzw. $\lambda = \phi/K$ konstant gehalten werden.

Die Wahl dieses speziellen Grenzüberganges ist durch eine Skalierungsüberlegung für den Nachlauf bzw. die Störung der Potentialströmung gegeben. Die Wärmezufuhr entlang der Platte bewirkt eine Dichtestörung im Nachlauf, die wiederum einen hydrostatischen Druckunterschied über den Nachlauf bewirkt. Die Potentialströmung muss nun diesen Druckunterschied ausgleichen. Formal kann das mittels einer Wirbelbelegung entlang des Nachlaufes bewirkt werden. Die Größe des Drucksprunges hängt jedoch vom Temperaturprofil im Nachlauf ab. Dieses hängt jedoch entscheidend von der Neigung des Nachlaufs und somit von der Störung der Potentialströmung ab.

Der Druckgradient im Nachlauf tangential zur Mittellinie des Nachlaufs ist einerseits proportional zur Neigung des Nachlaufs ($\sim$ K bzw. $\sim \phi$) und andererseits proportional zur vertikalen Komponente des Druckgradienten im Nachlauf ($\sim K\sqrt{Re}$). Insgesamt is daher die tangentiale Komponente des Druckgradienten im Nachlauf von der Größenordnung $K\Phi\sqrt{Re}$ bzw. $K^2\sqrt{Re}$. Um ein sinnvolles Grenzproblem zu erhalten, fordert man nun, dass diese Komponente des Druckgradienten von der Größenordnung 1 ist. Somit ergibt sich die gewählte Skalierung.

Die asymptotische Analyse mittels der Methode der angepassten Entwicklungen ergibt nun, dass zunächst folgende Gebiete unterschieden werden müssen: Das Gebiet der Potentialströmung, Grenzschichten auf der Ober- bzw. Unterseite der Platte, Nachlauf, und in der Nähe der Hinterkante jeweils ein Tripeldeck Problem mit Upper-, Main-, Lowerdeck für die Plattenober- bzw. Unterseite. Die Strömung im

Nachlauf und die Störung der Potentialströmung müssen nun simultan ermittelt werden. Dabei stellt sich heraus, dass Lösungen nur für positive Anströmwinkel ϕ (λ) existieren, falls der reduzierte Auftriebsparameter κ unterhalb eines kritischen (λ-abhängigen) Wertes ist. Im Nachlauf selbst bewirkt der Auftrieb eine Beschleunigung des Fluids. Die somit gewonnene Potentialströmung erfüllt die Kuttabedingung. Die Wirbelbelegung entlang des Nachlaufs bewirkt eine zusätliche Zirkulation, die den dynamischen Auftrieb aufgrund des Anstellwinkels der Platte gegenüber der Parallelströmung verringert, ja sogar zu einem negativen Auftrieb führen kann.

Die Beschreibung der Strömung in der Nähe der Hinterkante erfolgt nun im Rahmen des Konzepts wechselwirkender Grenzschichten. Alle Größen werden nun dargestellt als Summe eines bezüglich der horizontalen x-Achse symmetrischen bzw. antisymmetrischen Anteils. Da der Auftriebsparameter von der Größenordnung $Re^{-1/4}$ ist, erhält man für den symmetrischen Anteil das von Stewartson bzw. Messiter behandlte Hinterkantenproblem der Umströmng einer ebenen Platte in einer zur Platte parallelen Anströmung.

Für den antisymmetrischen Anteil, der den Einfluß des hydrostatischen Auftriebs beschreibt, erhält man ein lineares Problem. Die numerische Lösung ergibt nun das der Wechselwirkungsdifferenzdruck, der von der Größenordnung $Re^{-3/8}$ ist, an der Hinterkante unstetig ist. (Der führende vom Auftrieb induzierte Differenzdruck ist von der Größenordnung $Re^{-2/8}$ und ist nicht am Wechselwirkungsprozess beteiligt.) Zur Auflösung der Unstetigkeit des Wechselwirkungsdifferenzdruckes werden nun weitere Unterschichen mit den Abmessungen $Re^{-4/8}$ bzw. kann $Re^{-5/8}$ in x-Richtung eingeführt. Für den Differendruck erhält man jeweils eine elliptische Gleichung, die numerisch gelöst wird. In diesen Schichten kann die Unstetigkeit auf nur einen Punkt, nämlich die Hinterkante reduziert werden. Es wird vermutet, dass eine vollständige Auflösung der Drucksingularität an der Hinterkant erst auf einer Skala, auf der alle Reibungsterme von führender Größenordnung sind, möglich ist.

Wir erhalten somit das paradoxe Ergebnis, dass auf den Skalen der globalen Strömung in führender Ordnung die Kuttabedingung erfüllt ist, jedoch auf den Skalen des Wechselwirkungsproblems eine Umströmung der Hinterkante erfolgt. Die Resultate für die globale Strömung sind ebenfalls neu, und gehen über die Resultate von Schneider (2005) wesentlich hinaus, da (im Gegensatz zu Schneider) die Neigung des Nachlaufs berücksicht wurde und somit eine wesentliche technische Annahme, die Schneider traf, vermieden werden konnte. Bei der globalen Strömung belieben jedoch noch die Fragen offen, was den Zusammenbruch des gewählten numerischen Verfahrens bewirkt und wie die zweidimensionale Strömung in eine dreidimensionale Strömung eingebettet wird.

Die Arbeit ist methodisch korrekt sowohl vom Standpunkt der asymptotischen Analyse als auch der angewandten numerischen Methoden ausgeführt. Sowohl die Resultate bezüglich der globalen Strömung alsauch der lokalen Analyse der Hinterkantenumströmung sind in dieser Form neu und unerwartet.

Die Resultate sind leider nicht mit der nötigen Klarheit und Sorgfalt dargestellt, was darauf zurückzuführen ist, dass der Verfasser die Dissertation nicht in seiner Muttersprache (serbisch) verfasst hat. Aufgrund der interessanten Ergebnisse beurteile ich die vorliegende Dissertation dennoch mit

<center>

"Sehr gut (1)".

</center>

Wien, am 30. Mai 2006   A. o. Prof. Dr. Herbert Steinrück

DISSERTATION

Mixed convection flow past a horizontal plate

ausgeführt zum Zwecke der Erlangung des akademischen Grades eines Doktors der technischen Wissenschaften / der Naturwissenschaften unter der Leitung von

Ao.Univ.Prof. Dipl.-Ing. Dr. techn. Herbert Steinrück

E322 /

Institut für Strömungsmechanik und Wärmeübertragung

eingereicht an der Technischen Universität Wien

Fakultät für Maschinenwesen und Betriebswissenschaften

von

Dipl.-Ing. Ljubomir Savić

Martikelnummer: 0227349

Trappelgasse 3/1/2, 1040 Wien

Wien, im Mai 2006

Acknowledgements

Vienna, Mai 2006.   Ljubomir Savić

Abstract

The mixed convection flow past a horizontal plate which is aligned under a small angle of attack to a uniform free stream will be considered in a distinguish limit of large Reynolds Re and Grashof number Gr. Two aspects are investigated: the global two-dimensional flow field and the local behavior near the trailing edge.

A hydrostatic pressure difference across the wake induces a correction of the potential flow which influences the inclination of the wake. Thus the wake and the correction of the potential flow have to be determined simultaneously. However, it turns out that solutions exists only if the the angle of attack is sufficiently large. Solutions are computed numerically and the influence of the buoyancy on the lift coefficient is determined.

The influence of the buoyancy forces onto the flow near the trailing edge is analyzed in the frame work of the triple deck theory. The flow near the trailing edge can be decomposed into a symmetric and an anti-symmetric part. The symmetric part can be described by the classical triple deck theory (Stewartson 1969 and Messiter 1970), while for the anti-symmetric one, a new (linear) triple deck problem is formulated.

However, it turns out that the pressure of the anti-symmetric part is discontinuous at the trailing edge even on the triple deck scale ($x = O(\text{Re}^{-\frac{3}{8}})$). Thus new sub-layers of size $x = O(\text{Re}^{-\frac{4}{8}})$ and $x = O(\text{Re}^{-\frac{5}{8}})$ are introduced to resolve the discontinuity of the pressure.

Contents

List of Figures

1 Introduction

The boundary layers which include the temperature field always provoke the coupling between velocity and temperature distribution. These two fields can be considered as decoupled only if physical properties (density, viscosity, etc...) are constant, i.e. can be assumed to be independent of temperature and pressure. This is justified as long as the temperature and pressure differences are small.

However in the most general case, the material properties depend on the temperature and pressure and as a consequence there is the coupling of the velocity and temperature filed.
In fact, whenever the temperature of the fluid is nonuniform, there will be gradients in all properties, including the density. In general, the heat transfer influences the fluid motion by the buoyancy forces.

Due to the role of buoyancy, convection flows can be classified as forced, mixed and natural convection flows. If the buoyancy is the only source of fluid motion, one speaks of natural (free) convection. On the other hand, if the influence of the buoyancy forces is negligible, we speak of forced convection. In case of mixed convection, the flow is considerably influenced by buoyancy, but it is not the only driving force of the flow. Therefore, mixed convection is a combination of natural and forced convection, where the buoyancy forces can be treated in terms of the so-called Boussinesq approximation (Leal 1992).

The mechanism how the buoyancy force acts onto the boundary-layer flow is quite different in the case of the flow along vertical or inclined surface, than in case of the flow along horizontal or slightly inclined one.
In the first case buoyancy has a non-vanishing component in the main (tangential to the surface) flow direction, whereas in the second case the buoyancy is normal to the surface. Balancing this buoyancy force, a hydrostatic pressure gradient across the boundary layer builds up. Due to the variation of the boundary-layer thickness the gradient of this hydrostatic pressure distribution has a non-vanishing component tangential to the surface, thus affecting the boundary-layer flow. In the case of fluid with a positive thermal expansion coefficient this gradient is favorable (in the case of the flow above a heated surface) and it is opposing the flow in case of the flow above a cooled surface. Since buoyancy affects the boundary layer only via the hydrostatic pressure this mechanism is called an indirect buoyancy effect. This is in contrast to the case of the vertical surface, where buoyancy affects the flow directly.

The effects of the indirect buoyancy will be demonstrated in the following sketch (figure 1.1). It shows the reduction of the static pressure above a heated horizontal surface.
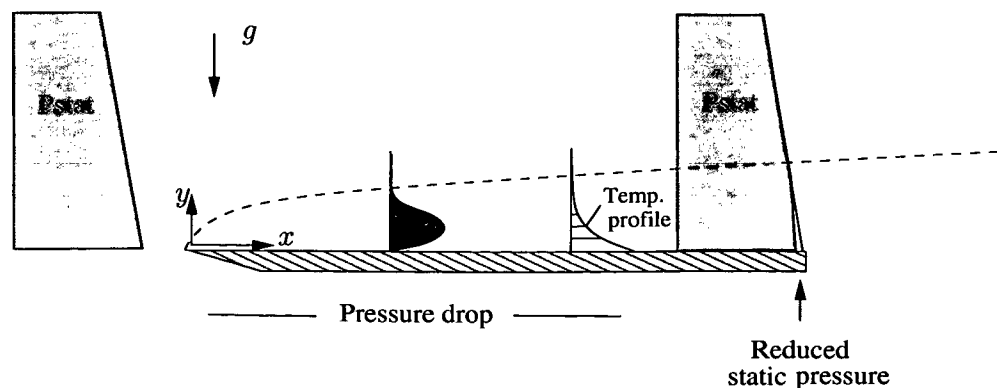
Figure 1.1 Forming of pressure gradient

A dimensionless measure of the strength of the buoyancy effects in the boundary layer above a horizontal surface is given by the buoyancy parameter $K = \mathrm{Gr}/\mathrm{Re}^{\frac{5}{2}}$ (Schneider 1979,

Schneider&Wasel 1985), where Gr and Re are Grashof and Reynolds number based on the plate length, respectively. The limiting cases of $K = 0$ and $K \to \infty$ correspond to forced and free convection.

For small buoyancy effects the boundary-layer flow is close to the forced convection case, whereas in the limit of large buoyancy forces the free convection boundary layer will be attained. In the case of a favorable indirect buoyancy nothing unexpected happens. For fluids with positive volumetric coefficient of thermal expansion ($\beta > 0$), the flow in the boundary layer is accelerated and can be computed with usual marching techniques for solving boundary-layer equations.

In the case of adverse buoyancy the situation is quite different. The oncoming flow faces an adverse pressure gradient. Thus the separation of the flow might be expected. Therefore it is of interest to determine how the boundary-layer flow approaches the point of vanishing wall shear stress, i.e. what kind of singularity occurs (Goldstein or Merkin type; Goldstein 1930, Merkin 1987).

However, the first attempts to compute the solution of the boundary-layer equations up to the point of separation by the matching procedure in flow direction failed. The solution terminated in the singularity (Schneider&Wasel 1985, Wickern 1991). Investigations done by Steinrück (1995) showed that the modified boundary equations are ill-posed in case of a cooled plate, which is responsible for several aspects of peculiarities:

- Non-uniqueness of the solution of the boundary-layer equations

- Break down of a numerical method based on a marching procedure (Schneider&Wasel 1985)

- Self-similar and connected solutions

- Upstream influence in the boundary layer (Denier&Duck 2005)

All previous studies considered the boundary-layer flow over a semi-infinite cooled plate, i.e. plate temperature below free-stream temperature.

Schneider (2000, 2001) was the first to investigate the mixed convection flow around a finite horizontal plate. In this case the temperature perturbation are not limited to the boundary layer at the plate, but are also present in the wake. Thus, they are inducing the hydrostatic pressure difference across the wake. The problem concerning the potential flow was solved in the limit of the vanishing Prandtl number (Pr $\to$ 0), using the vortex strength distribution along the wake and at the plate, respectively. The vortex strength was chosen to compensate the hydrostatic pressure jump across the wake.

However the solution of the potential flow was not satisfactory (the solution in the unbounded plane does not exist), thus a different approach has been preformed. In Schneider (2005) the potential flow was considered in a horizontal chanel with a width b depending on the Richardson number Ri ($b = \text{Ri}^{-n}$, with $n = \text{const} > 0$). This approach handled the matter.

In the present investigation a different approach will be pursued. The global two dimensional flow field will be analyzed by the asymptotic consideration in the distinguish limit of the Reynolds number Re $\to \infty$, buoyancy parameter $K \to 0$ and Prandtl number Pr $\sim O(1)$. To ensure the existence of the potential flow solution a small angle of inclination of the oncoming free stream will be assumed.

Furthermore, the flow in the vicinity of the trailing edge is associated with difficulties of transition into the wake region – the interaction mechanism between viscid sub-layer and outer (potential) flow enables the continues transition. Thus the correct implementation of the triple-deck concept (developed by several authors in 1969) in the global flow also represents a new interesting issue of the mixed convection flow around a finite plate.

Considering all peculiarities of the mixed-convection flow over a horizontal finite plate, the goals of investigation are twofold: the description of the global flow (potential flow, boundary layer and wake) on one hand and the local analysis of the trailing edge region on another. Of particular interest will be the implementation of the triple-deck concept into the global flow for small buoyancy parameters.

The thesis is organized as follows:

chapter 2 represents the problem formulation, with all necessary assumptions, governing equations and boundary conditions.

Chapter 3 deals with the global flow and interaction of the wake with the potential flow. Some interesting results are obtained here, since the potential flow and boundary layer are coupled. The two dimensionless parameters are introduced which describe the effects of buoyancy in the far wake region and influence of hydrostatic pressure difference across the wake as well.

The trailing edge properties with interaction mechanism for two coupled triple deck structures are considered in chapter 4. Also, the complete matching procedure is done here, confirming continuous transition of the displacement function into the center wake line.

Chapter 5 presents the numerical solution of the lower-deck equations were a pressure discontinuity occurs at the trailing edge in the lower-deck scale. This is a new phenomenon not observed by the comparable investigations (Stewartson&Brown 1970, Melnik&Chow 1975).

In order to resolve the pressure discontinuity in chapter 6 new sub-layers are introduced and analyzed.

Details of mathematical analysis and/or calculation routines used in thesis are given in the appendix.

2 The problem formulation

2.1 Basic assumptions

The two dimensional, laminar mixed convection flow, past a horizontal finite plate, aligned under small angle of attack to an oncoming free stream will be investigated for large values of the Reynolds number (Re) and weak buoyancy effects. The flow will be considered as steady and incompressible (Boussinesq approximation).
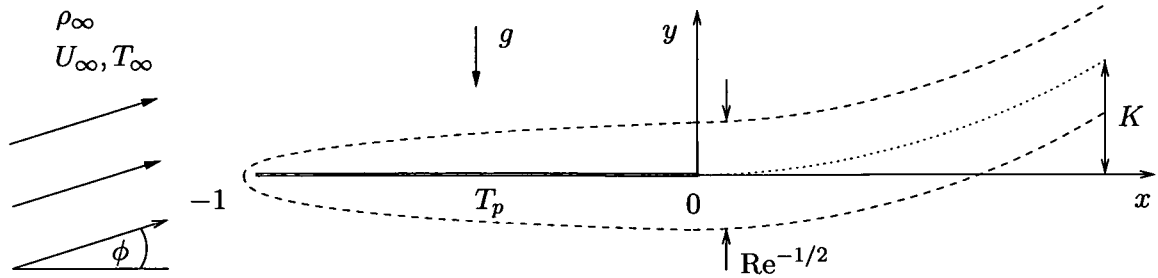
Figure 2.1 Mixed convection flow past a horizontal plate

A large Reynolds number represents a precondition for applying Prandtl's boundary layer concept and method of matched asymptotic expansions as well – since boundary layer theory is an asymptotic theory for large values of Re numbers. The assumptions of weak buoyancy (caused by temperature difference between plate and the free stream) and finite length of the plate will be elaborated.

The influence of buoyancy onto the complete flow will be characterized by the buoyancy parameter K, which in fact represents the Richardson number (Ri) : $K \sim \text{Ri}$.

The Richardson number is defined in terms of the total heat flux $\dot{Q}$ per unit depth of the plate (Schneider 2005):

$$\text{Ri} = \frac{g\beta\dot{Q}}{\rho c_p u_\infty^3} = \frac{\text{Gr}}{\text{Re}^{\frac{5}{2}}} \frac{1}{\text{Pr}} \frac{\text{Nu}}{\text{Re}^{\frac{1}{2}}} = K \frac{1}{\text{Pr}} \frac{\text{Nu}}{\text{Re}^{\frac{1}{2}}},$$

where $\text{Gr} = g\beta\Delta T L^3/\nu^2$, $\text{Re} = u_\infty L/\nu$, $\text{Nu} = \dot{Q}/k\Delta T$, $\text{Pr} = \rho c_p \nu/k$ are Grashof, Reynolds, Nusselt and Prandtl numbers, respectively and also ΔT, β, c_p, k, ν, ρ are the temperature difference, isothermal expansion coefficient, isobaric heat capacity, thermal conductivity, kinematic viscosity and density, respectively.

The assumptions of weak buoyancy effects, i.e. $\text{Ri} \ll 1$ simplifies the analysis and also it is a necessary condition for preventing boundary layer separation (Robertson 1973). Since we we are interesting in the limit $\text{Re} \rightarrow \infty, K \rightarrow 0$, the first idea was to take the interaction pressure (of order $O(\text{Re}^{-\frac{2}{8}})$) to be of the same power of the magnitude as the perturbation of the hydrostatic pressure across the boundary layer (classical interaction problem, Stewartson 1969). The coresponding scaling of the buoyancy parameter K implies that $K \sim O(\text{Re}^{-\frac{1}{8}})$ (Lagree 1999, 2001; Steinrück 2001). However, it turns out that such a scaling cannot enable the correct matching procedure with outer flow. The correct scaling for the buoyancy parameter K can be found from the scale analysis of the inclination of the center wake line.

The inclination of the center line of the wake is a consequence of the angle of attack of the free stream and of the buoyancy as well. The hydrostatic pressure gradient across the wake has a non-vanishing tangential component along the center line, affecting the equations of motion. Taking into account fact that pressure change across the wake is of order K and the thickness of the wake is of order $\text{Re}^{-\frac{1}{2}}$, we can estimate the component of the pressure gradient tangential to the center line of the wake:

$$\frac{\partial p}{\partial y} \sim K \mathrm{Re}^{\frac{1}{2}}$$

$$\Delta p \sim K, \quad \delta_w \sim \mathrm{Re}^{-\frac{1}{2}} \text{ (boundary-layer thickness)}$$
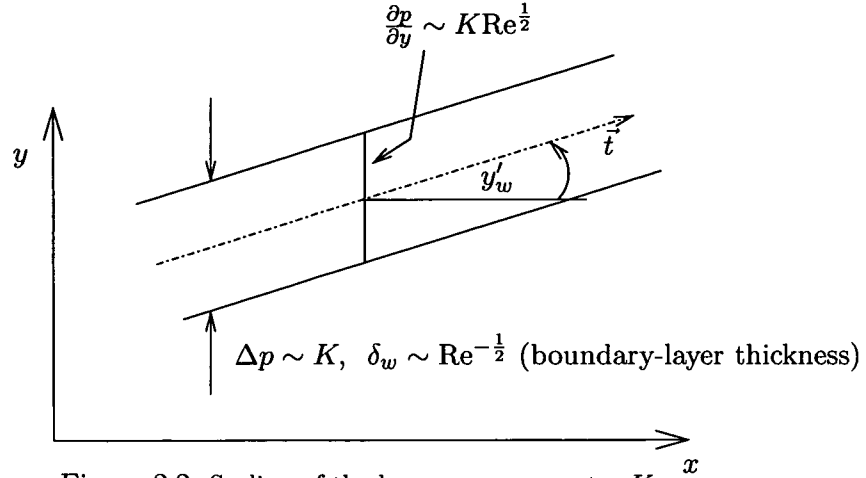
Figure 2.2 Scaling of the buoyancy parameter K

$$\frac{\partial p}{\partial \vec{t}} \sim \frac{\partial p}{\partial x} + \underbrace{\frac{\partial p}{\partial y} \frac{dy_w}{dx}}_{\sim K y'_w \sqrt{\mathrm{Re}}}$$

The inclination of the center wake line y'_w results from the two effects (buoyancy influence K and the angle of attack ϕ). In the far field we assume that the effects of buoyancy onto the potential flow have been vanished, thus we estimate the inclination of the wake center line by the angle of attack ($y'_w \sim \phi$).

In order to obtain the meaningfull asymptotic limit, we have to chose the factor $\phi K \sqrt{\mathrm{Re}}$ to be of order $O(1)$. K and ϕ are chosen to be of the same order of magnitude, namely $\phi \sim K \sim \mathrm{Re}^{-\frac{1}{4}}$ to take both effects, the buoyancy and an angle of attack, into account.

Thus we take a distinguish limit $\mathrm{Re} \to \infty, K \to 0, \phi \to 0$, with the two coupling parameters κ and λ (being of order $O(1)$) defined as:

- $\kappa = K \mathrm{Re}^{\frac{1}{4}}$ .... reduced buoyancy parameter

- $\lambda = \phi K \sqrt{\mathrm{Re}}$ .... reduced inclination parameter

We will later see that the parameter λ describes the effect of buoyancy in the far wake region, while κ is a measure of the hydrostatic pressure difference across the wake.

2.2 Governing equations

Taking into account all assumptions and phenomenons of mixed convection flow past a horizontal plate, the complete flow will be analyzed numerically and analytically using the method of matched asymptotic expansions and interacting boundary layers.

The analysis starts with complete Navier-Stokes equations (simplified by Boussinesq approximation), combined to continuity and energy equation.

The Boussinesq approximation treats density as a constant in all equations, except for the buoyancy term in momentum equations, in fact "the temperature variations in the field are small enough so material properties ρ, c_p, μ, k can be approximated by their values at the ambient temperature, except in the body force term of momentum equation" (Leal 1992, pp. 669).

The equations will be given in dimensional (vector) form, with following notation: $\frac{D}{Dt}$ is a material derivative, Δ represents a Laplacian operator:

$$\rho_\infty \frac{D\vec{V}}{Dt} = \rho_\infty \beta (T - T_\infty) g \vec{j} - \nabla p_d + \mu_\infty \Delta \vec{V},$$

$$\rho \, \text{div} \vec{V} = 0,$$

$$\rho_\infty \, c_{p\infty} \, \frac{DT}{Dt} = \text{div}(\lambda \, \text{grad} \, T)$$

and also in dimensionless form, using usual reference values: $L, U_\infty, \rho_\infty U_\infty^2, T_p - T_\infty$.

So, all the lengths are made dimensionless with the plate length L, velocities are nondimensionalized by u_∞ (the velocity of the unperturabated flow) and temperature differences are scaled by $T_p - T_\infty$.

In the dimensionless form the Navier-Stokes equations (momentum equations), continuity equation and energy equations read as:

$$uu_x + vu_y = -p_x + \frac{1}{\text{Re}}(u_{xx} + u_{yy}), \tag{2.1}$$

$$uv_x + vv_y = -p_y + \frac{\text{Gr}}{\text{Re}^2} \, \theta + \frac{1}{\text{Re}}(v_{xx} + v_{yy}), \tag{2.2}$$

$$u_x + v_y = 0, \tag{2.3}$$

$$u\theta_x + v\theta_y = \frac{1}{\text{Re Pr}}(\theta_{xx} + \theta_{yy}). \tag{2.4}$$

The subscripts "x" and "y" denote partial derivatives in horizontal and vertical direction, respectively.

At the plate the no-slip condition holds and the temperature of the plate is constant.

$$u(x,0) = v(x,0) = 0, \quad \theta(x,0) = 1 \, ; \quad -1 < x < 0 \tag{2.5}$$

In the far filed, the unperturabated flow is given by:

$$u(x,y) \rightarrow 1, \quad v(x,y) \rightarrow \phi, \quad \theta(x,0) \rightarrow 0, \quad x^2 + y^2 \rightarrow \infty. \tag{2.6}$$

For the analysis, the flow field is decomposed into four main regions (additional sub-layers will be introduced later):

- potential flow

- boundary layer (boundary layer at the plate)

- trailing edge (triple deck structure)

- wake (boundary layer)
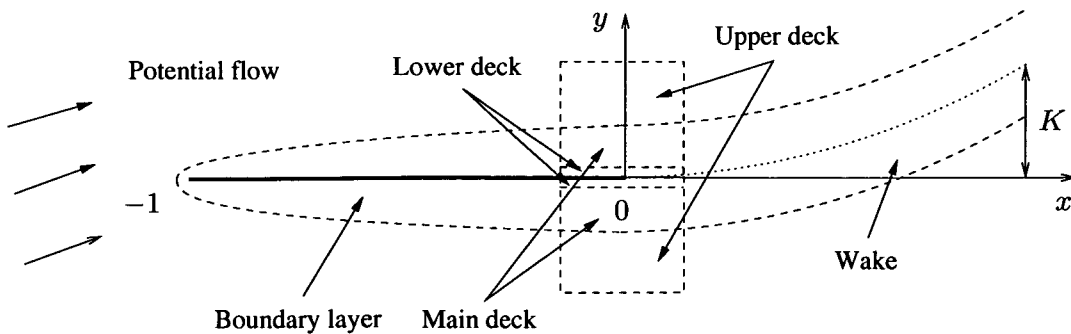
Figure 2.3 Regions of interest (schematic)

3 Global flow

3.1 Boundary layer and wake

The outer (potential) flow cannot satisfy the no-slip condition and as a consequence the boundary layer of thickness $O(\mathrm{Re}^{-\frac{1}{2}})$ forms along the plate. Since the solution of the boundary-layer equations can be continued into the wake (Goldstein 1930), the boundary layer approximation is valid here as well. Thus these two regions will be discussed together.

However, the position of the wake is not known a priorly – an inclination of the wake is expected. Thus the vertical boundary layer coordinate "$\bar{y}$" is defined as the scaled distance from the wake center line ($y = y_w(x) = \phi \bar{y}_w(x)$, figure 3.2). In fact, the boundary-layer equations will be formulated in local coordinates around the wake center line.
Along the plate $-1 < x < 0$ the value of $\bar{y}_w$ is zero.
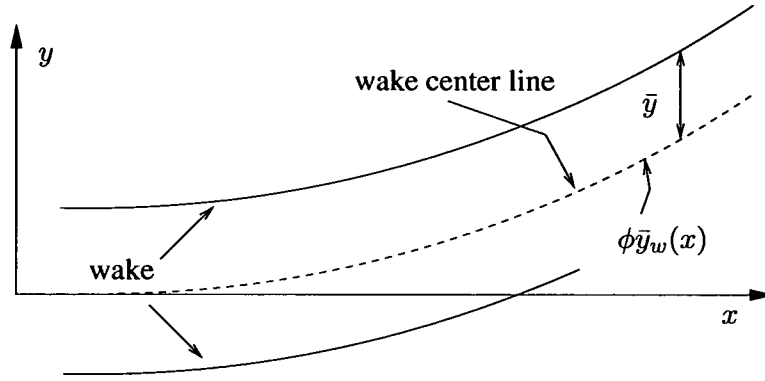
Figure 3.1 Scaled distance from a center line

$$\bar{y} = \Big(y - \phi\ \bar{y}_w(x)\Big)\sqrt{\mathrm{Re}},$$

$$\bar{v}_w(x,\bar{y}) = \Big(v - u(x,\phi\bar{y}_w)K\bar{y}_w'\Big)\sqrt{\mathrm{Re}}. \tag{3.1}$$

In equation (3.1) the vertical velocity component $\bar{v}_w$ is referred to the vertical velocity at the center line.

In order to obtain the relevant equations in this region, the following asymptotic expansions have to be involved as well, where the Reynolds number is the only perturbation parameter (κ and λ are identified as coupling parameters, cf. sub-section 2.1):

$$u(x,y) = \bar{u}_w(x,\bar{y};\kappa,\lambda) + O(\mathrm{Re}^{-\frac{1}{4}});$$

$$p(x,y) = \mathrm{Re}^{-\frac{1}{4}}\bar{p}_w(x,\bar{y};\kappa,\lambda) + \ldots; \quad \theta(x,y) = \bar{\theta}_w(x,\bar{y};\kappa,\lambda) + O(\mathrm{Re}^{-\frac{1}{4}}).$$

Inserting expansions for $u(x,y), p(x,y), \theta(x,y)$ into the governing equations (2.1-2.4), together with equation (3.1), the leading order approximation of boundary-layer equations is derived:

$$\bar{u}_w\bar{u}_{w,x} + \bar{v}_w\bar{u}_{w,\bar{y}} = \lambda\bar{y}_w'\bar{\theta}_w + \bar{u}_{w,\bar{y}\bar{y}}, \tag{3.2}$$

$$\bar{p}_{w,\bar{y}} = \kappa\bar{\theta}_w, \tag{3.3}$$

$$\bar{u}_{w,x} + \bar{v}_{w,\bar{y}} = 0, \tag{3.4}$$

$$\bar{u}_w\bar{\theta}_{w,x} + \bar{v}_w\bar{\theta}_{w,\bar{y}} = \frac{1}{\mathrm{Pr}}\bar{\theta}_{w,\bar{y}\bar{y}}. \tag{3.5}$$

The matching conditions to the potential flow are

$$\bar{u}_w(x, \bar{y} \to \pm\infty) = 1, \quad \bar{\theta}_w(x, \bar{y} \to \pm\infty) = 0. \tag{3.6}$$

At the plate the no-slip is given by:

$$\bar{u}_w(x, 0) = \bar{v}_w(x, 0) = 0 \,, \quad \bar{\theta}_w(x, 0) = 1 \,, \quad -1 < x < 0 \tag{3.7}$$

and a symmetry condition in the wake holds

$$\bar{u}_{w,\bar{y}}(x, 0) = \bar{v}_w(x, 0) = \bar{\theta}_{w,\bar{y}}(x, 0) = 0 \,, \quad x > 0. \tag{3.8}$$

The momentum equations (3.2 and 3.3) are of particular interest. Beside a component in y-direction (which is usual in mixed convection problem), the hydrostatic pressure gradient has a component tangential to the center line of the wake $(\lambda \bar{y}'_w \bar{\theta}_w)$. We point out that this term, since it has not been reported in the literature before! In Schneider (2005) this term was neglected, since the analysis was done for buoyancy parameter $K \ll \text{Pe}^{-\frac{1}{4}}$.

3.1.1 Boundary layer at the plate

At the plate, the inclination of the center wake line vanishes and equations (3.2-3.5) reduce to the boundary-layer equations for forced convection flow along the plate. Their solution is given by the well known Blasius similarity solution (Schlichting&Gersten 2000, pp. 156). Using the stream function $F_B(\zeta)$, function $D_B(\zeta)$ and similarity coordinate ζ we have:

$$\bar{u}_w(x, \bar{y}) = F'_B(\zeta), \quad \bar{\theta}_w(x, \bar{y}) = D_B(\zeta), \quad \zeta = \frac{\bar{y}}{\sqrt{x+1}},$$

where F_B, D_B represents the Blasius solution and the temperature profile at the plate, respectively.

$$2F'''_B + F_B F''_B = 0 \,; \quad F_B(0) = F'_B(0) = 0 \,, \quad F'_B(\infty) \to 1 \tag{3.9}$$

$$\frac{2}{\text{Pr}} D''_B + F_B D'_B = 0 \,; \quad D_B(0) = 1 \,, \quad D_B(\infty) = 0. \tag{3.10}$$

We will solve the system numerically and it will assure an initial profile at the trailing edge for investigation in the wake region. The solution is given in figure 3.2.
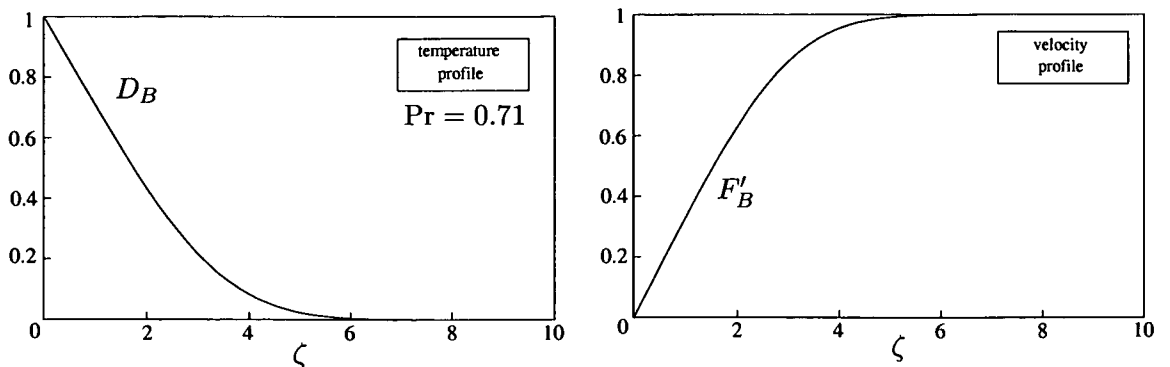
Figure 3.2 Similarity solution at the plate

3.1.2   The wake

Considering the wake, we will transform the wake equations (3.2-3.5) to the following variables which are appropriate to discuss the limiting behavior in far wake region ($x \to \infty$):

$$\psi = (x+1)^{\frac{3}{5}} F(x,\eta), \quad \bar{\theta}_w = \frac{1}{(x+1)^{\frac{3}{5}}} D(x,\eta), \quad \eta = \frac{\bar{y}}{(x+1)^{\frac{2}{5}}},$$

where ψ is the stream function and η is a "similarity" variable.

The tangential component of the velocity $\bar{u}_w = (x+1)^{\frac{1}{5}} F'(x,\eta)$ will grow unbounded for $x \to \infty$ (far wake) if F' tends to a non-vanishing limit. Thus we expect (due to the scaling) a velocity overshoot in the wake.

The transformed wake equations read as:

$$F''' + \frac{3}{5}F''F - \frac{1}{5}(F')^2 + \lambda \bar{y}'_w D = (x+1)(F'F'_x - F''F'_x), \tag{3.11}$$

$$\frac{1}{\text{Pr}}D'' + \frac{3}{5}(FD)' = (x+1)(F'D_x - D'F_x). \tag{3.12}$$

Here and in following, the derivatives with respect to η will be denoted with primes.

The boundary conditions have to be transformed and the initial condition (initial profile) at the trailing edge as well:

$$F(x,0) = F''(x,0) = D'(x,0) = 0, \quad F'(x,\infty) = \frac{1}{(x+1)^{\frac{1}{5}}}, \quad D(0,\infty) = 0, \tag{3.13}$$

$$F(0,\eta) = F_B(\eta), \quad D(0,\eta) = D_B(\eta). \tag{3.14}$$

Following Schneider (2005) and using the energy balance, we define the enthalpy flux $\dot{H} = \int_{-\infty}^{+\infty} \bar{u}_w \bar{\theta}_w \, d\bar{y}$. Integrating the energy equation (3.5) with respect to $\bar{y}$ we obtain that the enthalpy flux stays constant in the wake.

$$\bar{u}_w \bar{\theta}_{w,x} + \bar{v}_w \bar{\theta}_{w,\bar{y}} = \frac{1}{\text{Pr}} \bar{\theta}_{w,\bar{y}\bar{y}},$$

$$(\bar{u}_w \bar{\theta}_w)_x + (\bar{v}_w \bar{\theta}_w)_{\bar{y}} = \frac{1}{\text{Pr}} \bar{\theta}_{w,\bar{y}\bar{y}}, \quad \int_{-\infty}^{+\infty} d\bar{y},$$

$$\frac{d}{dx} \int_{-\infty}^{+\infty} \bar{u}_w \bar{\theta}_w \, d\bar{y} + \underbrace{\bar{v}_w \bar{\theta}_w|_{-\infty}^{+\infty}}_{\approx 0} = \underbrace{\frac{1}{\text{Pr}} \bar{\theta}_{w,\bar{y}}}_{\approx 0},$$

$$\Rightarrow \int_{-\infty}^{+\infty} \bar{u}_w \bar{\theta}_w \, d\bar{y} = \text{const} = \dot{H},$$

$$\dot{H} = \int_{-\infty}^{+\infty} \bar{u}_w \bar{\theta}_w \, d\bar{y} = \int_{-\infty}^{+\infty} F'D \, d\eta = 2 \int_{0}^{+\infty} F'_B D_B \, d\eta = \frac{\text{Nu}}{\text{Pr}\sqrt{\text{Re}}}. \tag{3.15}$$

Integrating the degenerated y-momentum equation (3.3) with respect to the vertical direction, the pressure difference across the wake is given by

$$\Delta \bar{p}_w(x) = \bar{p}_w(x,+\infty) - \bar{p}_w(x,-\infty) = \int_{-\infty}^{+\infty} \bar{\theta}_w \, d\bar{y} := \gamma_w(x). \tag{3.16}$$

Discussing the potential flow, $\gamma_w(x)$ will be interpreted as a vortex strength distribution along the center line of the wake. It has to compensate the hydrostatic pressure jump which occurs across the wake.

3.1.3 The limiting behavior of the wake

The transformed wake equations (3.11),(3.12) are in such a form, that the limiting behavior can be deduced just by setting the derivatives with respect to x equal to zero and take the limit $x \to \infty$ (far wake region). Assuming that the far potential flow field is given by the asymptotic condition (2.6), the scaled inclination of the wake $\bar{y}'_w$ tends to 1 ($\bar{y}'_w \to 1$).
Then for $\lambda > 0$ the similarity equations for the asymptotic flow and temperature profile are obtained. Using:

$$F(x,\eta) \sim a\hat{F}(\hat{\eta}), \quad D(x,\eta) \sim cD(\hat{\eta}), \quad \hat{\eta} = b\eta, \quad a = b = \left(\frac{\lambda \dot{H}}{2}\right)^{\frac{1}{5}}, \quad c = \frac{\dot{H}^{\frac{4}{5}}}{2^{\frac{4}{5}}\lambda^{\frac{1}{5}}}$$

the similarity equations can be normalized to:

$$\hat{F}''' + \frac{3}{5}\hat{F}''\hat{F} - \frac{1}{5}(\hat{F}')^2 + \hat{D} = 0 \;\; ; \;\; \frac{1}{\text{Pr}}\hat{D}'' + \frac{3}{5}(\hat{F}\hat{D})' = 0, \tag{3.17}$$

with the boundary conditions

$$\hat{F}(0) = \hat{F}''(0) = \hat{F}'(\infty) = 0 \,, \quad \int\limits_0^{+\infty} \hat{F}'\hat{D}\, d\hat{\eta} = 1. \tag{3.18}$$
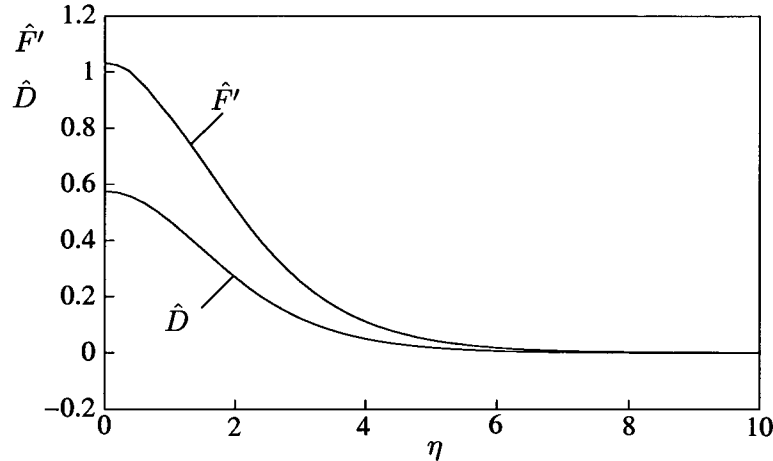
Figure 3.3 Similarity solution in the wake for Pr=0.71

A numerical solution of the equations (3.17) is shown in figure 3.3. It is a jet like profile. Due to the scaling we expect the following asymptotic behavior for the velocity and temperature profiles in the wake, respectively:

$$\bar{u}_w = (x+1)^{\frac{1}{5}}\hat{F}'(b\eta) + ..., \quad \bar{\theta}_w = (x+1)^{-\frac{3}{5}}c\hat{D}'(b\eta) + ...$$

Thus in the wake the maximum velocity is proportional to $\lambda^{\frac{2}{5}}x^{\frac{1}{5}}$ and the width of the far wake is proportional to $\dfrac{x^{\frac{1}{5}}}{\lambda^{\frac{2}{5}}}$.

Although the temperature perturbation decreases like $\lambda^{-\frac{1}{5}}x^{-\frac{3}{5}}$, the width of the wake is wide enough so that the resulting buoyancy force accelerates the flow ($\bar{u}_w$ increases as $x \to \infty$). As a consequence, the hydrostatic pressure difference across the wake decays to zero for $x \to \infty$.

$$\gamma_w(x) = \int\limits_{-\infty}^{+\infty} \bar{\theta}_w\, d\bar{y} \sim \frac{c}{(x+1)^{\frac{1}{5}}} \int\limits_{-\infty}^{+\infty} \hat{D}(\hat{\eta})\, d\hat{\eta} \tag{3.19}$$

The fact that the hydrostatic pressure difference decays in the wake guarantees the existence of the two-dimensional potential flow as we will see in the following sub-section.

3.2 Potential flow

The potential flow occupies the entire x, y-plane with the exception of the boundary layer along the plate and the wake. As already mentioned in sub-section 3.1, there is a hydrostatic pressure jump across the wake, which can be compensated by a vortex strength distribution along the center wake line and at the plate.
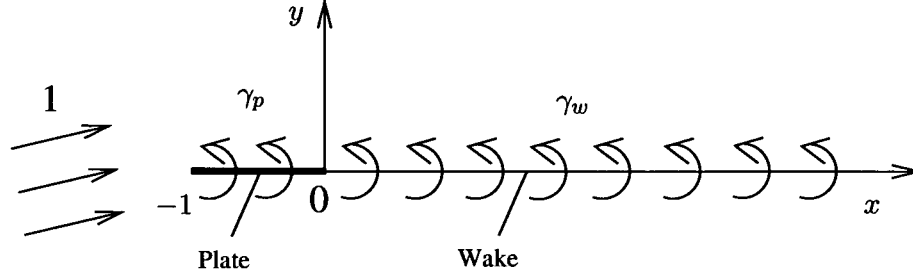
Figure 3.4 Outer flow with vortex distribution

Thus we expand the potential flow field in terms of the buoyancy parameter K, using the notation of complex functions of a complex variable $z = x + iy$ (Schneider 2005). The complex velocity field is decomposed into

$$u - iv \sim 1 - i\phi\sqrt{\frac{z}{z+1}} + K(u_1 - iv_1). \tag{3.20}$$

The first correction gives the perturbation of the flow field due to the angle of attack ϕ. The value ϕ is assumed to be small and of comparable size to the buoyancy parameter $K = O(\mathrm{Re}^{-\frac{1}{4}})$. The second term is induced by the vortex distribution γ_w and is therefore of order K.

Boundary conditions for the potential flow correction $u_1 - iv_1$ are given at the plate as vanishing vertical velocity component, since the plate is a solid body.

$$v_1(x, 0) = 0, \quad -1 < x < 0 \tag{3.21}$$

and along the wake where the pressure has a jump (discontinuity) given by (3.16). Using the linearized Bernoulli equation this condition can be formulated as

$$-u_1(x, 0+) + u_1(x, 0-) = \gamma_w(x). \tag{3.22}$$

According to Schneider (2005), the potential flow is represented in terms of a vortex distribution along the x-axis. Note that deviation of the center line of the wake is small (of the order of the buoyancy parameter) on the scales of the original coordinates x, y which justifies the fact to place the vortices along the x-axis instead on the center line. Thus we have

$$u_1 - iv_1 = -\frac{1}{2\pi} \int\limits_{-1}^{+\infty} \gamma_w(\xi) \, \frac{y + i(x - \xi)}{(x - \xi)^2 + y^2} \, d\xi,$$

with

$$\gamma(x) = \begin{cases} \gamma_p(x) & -1 < x < 0 \\ \gamma_w(x) & x > 0 \end{cases}.$$

Thus the jump condition for the horizontal velocity component along the x-axis (3.21) is satisfied. It remains to determine the vortex distribution $\gamma_p(x)$ along the plate. From condition (3.21) we obtain the integral equation

$$v_1(x, 0) = \int\limits_{-1}^{0} \frac{\gamma_p(\xi) \, d\xi}{x - \xi} + \int\limits_{0}^{\infty} \frac{\gamma_w(\xi) \, d\xi}{x - \xi} = 0, \tag{3.23}$$

with the solution, cf. Schneider (1978, pp. 142)

$$\gamma_p(x) = -\frac{1}{\pi}\sqrt{-\frac{x}{x+1}}\int_0^\infty \frac{\gamma_w(\xi)}{x-\xi}\sqrt{\frac{\xi+1}{\xi}}d\xi, \quad -1 < x < 0 \tag{3.24}$$

and thus

$$v_1(x) = \frac{1}{2\pi}\sqrt{\frac{x}{x+1}}\int_0^\infty \frac{\gamma_w(\xi)}{x-\xi}\sqrt{\frac{\xi+1}{\xi}}d\xi, \quad x > 0. \tag{3.25}$$

Finally the scaled inclination of the wake is given by

$$\bar{y}'_w(x) = \sqrt{\frac{x}{x+1}} + \frac{\kappa^2}{\lambda}v_1(x). \tag{3.26}$$

The scaled inclination of the wake $\bar{y}'_w(x)$ consists of two terms, where first $\sqrt{\dfrac{x}{x+1}}$ represents the influence of angle of attack ϕ and second one which is induced by γ_w expressing the influence of the hydrostatic pressure difference across the wake onto the potential flow.

We note that the integrals in (3.24), (3.25) exist only if γ_w tends to zero as $x \to \infty$ (similar problem also by Schneider 2005).

In Schneider (2005) γ_w is a constant ($\gamma_w = const$) and thus he placed the flow problem between two parallel plates. Then the kernel of the integral in (3.25) is replaced by $\dfrac{1}{x-\xi}$ and the integral exist.

The scaled inclination of the center line $\bar{y}'_w(x)$ (3.26) will be used to define the "final" transformation of the wake equation:

$$F''' + \frac{3}{5}F''F - \frac{1}{5}(F')^2 + \left(\lambda\sqrt{\frac{x}{x+1}} + \kappa^2 v_1(x)\right)D = (x+1)(F'F'_x - F''F'_x) \tag{3.27}$$

Thus equations (3.27), (3.26), (3.25), (3.19) have to be solved simultaneously.

Thus the wake and the potential flow interact with each other.

3.3 Results

3.3.1 Numerical solution

For given set of parameters $(\text{Pr}, \lambda, \kappa)$ we pursue the following solution strategy (numerical scheme).

$v_1^{(0)}$ – starting velocity distribution

$v_1^{(i)}$ – velocity distribution as a function of $\gamma_w^{(i)}$

$\gamma_w^{(i)}$ – vortex distribution as a function of $v_1^{(i-1)}$
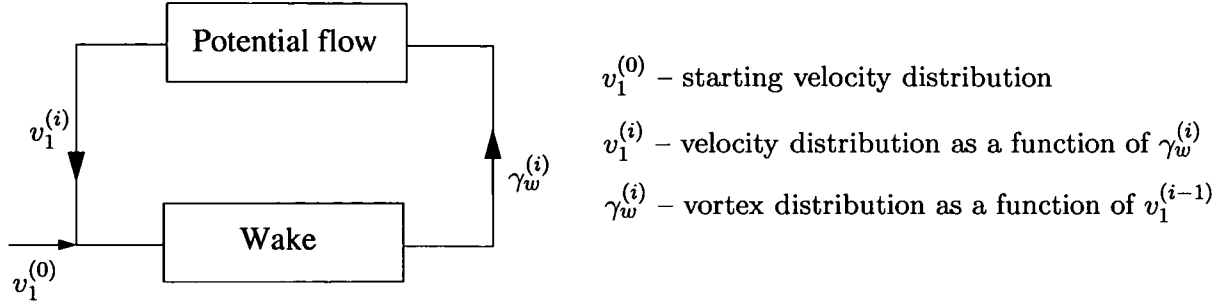
Figure 3.5 Numerical algorithm

First we assume an initial guess for the vertical velocity distribution $v_1^{(0)}$ and solve the wake equations starting at the trailing edge $(x = 0)$ by a marching technique (parabolic problem). Since it is expected that velocity and temperature converge slowly to their limiting similarity profiles, the integration has to be preformed over a large distance. Thus we increase the step size in x-direction after each step by a constant factor, say $f = 1.011$ (non-uniform mesh). On the other hand, we want to resolve profiles near the trailing edge accurately, thus we start here with a step size of $\Delta x = 10^{-7}$. Taking $N_x = 4000$ steps in x-direction, the last grid point is of the order 10^{13}.

The wake equations are discretized in x-direction by a simple first order difference scheme. Thus we get at each grid point a system of ordinary differential equations, which is solved by a well proven ODE solver – COLPAR (Uscher et al. 1981).

We start with $v_1^{(0)} = 0$. In this way first guesses for the velocity, temperature profiles and vortex distribution in the wake are obtained. Then the integral (3.25) has to be evaluated for an improved guess for $v_1^{(1)}$.

To evaluate the integral (3.25), $\gamma_w(\xi)\sqrt{\xi + 1}$ is replaced by a piecewise linear function so that the integral can be integrated exactly near the trailing edge and in the far wake region. With the new guess for v_1, the integration of the equation (3.27) can be done again and repeated until convergence is obtained. Usually it takes only 3 to 5 iterations.

Note that in the case when $\lambda > 0, \kappa = 0$ the iteration is not necessary. The inclination of the wake is solely determined by the angle of attack ϕ. In that case the hydrostatic pressure difference across the wake is too small to influence the potential flow significantly. However, buoyancy is limited to the flow behavior in the wake. The flow is accelerated and a velocity overshoot develops for $x \to \infty$.

Cases when λ and κ are of the same order are of the interest and will be further investigated. In following examples, λ and the Prantdtl number will be fixed $(\lambda = 1, \text{Pr} = 0.71)$ and κ will be varied, starting from the $\kappa = 0$.

However, convergence could not be achieved for $\kappa > 0.915$. In fact, solutions exist only for $\lambda > 0$ and κ less than a critical value.

3.3.2 The vortex distribution in the wake

Using the procedure described in sub-section (3.3.1) the solution of the coupled problem (potential flow/wake) is obtained. The solution of the potential flow will be discussed first.
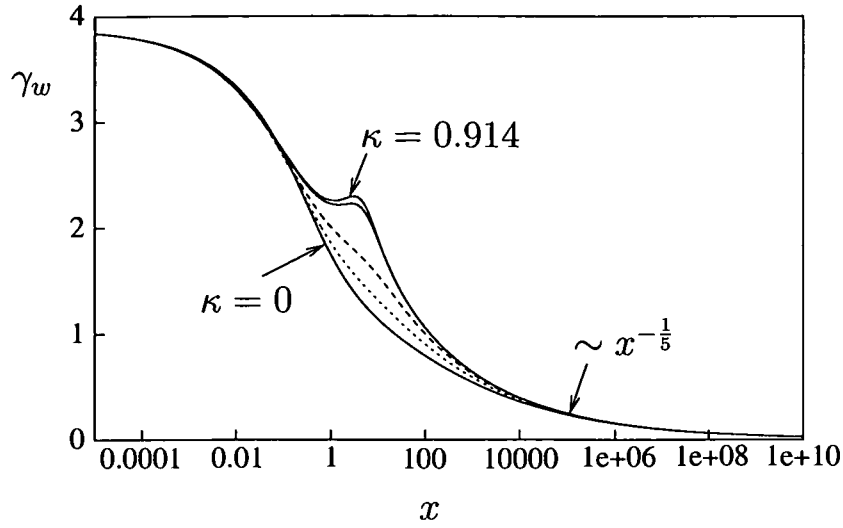
Figure 3.6 Vortex strength in the wake for Pr $= 0.71$; $\lambda = 1$; $\kappa = 0$, 0.5, 0.6. 0.85, 0.91

In figure 3.6 the vortex strength distribution $\gamma_w(x)$ is shown as a function of the horizontal coordinate x and the reduced buoyancy parameter κ.

At the trailing edge γ_w has a prescribed value $\gamma_w = 2 \int\limits_{0}^{\infty} D_B \, d\eta$ and then it starts to decay monotonically like $x^{-\frac{1}{5}}$ to zero for $\kappa = 0$. For small values of κ there are only small deviations of γ_w in the range from 1 to 100. About $\kappa = 0.7$ this deviation becomes markedly pronounced, (cf. $\kappa = 0.85$). For $\kappa = 0.91$ the vortex distribution γ_w has a plateau at $x = 10$ and at $\kappa = 0.914$ is has even a local maximum. It turns out that the solution is here very sensible to even very small perturbations in κ!

The described solution method fails for $\kappa > 0.915$.

3.3.3 Local behavior near trailing edge

Although the boundary layer equations are valid along the plate and in the wake their solution has a singularity at the the trailing edge due to the "sudden" change of the boundary conditions. At the plate the no-slip boundary condition for the velocity and the Dirichlet condition for the temperature hold.

In the wake all quantities, like velocity, shear rate $\dfrac{\partial \bar{u}_w}{\partial \bar{y}}$, temperature and heat flux $\dfrac{\partial \bar{\theta}_w}{\partial \bar{y}}$ have to be continuous. It has been shown that for the velocities and temperature the following asymptotic representation holds (Sychev 1998, pp. 100).

$$\bar{u}(x,\bar{y}) = f_B'(\bar{y}) + x^{\frac{1}{3}} \left(\hat{f}'(\zeta) - k_1 \left(f_B''(0)\zeta - f_B''(\bar{y}) \right) \right) + ..., \qquad \zeta = \frac{\bar{y}}{x^{\frac{1}{3}}},$$

$$\bar{\theta}(x,\bar{y}) = D_B(\bar{y}) + x^{\frac{1}{3}} \left(\hat{D}'(\zeta) - k_1 \left(D_B'(0)\zeta - D_B'(\bar{y}) \right) \right) + ...,$$

where k_1 is a constant given in Sychev (1998). As a consequence we obtain for the vortex distribution in the wake:

$$\gamma_w(x) = \int\limits_{-\infty}^{\infty} \bar{\theta}(x,\bar{y}) \, d\bar{y} \sim \gamma_{w,0} + \gamma_{w,1} \, x^{\frac{1}{3}},$$

$$\gamma_{w,0} = 2 \int\limits_{0}^{\infty} D_B(\bar{y}) \, d\bar{y}, \quad \gamma_{w,1} = -2k_1 D_B(0) = -2k_1,$$

where $\gamma_{w,0}$ is the prescribed value at the trailing edge and $\gamma_{w,1}$ is a coefficient which has to be determined by a numerical calculation.

Considering that v_1 vanishes at the plate and using analytical functions and complex analysis, the velocity field can be expanded (locally)

$$u_1 - i v_1 \sim -\frac{\gamma_0}{2} - \gamma_1 |z|^{\frac{1}{3}} e^{\frac{\varphi - \pi}{3}},$$

with $\varphi = \arctan \frac{y}{x}$, $|z| = \sqrt{x^2 + y^2}$ and the result is obtained

$$u_1(x,0) = \left\{ \begin{array}{llll} -\frac{\gamma_w}{2} & \sim & -\frac{\gamma_{w,0}}{2} - \frac{\gamma_{w,1}}{2} |x|^{\frac{1}{3}} & x > 0 \\ -\frac{\gamma_p}{2} & \sim & -\frac{\gamma_{w,0}}{2} - \gamma_{w,1} |x|^{\frac{1}{3}} & x < 0, \end{array} \right. \tag{3.28}$$

$$v_1 \sim -\frac{\sqrt{3}}{2} \gamma_{w,1} x^{\frac{1}{3}}, \quad x > 0.$$
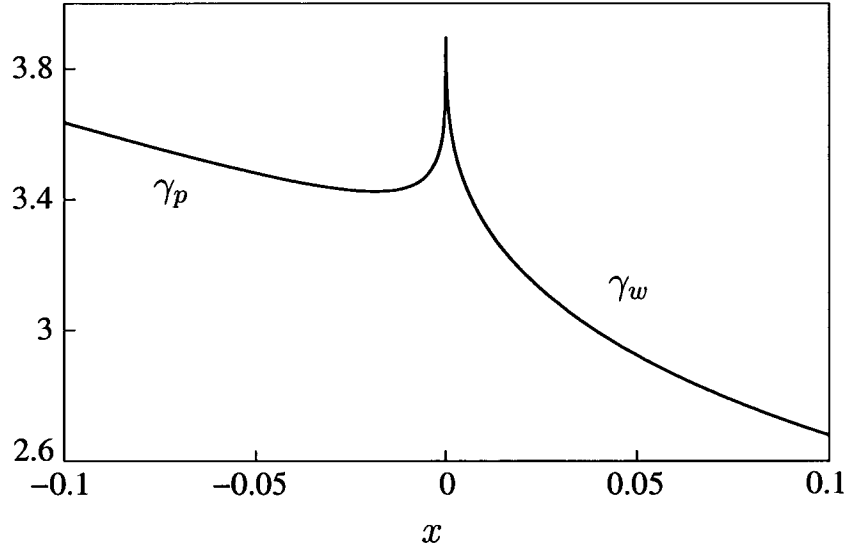
Figure 3.7 The local behavior near trailing edge

In figure 3.7 the local behavior of the vortex strength near the trailing edge for $\lambda = 1$, $\kappa = 0$ is shown. The vorticity is continuous there, satisfying the Kutta condition, but the derivative is obviously singular as expected.

This local behavior (3.28) enables us to match the potential flow to the local solution described in sub-section 4.4.

3.3.4 The wake

In the wake, after the plate, there is a deficit $\dot{I}$ in the momentum flux due to the no-slip boundary condition at the plate (the peculiarities of transition plate/wake will be explained in Section 4.).

Integrating the boundary-layer (wake) equations the balance equation for the momentum deficit is obtained

$$\frac{\mathrm{d}}{\mathrm{d}x} \dot{I} := \frac{\mathrm{d}}{\mathrm{d}x} \int_0^\infty \bar{u}_w (\bar{u}_w - 1)\, \mathrm{d}\bar{y} = \frac{\lambda \bar{y}_w' \gamma_w}{2}, \quad x > 0.$$

In a non-buoyant wake ($\lambda = 0$) the momentum deficit would be constant along the wake. The width of the wake would increase and the velocity profile would tend to the unperturbed velocity profile with increasing distance from the plate.

Here the situation is different. The buoyancy force due to a slight inclination of the wake gives a contribution to the momentum flux balance. This can lead, as in the present case, to a velocity overshoot in the wake (figure 3.8).
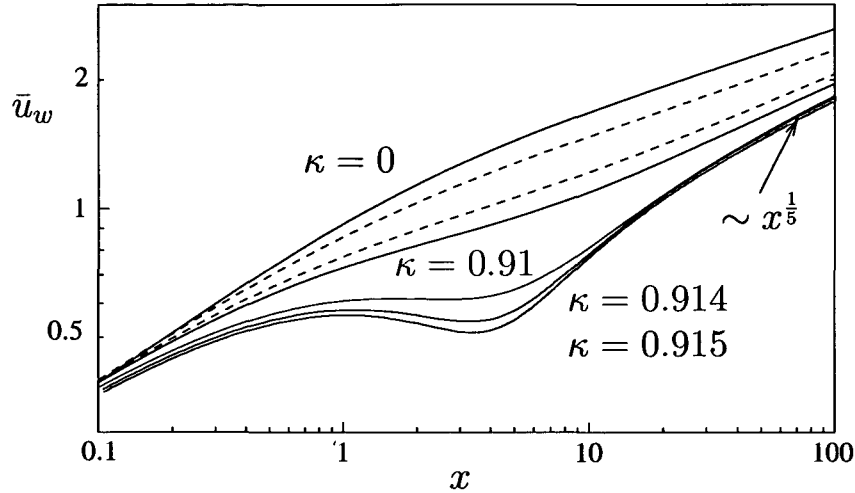
Figure 3.8 Horizontal velocity at the center line of the wake, $Pr = 0.71$, $\lambda = 1$, $\kappa =0$, 0.5, 0.6, 0.85, 0.91, 0.914, 0.915

In figure 3.8 the horizontal velocity component at the center line of the wake is shown. In the near wake region ($x \ll 1$), the velocity is not much influenced by buoyancy, since it first recovers from the velocity deficit (no-slip condition). About $x = 1$, for $\kappa = 0$ it has the value of the outside potential flow. Further downstream buoyancy accelerates the flow and a velocity overshoot forms. The behavior in far wake region is like $x^{\frac{1}{5}}$.

With increasing values of the reduced buoyancy parameter κ, the induced potential flow deforms the wake such that $\bar{u}_w(x,0)$ is reduced compared to the case $\kappa = 0$ and for $\kappa = 0.91$ a plateau forms. The solution is here very sensible to variations of κ and for $\kappa > 0.915$ the procedure fails, as already been said.

This break-down of the numerical solution (no convergence) can be a consequence of a dissatisfactory numerical scheme, or may be caused by "the physics" — a small region of a reversed flow which breaks the boundary-layer concept, concept of parabolic equations. Since, the velocity profile $\bar{u}_w(x, 0)$ has an obvious minimum (at $x \sim 2.2$), we expect that with increasing value of κ, this minimum could reach the zero value, so a reverse flow region might form.

In order to explain the break-down of numerics, in fact to "reach the reverse flow" (to obtain solutions for $\kappa > 0.915$), the numerical procedure has to be formulated differently. Certainly, the further investigations are desirable.

The influence of the vorticity distribution γ_w onto the form of the wake can be seen in figures 3.9 and 3.10.
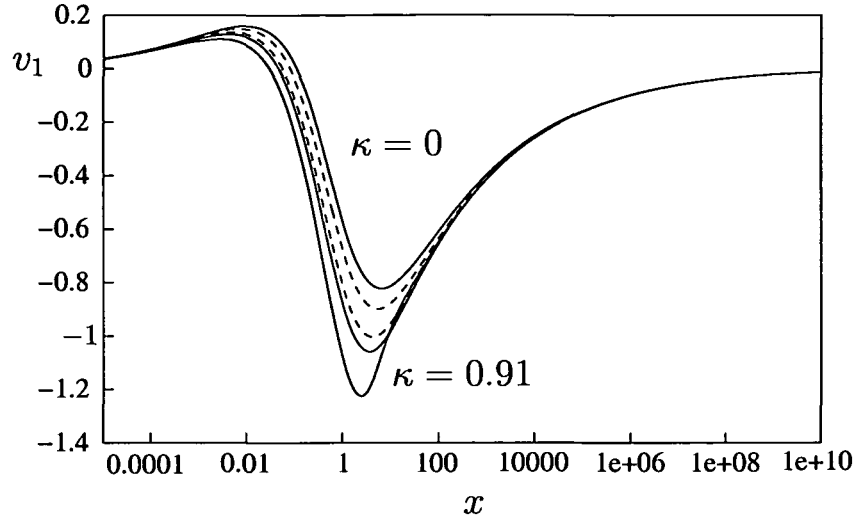
Figure 3.9 Vertical velocity at the center wake line, $Pr = 0.71$, $\lambda = 1$, $\kappa = 0$, 0.5, 0.6, 0.85, 0.91
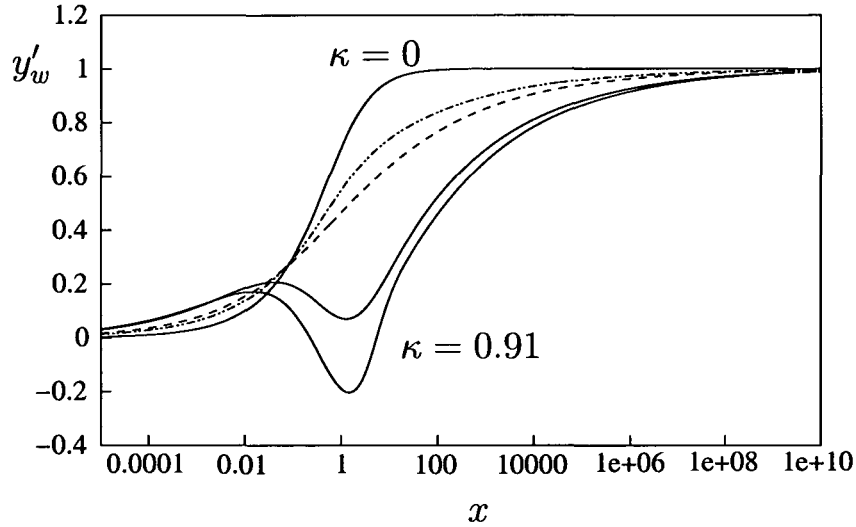
Figure 3.10 Scaled inclination of the wake center line, $Pr = 0.71$, $\lambda = 1$, $\kappa = 0$, 0.5, 0.6, 0.85, 0.91

The first one shows the induced vertical velocity component v_1 in the wake.

Starting at zero from the trailing edge it attains a positive maximum and then decreases rapidly to a negative minimum and finally increases slowly to its limiting value zero at infinity. This zero value is a confirmation that divergence of integrals (3.24) and (3.25) does not occur!

In figure 3.10 the scaled inclination of the wake y'_w is shown.

For $\kappa = 0$ it is the inclination of the wake after a plate with the small angle of attack ϕ. It is not affected by buoyancy. Shortly after the plate buoyancy tends to bend the wake upwards, but at $x \sim 0.1$ buoyancy tends to bend the wake downwards. For $\kappa = 0.91$ the wake has near $x = 1$ a section with negative inclination! Near this limiting value of κ one sees that the inclination is very sensitive to κ. This seems to be an indication that around $\kappa = 0.915$ a bifurcation or a singularity occurs.

3.3.5 Vortex distribution at the plate – lift coefficient

The pressure due to the potential flow with circulation gives rise to a normal force acting on the plate, i.e. a lift coefficient. So the total vortex strength distribution along the plate will be used to define the lift coefficient.

$$\Gamma_P(x) = \phi\gamma_\phi(x) + K\gamma_p(x) = -\phi\left(2\sqrt{\frac{-x}{x+1}} - \frac{\kappa^2}{\lambda}\gamma_p(x)\right). \tag{3.29}$$

The total vortex strength includes the influence of the inclination angle, term $\phi \gamma_\phi(x)$ and a buoyancy term, characterized by parameter $\dfrac{\kappa^2}{\lambda}$ (sub-section 3.2).
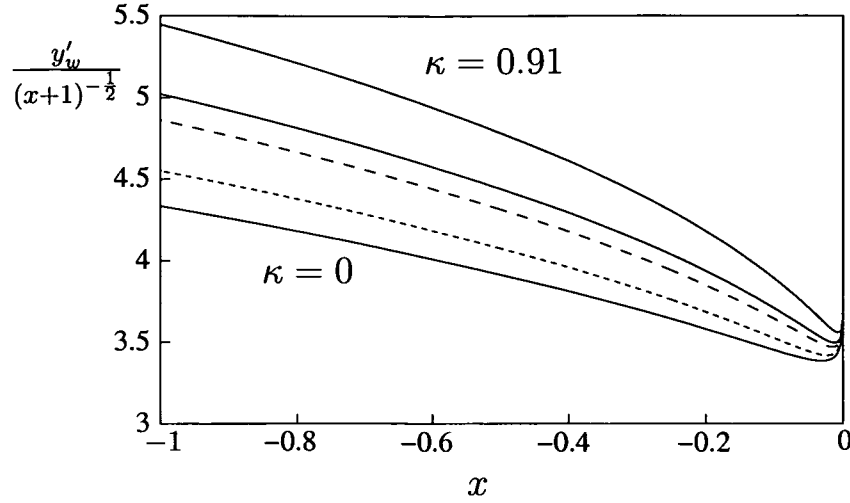
Figure 3.11 Vortex strength distribution at the plate, $\mathrm{Pr} = 0.71$, $\lambda = 1$, $\kappa = 0, 0.5, 0.6, 0.85, 0.91$

Accounting for the contributions from the upper and lower surfaces of the plate and referring the lift force to the free stream stagnation pressure and the plate area we obtain for the lift coefficient C_L

$$C_L = -4 \int_{-1}^{0} p(x, 0+) \, dx = -2 \int_{-1}^{0} \Gamma_p(x) \, dx = \phi \left(2\pi - \frac{2\kappa^2}{\lambda} \int_{-1}^{0} \gamma_p(x) \, dx \right). \qquad (3.30)$$
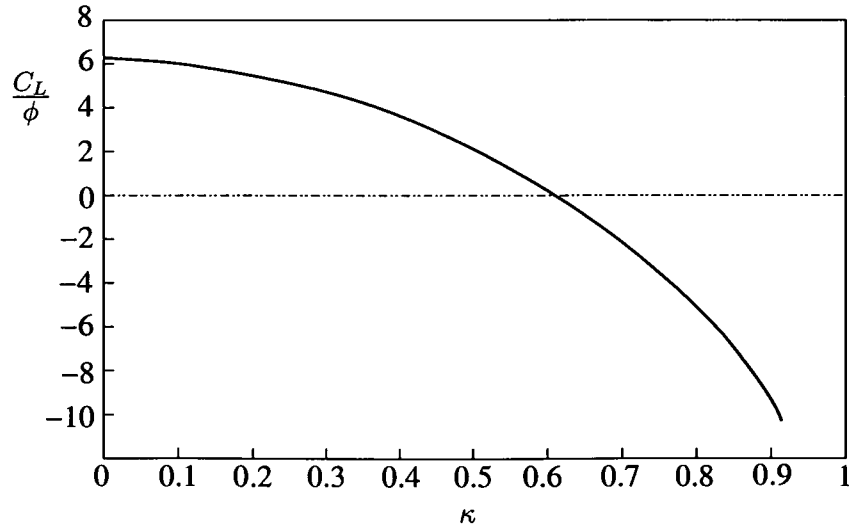
Figure 3.12 Lift coefficient, $\mathrm{Pr} = 0.71$, $\lambda = 1$

Figure 3.12 shows that buoyancy reduces the lift force. For $\kappa \sim 0.6$ the resulting lift force is zero and for larger values of κ a negative lift is obtained. This result is in accordance with Schneider (2005) who also obtained a negative lift.

3.4 Heat transfer

In this section we consider the effects of buoyancy onto the heat transfer from the plate to the fluid. Starting point are the modified boundary-layer equations (cf. Schneider (1979), Schneider&Wasel (1985), Steinrück (1994), Steinrück (1995), etc...) using the (original) buoyancy parameter K.

The potential flow is also affected by buoyancy and is assumed to have an expansion of the form (3.20) with $\phi \sim K$.

As usual we distinguish between a local Nusselt number $\mathrm{Nu}_x = \frac{\dot{q}_w(x)x}{k(T_p - T_\infty)}$, where $\dot{q}_w$ is the local heat flux $\dot{q}_w(x) = -k\frac{\partial T}{\partial y}$ and a global Nusselt number $\mathrm{Nu} = \frac{\bar{q}L}{k(T_p - T_\infty)}$, where $\bar{q}$ is a average wall heat flux. The thermal conductivity k is assumed to be constant. We will expand both Nusselt numbers in terms of K:

$$\mathrm{Nu} = \mathrm{Nu}_0 + K\,\mathrm{Nu}_1 + ... \ ; \quad \mathrm{Nu}_x = \mathrm{Nu}_{x0} + K\,\mathrm{Nu}_{x1} + ..., \tag{3.31}$$

where Nu_0 is the classical forced convection Nusselt number, which is function of the Prandtl number (Pr) only. Thus Nu_1 is the correction due to buoyancy and it will be of particular interest.

We start from the modified boundary layer equations at the plate (Schneider&Wasel 1985) formulated in terms of the stream function $\bar{\psi}(x, \bar{y})$:

$$\bar{\psi}_{\bar{y}}\bar{\psi}_{\bar{y},x} - \bar{\psi}_x\bar{\psi}_{\bar{y},\bar{y}} = -\bar{p}_x + \bar{\psi}_{\bar{y}\bar{y}\bar{y}}, \tag{3.32}$$

$$\bar{p}_{\bar{y}} = K\bar{\theta}, \tag{3.33}$$

$$\bar{\psi}_{\bar{y}}\bar{\theta}_x - \bar{\psi}_x\bar{\theta}_{\bar{y}} = \frac{1}{\mathrm{Pr}}\bar{\theta}_{\bar{y}\bar{y}}, \tag{3.34}$$

with the boundary conditions:

$$\bar{\psi}(x,0) = \bar{\psi}_{\bar{y}}(x,0) = 0, \ \ \hat{\theta}(0) = 1, \tag{3.35}$$

$$\bar{\psi}_{\bar{y}}(x, \bar{y} \to \infty) \to 1 + Ku_1, \ \ \hat{\theta}(x, \bar{y} \to \infty) = 0. \tag{3.36}$$

In contrast to the investigations concerning the semi-infinite plate (Schneider 1979, Schneider&Wasel 1985, etc...) where the outer potential flow is assumed to be uniform parallel flow, we have to take the pressure perturbations in the potential flow into account

$$\bar{p}(x, \bar{y} \to \infty) \to 1 + Ku_1. \tag{3.37}$$

Transforming the modified boundary equations using the similarity variable $\hat{\eta} = \frac{\bar{y}}{\sqrt{x}}$ and functions $\bar{\psi}(x, \bar{y}) = \sqrt{x}\,\hat{f}(\hat{\eta})$, $\bar{\theta}(x, \bar{y}) = \hat{\theta}(\hat{\eta})$, $\bar{p}(x, \bar{y}) = \sqrt{x}\,\hat{p}(\hat{\eta})$ we obtain:

$$\hat{f}''' + \frac{1}{2}\hat{f}\hat{f}'' + \frac{\sqrt{x}}{2}(\hat{p} - \hat{\eta}\hat{p}') = 0, \tag{3.38}$$

$$\hat{p}' = K\hat{\theta}, \tag{3.39}$$

$$\frac{1}{\mathrm{Pr}}\hat{\theta}'' + \frac{\sqrt{x}}{2}\hat{f}\hat{\theta}' = 0, \tag{3.40}$$

subject to the boundary conditions:

$$\hat{f}(0) = \hat{f}'(0) = 0, \ \ \hat{\theta}(0) = 1, \ \ \hat{\eta} = 0, \tag{3.41}$$

$$\hat{f}'(\hat{\eta} \to \infty) \to 1, \ \ \hat{p}(\hat{\eta} \to \infty) \to \frac{1}{2}\gamma_p(x), \ \ \hat{\theta}(\hat{\eta} \to \infty) = 0. \tag{3.42}$$

The primes denote the derivatives with respect to $\hat{\eta}$.

We expand the $\hat{f}, \hat{p}, \hat{\theta}$ in terms of K:

$$\hat{f} = \hat{f}_0(\hat{\eta}) + K\hat{f}_1(x, \hat{\eta}; \lambda, \kappa^2) + ...; \quad \hat{\theta} = \hat{\theta}_0(\hat{\eta}) + K\hat{\theta}_1(x, \hat{\eta}; \lambda, \kappa^2) + ...; \quad \hat{p} = \hat{p}_0(\hat{\eta}) + K\hat{p}_1(x, \hat{\eta}; \lambda, \kappa^2) + ...,$$

where the leading order terms are not affected by the buoyancy at all ("zero" indices) and the first order terms take into account buoyancy induced disturbaces from the outer potential flow. Combing these expansion with the equations (3.38-3.40) we obtain the forced convection problem for leading order terms:

$$\hat{f}_0''' + \frac{1}{2}\hat{f}_0\hat{f}_0'' + \frac{\sqrt{x}}{2}(\hat{p}_0 - \hat{\eta}\hat{p}_0') = 0, \tag{3.43}$$

$$\hat{p}_0' = 0, \tag{3.44}$$

$$\frac{1}{\text{Pr}}\hat{\theta}_0'' + \frac{\sqrt{x}}{2}\hat{f}_0\hat{\theta}_0' = 0, \tag{3.45}$$

with boundary conditions: $\quad \hat{f}_0(0) = \hat{f}_0'(0) = 0, \quad \hat{\theta}_0(0) = 1, \quad \hat{\eta} = 0, \tag{3.46}$

$$\hat{f}_0'(\hat{\eta} \to \infty) \to 1, \quad \hat{\theta}_0(\hat{\eta} \to \infty) = 0, \quad \hat{p}_0(\hat{\eta} \to \infty) = 0 \tag{3.47}$$

and the first order approximation (correction):

$$\hat{f}_0''' + \frac{1}{2}(\hat{f}_0\hat{f}_1'' + \hat{f}_1\hat{f}_0'') + \frac{\sqrt{x}}{2}(\hat{p}_1 - \hat{\eta}\hat{p}_1') = 0, \tag{3.48}$$

$$\hat{p}_1' = \hat{\theta}_0, \tag{3.49}$$

$$\frac{1}{\text{Pr}}\hat{\theta}_1'' + \frac{\sqrt{x}}{2}(\hat{f}_0\hat{\theta}_1' + \hat{f}_1\hat{\theta}_0') = 0, \tag{3.50}$$

with boundary conditions: $\quad \hat{f}_1(0) = \hat{f}_1'(0) = 0, \quad \hat{\theta}_1(0) = 0, \quad \hat{\eta} = 0, \tag{3.51}$

$$\hat{f}_1'(\infty) = -\frac{1}{2}\gamma_p(x; \lambda, \kappa^2), \quad \hat{\theta}_1(\infty) = 0, \quad \hat{p}_1(\infty) = \frac{1}{2}\gamma_p(x; \lambda, \kappa^2). \tag{3.52}$$

Following Schneider (2005) the local correction of Nusselt number can be written as:

$$\text{Nu}_{1x} = -K \sqrt{\text{Pe}} \sqrt{x} \frac{\partial\hat{\theta}_1}{\partial\hat{\eta}}, \tag{3.53}$$

where Pe is a Peclet number Re Pr = Pe. The temperature profile in (3.53) has to be calculated from the equations (3.43-3.52).

However of the interest is the global correction of the Nusselt number and it is given in figure 3.13.
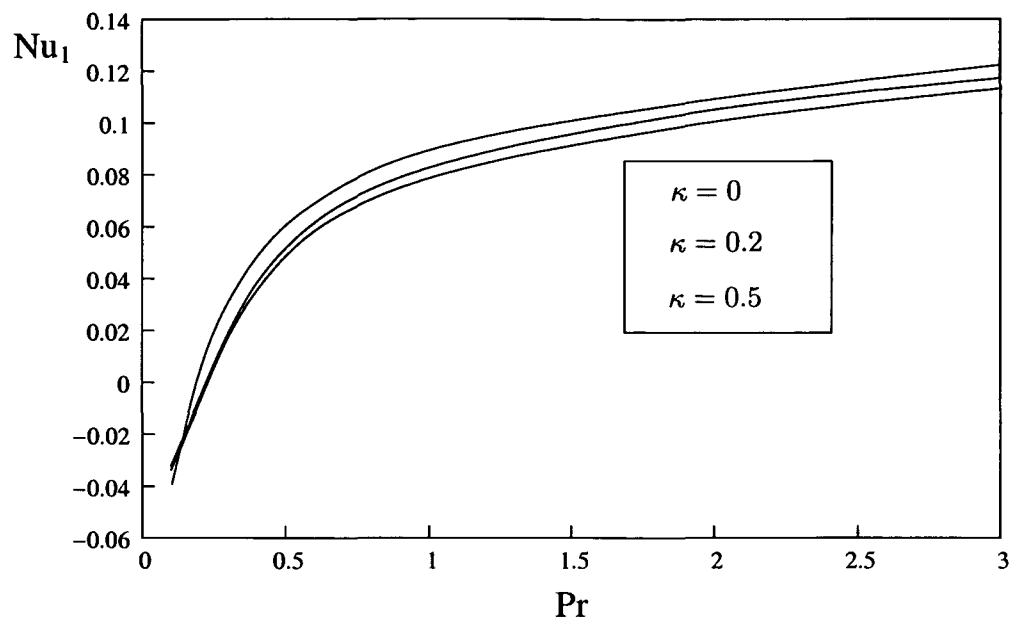
Figure 3.13 The correction of the global Nusselt number as function of κ and Prandtl number by $\lambda = 1$

The figure 3.13 confirms that the heat transfer is getting more intensive by the increasing values of Prandtl number and reduced buoyancy parameter κ. Recalling the investigations in the global flow (figure 3.11) such result was to expect.

It is important to note that values near the zero-point are not of particular relevance for the present investigation, since the study done in Schneider (2005) deals with case of $Pr \rightarrow 0$ in details.

4 Trailing edge region

4.1 Interacting boundary layers and mixed convection

It is well known that the inviscid and boundary layer description break down near separation points or near singular points of the geometry, such as sharp leading edges, corners and trailing edges.

The singularity at the trailing edge is very sever since the nonuniformaty of the basic expansions is caused by a discontinuity in the surface boundary condition (sudden change of no-slip to symmetry condition) and by a singularity in the inviscid solution (outer flow) as well. The discontinuity in the inviscid solution is described by Goldstein's near wake solution (1930), which shows the singularity in the vertical component of velocity. On the other hand, the second order inviscid solution is singular too, since the induced pressure perturbations obtain the values of plus/minus infinity on the downstream/upstream side of the trailing edge.

The singularity caused by the trailing edge is so strong that only a local expansion deep within the boundary layer can remove it. This requires a major change in the way the expansions are formulated and there were numerous attempts to correct mentioned defects in order to develop the asymptotic theory that is uniformly valid at the trailing edge.

The derivation of the suitable theory to study disturbances in the boundary layer emerged in four different papers around 1969. Stewartson (1969) and Messiter (1970) considered the trailing edge problem and Stewartson&Williams (1969) and Neiland (1969) considered separation problem. In these papers it was shown that the flow develops a characteristic multilayer structure near trailing edges and separation points. This structure is noted as a triple deck (Stewartson).

The flow upstream and downstream of the triple deck region is governed by the standard inviscid and boundary layer equations. The leading term in the outer inviscid region is given by a uniform flow, while the solution in the upstream boundary layer is given by the Blasius solution and in the downstream by Goldstein near wake. However, in the present case, in the outer potential flow the pressure perturbations have to be taken into account.

The mentioned multilayer structure is characterized by:

- the potential perturbations in the upper deck

- an inviscid rotational disturbance in the main deck, outer part of the boundary layer

- the boundary layer type disturbance in the lower deck (viscid sub-layer)
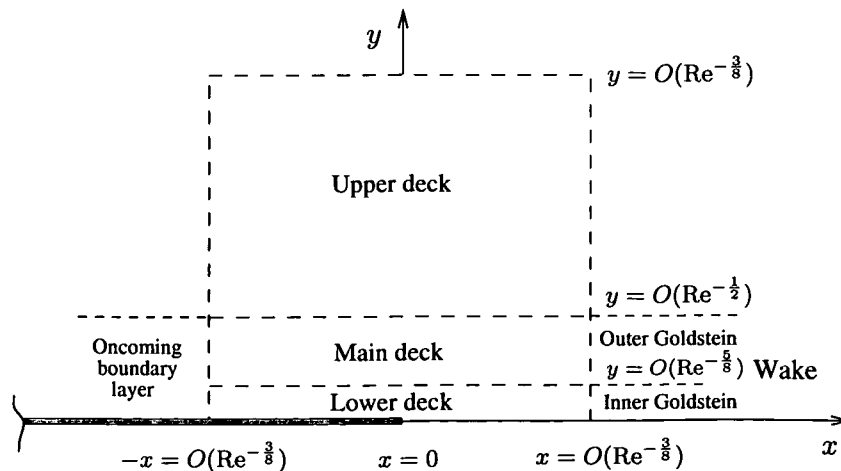
Figure 4.1 Triple deck structure (schematic)

Connecting the three decks is a pressure perturbation (and displacement function) which has to be determined by allowing the decks to interact with each other via matched asymptotic

expansions. That was the key idea of Stewartson's and Messiter's studies, to associate the potential flow (outer flow) with pressure perturbation which will affect flow near the trailing edge.

The preceding discussion explains that the triple deck formulation leads to a description of the flow as the interaction between the outer inviscid stream and vicious sub-layer (generation of the displacement function by the lower deck).

The solution in the inviscid upper deck can be reduced to the integral relationship (Hilbert integral) between pressure and the flow deflection generated by the sub-layer. On the other hand, the complete solution of the triple deck problem is then reduced to determine the solution in the viscid sub-layer (extended boundary layer equations). These solutions have to match the rotational flow in the main deck and must result in the displacement thickness and pressure distribution that satisfies the Hilbert integral arising from the outer solution.

For further details concerning the interactive boundary-layer flow see Kluwick (1998) or Sobey (2000, pp. 76).

In the present study the interaction problem will be extended to weak buoyancy effects.

In a first attempt one might assume that the buoyancy induced pressure perturbations and the interaction pressure can be of the same order of magnitude ($p = O(\mathrm{Re}^{-\frac{1}{8}})$ if $K = (\mathrm{Re}^{-\frac{1}{8}})$), cf. Lagree (1999, 2001) and Steinrück (2001). However, it can be shown that the resulting triple-deck problem for the trailing edge has no solution which can be matched to the wake solution. In accordance with the analysis of the wake and potential flow, we have to chose buoyancy parameter K of order $O(\mathrm{Re}^{-\frac{1}{4}})$. Thus, the applicability of the triple-deck concepts in present investigation is possible only with above specified value of K!

Since the flow condition on the upper and lower side of the plate are different, we have to consider two triple-deck problems: one at lower and one at the upper side. This resembles the triple deck at the trailing edge of the plate in a uniform stream at a small angle of attack studied by Stewartson&Brown (1970).
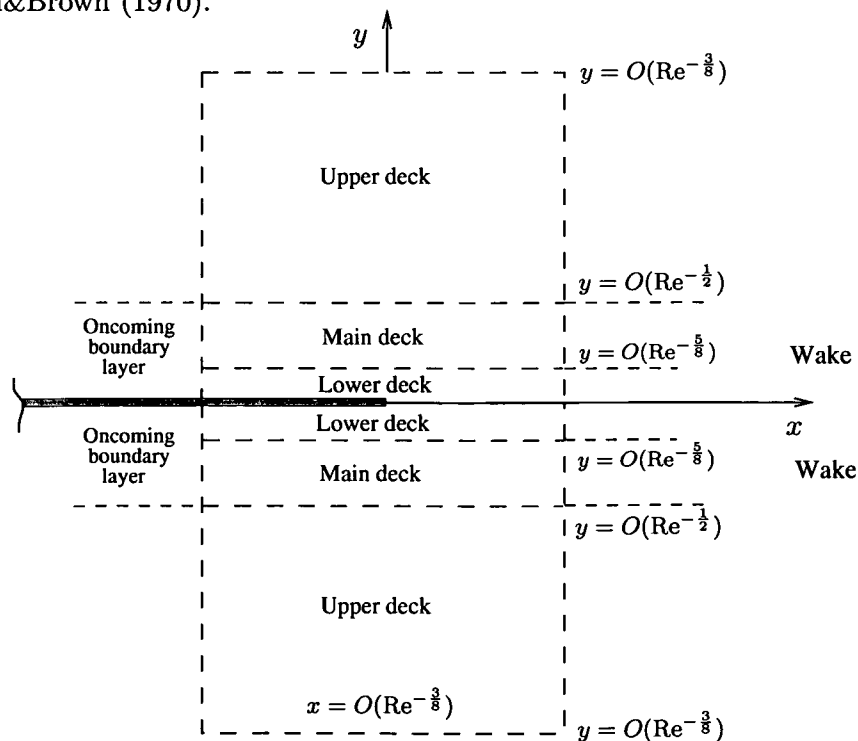
Figure 4.2 Triple deck structure for mixed convection (schematic)

To discuss the trailing edge problem the governing equations (2.1-2.4) will be used in combination with physical properties and length scales of each layer inside the triple-deck.

4.2 Notation

One difficulty in understanding the interaction near the trailing edge is that of developing a clear and easy visualized notation for such a complex problem.

The length scales are already shown in figure 4.2, but inside of the triple deck the notation will be changed. The independent variables will be denoted using the scheme where the indices represent the scaling factor by the Reynolds number:

$$x_l = \mathrm{Re}^{\frac{l}{8}}x \;\; ; \;\; y_m = \mathrm{Re}^{\frac{m}{8}}x \;\; ; \;\; l = 0,1,2,\dots \,, \;\; m = 0,1,2,\dots$$

In the further analysis $f^{(l,m)}$ will denote a depended variable (like $u,v,\theta,p\dots$), which is a function of x_l and y_m. In particular we consider the following regions:

- potential flow (no scaling) $\;\; x_0 = \mathrm{Re}^{\frac{0}{8}}x, \;\; y_0 = \mathrm{Re}^{\frac{0}{8}}y, \;\; f^{(0,0)}$

- boundary layer $\;\; x_0 = \mathrm{Re}^{\frac{0}{8}}x, \;\; y_4 = \mathrm{Re}^{\frac{4}{8}}y, \;\; f^{(0,4)}$

- upper deck $\;\; x_3 = \mathrm{Re}^{\frac{3}{8}}x, \;\; y_3 = \mathrm{Re}^{\frac{3}{8}}y, \;\; f^{(3,3)}$

- main deck $\;\; x_0 = \mathrm{Re}^{\frac{0}{8}}x, \;\; y_4 = \mathrm{Re}^{\frac{4}{8}}y, \;\; f^{(0,4)}$

- lower deck $\;\; x_3 = \mathrm{Re}^{\frac{3}{8}}x, \;\; y_5 = \mathrm{Re}^{\frac{5}{8}}y, \;\; f^{(3,5)}$

For convenience we decompose the flow into a symmetric and anti-symmetric problem. A similar technique was used by Stewartson&Brown (1970) and this procedure exactly "follows" the nature of the buoyancy, since it causes the anti-symmetric effect.

On the other hand, the symmetric case stays similar to the classical interaction problem.

This new decomposition of the flow field (symm./antisymm.) demands a formulation of sums and differences (of the values over and under the plate).

$$\bar{f} = \frac{f(x,y)+f(x,-y)}{2} \;\; ; \;\; \Delta f = \frac{f(x,y)-f(x,-y)}{2K} \;\; ; \;\; K = O(\mathrm{Re}^{-\frac{1}{4}}),$$

$$\text{but} \quad \bar{v} = \frac{v(x,y)-v(x,-y)}{2} \;\; ; \;\; \Delta v = \frac{v(x,y)+v(x,-y)}{2K}.$$

In order to make the notation system "easier to follow", all variables, together with reference values, will be shown in table 4.1:

Variable	Zones					
	Potential flow		Boundary layer		Wake	
x	$x^{(0,0)}$	(L)	$x^{(0,0)}$	(L)	$x^{(0,0)}$	(L)
y	$y^{(0,0)}$	(L)	$y^{(0,4)}$	$(U_\infty\mathrm{Re}^{-\frac{1}{2}})$	$y^{(0,4)}$	$(U_\infty\mathrm{Re}^{-\frac{1}{2}})$
u	$\bar{u}^{(0,0)}, \Delta u^{(0,0)}$	(U_∞)	$\bar{u}^{(0,4)}, \Delta u^{(0,4)}$	(U_∞)	$\bar{u}_w^{(0,4)}, \Delta u_w^{(0,4)}$	(U_∞)
v	$\bar{v}^{(0,0)}, \Delta v^{(0,0)}$	(U_∞)	$\bar{v}^{(0,4)}, \Delta v^{(0,4)}$	$(U_\infty\mathrm{Re}^{-\frac{1}{2}})$	$\bar{v}_w^{(0,4)}, \Delta v_w^{(0,4)}$	$(U_\infty\mathrm{Re}^{-\frac{1}{2}})$
p	$\bar{p}^{(0,0)}, \Delta p^{(0,0)}$	$(\rho_\infty U_\infty^2)$	$\bar{p}^{(0,4)}, \Delta p^{(0,4)}$	$(\rho_\infty U_\infty^2)$	$\bar{p}_w^{(0,4)}, \Delta p_w^{(0,4)}$	$(\rho_\infty U_\infty^2)$
θ	/	/	$\bar{\theta}^{(0,4)}, \Delta\theta^{(0,4)}$	$(T_0 - T_\infty)$	$\bar{\theta}_w^{(0,4)}, \Delta\theta_w^{(0,4)}$	$(T_0 - T_\infty)$

Trailing edge						
Variable	upper deck		main		lower	
x	x_3	$(L\mathrm{Re}^{-\frac{3}{8}})$	x_3	$(L\mathrm{Re}^{-\frac{3}{8}})$	x_3	$(L\mathrm{Re}^{-\frac{3}{8}})$
y	y_3	$(L\mathrm{Re}^{-\frac{3}{8}})$	y_4	$(L\mathrm{Re}^{-\frac{1}{2}})$	y_5	$(L\mathrm{Re}^{-\frac{5}{8}})$
u	$\bar{u}^{(3,3)}$, $\triangle u^{(3,3)}$	(U_∞)	$\bar{u}^{(3,4)}$, $\triangle u^{(3,4)}$	(U_∞)	$\bar{u}^{(3,5)}$, $\triangle u^{(3,5)}$	(U_∞)
v	$\bar{v}^{(3,3)}$, $\triangle v^{(3,3)}$	(U_∞)	$\bar{v}^{(3,4)}$, $\triangle v^{(3,4)}$	$(U_\infty\mathrm{Re}^{-\frac{1}{2}})$	$\bar{v}^{(3,5)}$, $\triangle v^{(3,5)}$	$(U_\infty\mathrm{Re}^{-\frac{1}{2}})$
p	$\bar{p}^{(3,3)}$, $\triangle p^{(3,3)}$	$(\rho_\infty U_\infty^2)$	$\bar{p}^{(3,4)}$, $\triangle p^{(3,4)}$	$(\rho_\infty U_\infty^2)$	$\bar{p}^{(3,5)}$, $\triangle p^{(3,5)}$	$(\rho_\infty U_\infty^2)$
θ	/	/	$\bar{\theta}^{(3,4)}$, $\triangle\theta^{(3,4)}$	$(T_0 - T_\infty)$	$\bar{\theta}^{(3,5)}$, $\triangle\theta^{(3,5)}$	$(T_0 - T_\infty)$

Table (4.1) shows the variables and their reference values

The analysis of the three decks follows the sequence of main deck where an inviscid rotation disturbance introduces two functions of x, the pressure gradient and the displacement function; the upper deck where a potential flow solution provides a link between the pressure gradient and the displacement function; and finally the lower deck where the solution of a non-linear boundary-layer type equation generates the unknown pressure and displacement function.

All mentioned equations will be obtained from the governing system (2.1-2.4), but now formulated for the symmetric and anti-symmetric part of the solution (flow).

Equations for the symmetric part:

$$\bar{u}^{(0,0)}\bar{u}_{x_0}^{(0,0)} + \bar{v}^{(0,0)}\bar{u}_{y_0}^{(0,0)} + K^2(\triangle u^{(0,0)}\,\triangle u_{x_0}^{(0,0)} + \triangle v^{(0,0)}\,\triangle u_{y_0}^{(0,0)}) =$$

$$-\bar{p}_{x_0}^{(0,0)} + \frac{1}{\mathrm{Re}}(\bar{u}_{x_0 x_0}^{(0,0)} + \bar{u}_{y_0 y_0}^{(0,0)}),$$

$$\bar{u}^{(0,0)}\bar{v}_{x_0}^{(0,0)} + \bar{v}^{(0,0)}\bar{v}_{y_0}^{(0,0)} + K^2(\triangle u^{(0,0)}\,\triangle v_{x_0}^{(0,0)} + \triangle v^{(0,0)}\,\triangle v_{y_0}^{(0,0)}) =$$

$$-\bar{p}_{y_0}^{(0,0)} + \frac{\mathrm{Gr}}{\mathrm{Re}^2}\,K\,\triangle\theta^{(0,0)} + \frac{1}{\mathrm{Re}}(\bar{v}_{x_0 x_0}^{(0,0)} + \bar{v}_{y_0 y_0}^{(0,0)}),$$

$$\bar{u}_{x_0}^{(0,0)} + \bar{v}_{y_0}^{(0,0)} = 0,$$

$$\bar{u}^{(0,0)}\bar{\theta}_{x_0}^{(0,0)} + \bar{v}^{(0,0)}\bar{\theta}_{y_0}^{(0,0)} + K^2(\triangle u^{(0,0)}\,\triangle\theta_{x_0}^{(0,0)} + \triangle v^{(0,0)}\,\triangle\theta_{y_0}^{(0,0)}) =$$

$$\frac{1}{\mathrm{Re}\,\mathrm{Pr}}(\bar{\theta}_{x_0 x_0}^{(0,0)} + \bar{\theta}_{y_0 y_0}^{(0,0)}). \qquad (4.1)$$

Equations for the anti-symmetric part:

$$\bar{u}^{(0,0)}\,\triangle u_{x_0}^{(0,0)} + \triangle u^{(0,0)}\,\bar{u}_{x_0}^{(0,0)} + \bar{v}^{(0,0)}\,\triangle u_{y_0}^{(0,0)} + \triangle v^{(0,0)}\,\bar{u}_{y_0}^{(0,0)} =$$

$$-\triangle p_{x_0}^{(0,0)} + \frac{1}{\mathrm{Re}}(\triangle u_{x_0 x_0}^{(0,0)} + \triangle u_{y_0 y_0}^{(0,0)}),$$

$$\bar{u}^{(0,0)}\,\triangle v_{x_0}^{(0,0)} + \triangle u^{(0,0)}\,\bar{v}_{x_0}^{(0,0)} + \bar{v}^{(0,0)}\,\triangle v_{y_0}^{(0,0)} + \triangle v^{(0,0)}\,\bar{v}_{y_0}^{(0,0)} =$$

$$-\triangle p_{y_0}^{(0,0)} + \frac{\mathrm{Gr}}{\mathrm{Re}^2 K}\bar{\theta}^{(0,0)} + \frac{1}{\mathrm{Re}}(\triangle v_{x_0 x_0}^{(0,0)} + \triangle v_{y_0 y_0}^{(0,0)}),$$

$$\triangle u_{x_0}^{(0,0)} + \triangle v_{y_0}^{(0,0)} = 0,$$

$$\bar{u}^{(0,0)} \, \triangle\theta_{x_0}^{(0,0)} + \triangle u^{(0,0)} \, \bar{\theta}_{x_0}^{(0,0)} + \bar{v}^{(0,0)} \, \triangle\theta_{y_0}^{(0,0)} + \triangle v^{(0,0)} \, \bar{\theta}_{y_0}^{(0,0)} =$$

$$\frac{1}{\mathrm{RePr}}(\triangle\theta_{x_0 x_0}^{(0,0)} + \triangle\theta_{y_0 y_0}^{(0,0)}). \tag{4.2}$$

It seems that after the transformation, the system of equations is more complicated than it used to be (by "separated" top and bottom of the plate), but in reality this procedure makes the investigation much easier (both analytically and numerically).

With specified value of K (defined in investigation of the global flow), namely $K = O(\mathrm{Re}^{-\frac{1}{4}})$, the problem (4.2) becomes linear, where the symmetric part of the solution is given by classic triple deck concept (1969). Thus the anti-symmetric part can be interprated as "next approximation", or the slightly disturbed Stewartson case of interaction.

4.3 Flow structure at the trailing edge

4.3.1 Main deck

The equations valid in main deck are obtained by inserting the asymptotic expansions of the dependent variables into the equations (4.1, 4.2).

For the anti-symmetric part there are:

$$\triangle u^{(3,4)}(x_3, y_4) = C_{11} \ln \mathrm{Re} + \triangle u_0^{(3,4)}(x_3, y_4) + \mathrm{Re}^{-\frac{1}{8}} \triangle u_1^{(3,4)}(x_3, y_4) + ...,$$

$$\triangle v^{(3,4)}(x_3, y_4) = \mathrm{Re}^{-\frac{1}{8}} \triangle v_0^{(3,4)}(x_3, y_4) + \mathrm{Re}^{-\frac{2}{8}} \triangle v_1^{(3,4)}(x_3, y_4) + ...,$$

$$\triangle p^{(3,4)}(x_3, y_4) = \triangle p_0^{(3,4)}(x_3, y_4) + \mathrm{Re}^{-\frac{1}{8}} \triangle p_1^{(3,4)}(x_3, y_4) + ...,$$

$$\triangle \theta^{(3,4)}(x_3, y_4) = C_{11} \ln \mathrm{Re} + \triangle \theta_0^{(3,4)}(x_3, y_4) + \mathrm{Re}^{-\frac{1}{8}} \triangle \theta_1^{(3,4)}(x_3, y_4) + ...$$

We will see later that expansions for $\triangle u^{(3,4)}$ and $\triangle \theta^{(3,4)}$ have to have the $\ln \mathrm{Re}$-term (sub-section 4.5).

For the symmetric part we have:

$$\bar{u}^{(3,4)}(x_3, y_4) = \bar{u}_0^{(0,4)}(y_4) + \mathrm{Re}^{-\frac{1}{8}} \bar{u}_1^{(3,4)}(x_3, y_4) + ...,$$

$$\bar{v}^{(3,4)}(x_3, y_4) = \mathrm{Re}^{-\frac{2}{8}} \bar{v}_1^{(3,4)}(x_3, y_4) + ...,$$

$$\bar{p}^{(3,4)}(x_3, y_4) = \mathrm{Re}^{-\frac{2}{8}} \bar{p}_1^{(3,4)}(x_3, y_4) + ...,$$

$$\bar{\theta}^{(3,4)}(x_3, y_4) = \bar{\theta}_0^{(0,4)}(y_4) + \mathrm{Re}^{-\frac{1}{8}} \bar{\theta}_1^{(3,4)}(x_3, y_4) + ...$$

The main deck equations (symmetric/antisymmetic) for the leading order terms are:

$$\bar{u}_0^{(0,4)}\bar{u}_{1,x_3}^{(3,4)} + \bar{v}_1^{(3,4)}\bar{u}_{0,y_4}^{(0,4)} = 0, \tag{4.3}$$

$$\bar{p}_{1,y_4}^{(3,4)} = 0, \tag{4.4}$$

$$\bar{u}_{1,x_3}^{(3,4)} + \bar{v}_{1,y_4}^{(3,4)} = 0, \tag{4.5}$$

$$\bar{u}_0^{(0,4)}\bar{\theta}_{1,x_3}^{(3,4)} + \bar{v}_1^{(3,4)}\bar{\theta}_{0,y_4}^{(0,4)} = 0, \tag{4.6}$$

where $\bar{u}_0^{(0,4)} \equiv F_B'$, F_B is the Blasius function and $\bar{\theta}_0^{(0,4)} \equiv D_B$ is the temperature profile at the plate (cf. Subsection 3.1.1).

The obtained system describes the rotational inviscid flow and it can be solved analytically using the unknown function $\bar{A}(x_3)$ – Stewartson's displacement function.

$$\bar{u}_1^{(3,4)} = \bar{A}(x_3) \, \bar{u}_{0,y_4}^{(0,4)}, \tag{4.7}$$

$$\bar{v}_1^{(3,4)} = -\bar{A}'(x_3) \, \bar{u}_0^{(0,4)}(y_4), \tag{4.8}$$

$$\bar{p}_1^{(3,4)} = C_1^{(3,4)}(x_3), \tag{4.9}$$

$$\bar{\theta}_1^{(3,4)} = \bar{A}(x_3) \, \bar{\theta}_{0,y_4}^{(0,4)}. \tag{4.10}$$

Similar equations hold for the anti-symmetric case:

$$\bar{u}_0^{(0,4)}\triangle u_{0,x_3}^{(3,4)} + \triangle v_0^{(3,4)}\bar{u}_{0,y_4}^{(0,4)} = 0, \tag{4.11}$$

$$\triangle p_{0,y_4}^{(3,4)} = \bar{\theta}_0^{(0,4)}, \tag{4.12}$$

$$\triangle p_{1,y_4}^{(3,4)} = \bar{\theta}_1^{(3,4)},$$ (4.13)

$$\triangle u_{0,x_3}^{(3,4)} + \triangle v_{0,y_4}^{(3,4)} = 0,$$ (4.14)

$$\bar{u}_0^{(0,4)} \triangle \theta_{0,x_3}^{(3,4)} + \triangle v_0^{(3,4)} \bar{\theta}_{0,y_4}^{(0,4)} = 0,$$ (4.15)

with the solution:

$$\triangle u_0^{(3,4)} = \triangle A(x_3)\, \bar{u}_{0,y_4}^{(0,4)} + C_2^{(3,4)}(y_4),$$ (4.16)

$$\triangle v_0^{(3,4)} = -\triangle A'(x_3)\, \bar{u}_0^{(0,4)}(y_4),$$ (4.17)

$$\triangle \theta_0^{(3,4)} = \triangle A(x_3)\, \bar{\theta}_{0,y_4}^{(0,4)} + C_3^{(3,4)}(y_4),$$ (4.18)

$$\triangle p_0^{(3,4)} = \int_0^{y_4} \bar{\theta}_0^{(0,4)}\, dy_4 \;\Rightarrow\; \triangle p_0^{(3,4)} = \triangle p_0^{(3,4)}(y_4),$$ (4.19)

$$\triangle p_1^{(3,4)} = \bar{A}(x_3)\, \bar{\theta}_0^{(0,4)} + C_4^{(3,4)}(x_3).$$ (4.20)

The constants of integration $C_2^{(3,4)}, C_3^{(3,4)}$ present in the solution of anti-symmetric case will be determined by matching procedure (in classical interaction these terms are zero). The unknown function $\triangle A'(x_3)$ is "the difference of the displacement functions" on the upper and lower side of the plate.

4.3.2 Upper deck

The upper deck represents the disturbed potential flow.
The procedure for deriving the equations valid in upper deck has been already explained in the previos sub-section and we start with asymptotic expansions for the symmetric part:

$$\bar{u}^{(3,3)}(x_3, y_3) = 1 + \mathrm{Re}^{-\frac{2}{8}} \bar{u}_1^{(3,3)}(x_3, y_3) + ...,$$

$$\bar{v}^{(3,3)}(x_3, y_3) = \mathrm{Re}^{-\frac{2}{8}} \bar{v}_1^{(3,3)}(x_3, y_3) + ...,$$

$$\bar{p}^{(3,4)}(x_3, y_4) = \mathrm{Re}^{-\frac{2}{8}} \bar{p}_1^{(3,3)}(x_3, y_3) + ...$$

and for the anti-symmetric:

$$\triangle u^{(3,3)}(x_3, y_3) = \mathrm{Re}^{-\frac{1}{8}} \triangle u_0^{(3,3)}(x_3, y_3) + \mathrm{Re}^{-\frac{2}{8}} \triangle u_1^{(3,3)}(x_3, y_3) + ...,$$

$$\triangle v^{(3,3)}(x_3, y_3) = \mathrm{Re}^{-\frac{1}{8}} \triangle v_0^{(3,3)}(x_3, y_3) + \mathrm{Re}^{-\frac{2}{8}} \triangle v_1^{(3,3)}(x_3, y_3) + ...,$$

$$\triangle p^{(3,3)}(x_3, y_3) = \triangle p_0^{(3,3)}(x_3, y_3) + \mathrm{Re}^{-\frac{1}{8}} \triangle p_1^{(3,3)}(x_3, y_3) + ...$$

Matching the v-component of the main deck with the v-component of the upper deck yields:

$$\bar{v}_1^{(3,3)}(x_3, 0) = \bar{v}_1^{(3,4)}(x_3, \infty) = -\bar{A}'(x_3).$$ (4.21)

Thus the potential flow in the upper deck can be represented by a source distribution on the x_3-axis (Schneider 1978, pp. 142). Together with the linearized Bernoulli equation we obtain for the pressure distribution:

$$\bar{p}_1^{(3,3)}(x_3, 0) = \mathcal{F}\left\{ \frac{1}{\pi} \int_{-\infty}^{+\infty} \frac{\bar{A}'(\zeta)}{x_3 - \zeta}\, d\zeta \right\}$$

The pressure perturbation and displacement function are "connected" by Hilbert's integral, where the Cauchy principal value and also Hadamard's notion (finite part of integral, cf. Hadamard (1932)) have to be involved.

The source distribution procedure holds for the anti-symmetric part as well and we have

$$\Delta p_1^{(3,3)}(x_3, 0) = \mathcal{F}\left\{ \frac{1}{\pi} \int\limits_{-\infty}^{+\infty} \frac{\Delta A'(\zeta)}{x_3 - \zeta} \, d\zeta \right\}.$$

Now, considering the pressure perturbations by the matching principle (matching the upper with the main deck) the complete form of the pressure corrections in the trailing edge region is given by:

$$\bar{p}_1^{(3,4)}(x_3) = \mathcal{F}\left\{ \frac{1}{\pi} \int\limits_{-\infty}^{+\infty} \frac{\bar{A}'(\zeta)}{x_3 - \zeta} \, d\zeta \right\}, \tag{4.22}$$

$$\Delta p_1^{(3,4)}(x_3) = \bar{A}(x_3)\bar{\theta}_0^{(0,4)}(y_4) + \mathcal{F}\left\{ \frac{1}{\pi} \int\limits_{-\infty}^{+\infty} \frac{\Delta A'(\zeta)}{x_3 - \zeta} \, d\zeta \right\}. \tag{4.23}$$

4.3.3 Lower deck

Also in the lower deck the analysis starts from the governing equations and the asymptotic expansions, thus for symmetric part we have:

$$\bar{u}^{(3,5)}(x_3, y_5) = \mathrm{Re}^{-\frac{1}{8}} \bar{u}_1^{(3,5)}(x_3, y_5) + \ldots,$$

$$\bar{v}^{(3,5)}(x_3, y_5) = \mathrm{Re}^{-\frac{3}{8}} \bar{v}_1^{(3,5)}(x_3, y_5) + \ldots,$$

$$\bar{p}^{(3,5)}(x_3, y_5) = \mathrm{Re}^{-\frac{2}{8}} \bar{p}_1^{(3,5)}(x_3, y_5) + \ldots,$$

$$\bar{\theta}^{(3,5)}(x_3, y_5) = \mathrm{Re}^{-\frac{1}{8}} \bar{\theta}_1^{(3,5)}(x_3, y_5) + \ldots$$

and for anti-symmetric part:

$$\Delta u^{(3,5)}(x_3, y_5) = \Delta u_0^{(3,3)}(x_3, y_5) + \mathrm{Re}^{-\frac{1}{8}} \Delta u_1^{(3,5)}(x_3, y_5) + \ldots,$$

$$\Delta v^{(3,5)}(x_3, y_5) = \mathrm{Re}^{-\frac{2}{8}} \Delta v_0^{(3,5)}(x_3, y_5) + \mathrm{Re}^{-\frac{3}{8}} \Delta v_1^{(3,5)}(x_3, y_5) + \ldots,$$

$$\Delta p^{(3,5)}(x_3, y_5) = \Delta p_0^{(3,5)}(x_3, y_5) + \mathrm{Re}^{-\frac{1}{8}} \Delta p_1^{(3,5)}(x_3, y_5) + \ldots,$$

$$\Delta \theta^{(3,5)}(x_3, y_5) = \Delta \theta_0^{(3,5)}(x_3, y_5) + \mathrm{Re}^{-\frac{1}{8}} \Delta \theta_1^{(3,5)}(x_3, y_5) + \ldots.$$

The equations valid inside of lower deck (thin, viscid sub-layer) for the symmetric part are:

$$\bar{u}_1^{(3,5)} \bar{u}_{1,x_3}^{(3,5)} + \bar{v}_1^{(3,5)} \bar{u}_{1,y_5}^{(3,5)} = -\bar{p}_{1,x_3}^{(3,5)} + \bar{u}_{1,y_5 y_5}^{(3,5)}, \tag{4.24}$$

$$\bar{p}_1^{(3,5)}(x_3) = \mathcal{F}\left\{ \frac{1}{\pi} \int\limits_{-\infty}^{+\infty} \frac{\bar{A}'(\zeta)}{x_3 - \zeta} \, d\zeta \right\}, \tag{4.25}$$

$$\bar{u}_{1,x_3}^{(3,5)} + \bar{v}_{1,y_5}^{(3,5)} = 0, \tag{4.26}$$

$$\bar{u}_1^{(3,5)} \bar{\theta}_{1,x_3}^{(3,5)} + \bar{v}_1^{(3,5)} \bar{\theta}_{1,y_5}^{(3,5)} = \frac{1}{\mathrm{Pr}} \bar{\theta}_{1,y_5 y_5}^{(3,5)}, \tag{4.27}$$

with boundary conditions (no-slip and symmetry condition)

$$\bar{u}_1^{(3,5)}(x_3,0) = \bar{v}_1^{(3,5)}(x_3,0) = \bar{\theta}_1^{(3,5)}(x_3,0) = 0 \ ; \quad x_3 < 0, \tag{4.28}$$

$$\bar{u}_{1,y_5}^{(3,5)}(x_3,0) = \bar{v}_1^{(3,5)}(x_3,0) = \bar{\theta}_{1,y_5}^{(3,5)}(x_3,0) = 0 \ ; \quad x_3 > 0, \tag{4.29}$$

matching conditions

$$\bar{u}_1^{(3,5)}(x_3,\infty) \sim y_5 + \bar{A}(x_3) \ ; \quad \bar{\theta}_1^{(3,5)}(x_3,\infty) \sim y_5 + \bar{A}(x_3), \tag{4.30}$$

and initial condition

$$\bar{u}_1^{(3,5)}(x_3 \to -\infty) \sim y_5. \tag{4.31}$$

For the anti-symmetric part we have:

$$\bar{u}_1^{(3,5)}\triangle u_{0,x_3}^{(3,5)} + \triangle u_0^{(3,5)}\bar{u}_{1,x_3}^{(3,5)} + \bar{v}_1^{(3,5)}\triangle u_{0,y_5}^{(3,5)} + \triangle v_0^{(3,5)}\bar{u}_{1,y_5}^{(3,5)} = -\triangle p_{1,x_3}^{(3,5)} + \triangle u_{0,y_5 y_5}^{(3,5)}, \tag{4.32}$$

$$\triangle p_1^{(3,5)}(x_3) = \bar{A}(x_3) + \mathcal{F}\Big\{\frac{1}{\pi}\int\limits_{-\infty}^{+\infty}\frac{\triangle A'(\zeta)}{x_3 - \zeta}\, d\zeta\Big\}, \tag{4.33}$$

$$\triangle u_{0,x_3}^{(3,5)} + \triangle v_{0,y_5}^{(3,5)} = 0, \tag{4.34}$$

$$\bar{u}_1^{(3,5)}\triangle\theta_{0,x_3}^{(3,5)} + \triangle u_0^{(3,5)}\bar{\theta}_{1,x_3}^{(3,5)} + \bar{v}_1^{(3,5)}\triangle\theta_{0,y_5}^{(3,5)} + \triangle v_0^{(3,5)}\bar{\theta}_{1,y_5}^{(3,5)} = \frac{1}{\mathrm{Pr}}\,\triangle\theta_{0,y_5 y_5}^{(3,5)}, \tag{4.35}$$

with the boundary conditions:

$$\triangle u_0^{(3,5)}(x_3,0) = \triangle v_0^{(3,5)}(x_3,0) = \triangle\theta_0^{(3,5)}(x_3,0) = 0 \ ; \quad x_3 < 0, \tag{4.36}$$

$$\triangle u_0^{(3,5)}(x_3,0) = \triangle p_0^{(3,5)}(x_3,0) = \triangle\theta_0^{(3,5)}(x_3,0) = 0 \ ; \quad x_3 > 0. \tag{4.37}$$

The symmetric part of the solution (4.24-4.27) is the triple-deck problem for the flow past a finite plate considered by Stewartson (1969) and Messiter (1970) and thus the solution is well known (classical interaction, no buoyancy influence).

However, the anti-symmetric part (4.32-4.35) can only be solved, after the determination of the solution of the classical interaction problem. Due to the scaling of the buoyancy parameter, the anti-symmetric part of the solution does not influence the symmetic one.

In order to complete the formulation of the tripe-deck problem for the anti-symmetric case, the asymptotic behavior for $x_3 \to -\infty$ has to be analyzed, which is done in the following subsection.

4.4 Asymptotic behavior for $x_3 \to \pm\infty$

In order to define an adequate numerical scheme to solve the system of equations (4.24–4.37), a detailed analysis of the problem is necessary. The asymptotic behavior of the unknown variables in the region of the trailing edge and infinity are of particular interest. Since the problem is of elliptic/parabolic nature, it will be sensitive to any changes in asymptotic of pressure distribution and displacement function, respectively.

4.4.1 Symmetric part

We start with the symmetric problem (Stewartson's solution) and recall the asymptotic behavior of its solution (Melnik&Chow 1975):

$$\bar{u}^{(3,5)}(x_3, y_5) = \left\{ \begin{array}{ll} y_5 & x_3 \to -\infty \\ x_3^{\frac{1}{3}} U_s(\zeta) & x_3 \to +\infty \end{array} \right. \quad \zeta = y_5/x_3^{\frac{1}{3}} \quad ,$$

$$\bar{v}^{(3,5)}(x_3, y_5) = \left\{ \begin{array}{ll} 0 & x_3 \to -\infty \\ x_3^{-\frac{1}{3}} V_s(\zeta) & x_3 \to +\infty \end{array} \right. \quad ,$$

$$\bar{A}^{(3,5)}(x_3) = \left\{ \begin{array}{ll} 0 & x_3 \to -\infty \\ x_3^{\frac{1}{3}} a_s & x_3 \to +\infty \end{array} \right. \quad ,$$

where $a_s = 0.892$ is the Stewartson's constant and U_s, V_s are the Goldstein's similarity solutions (1930), respectively.

4.4.2 Anti-symmetric part

Since the flow in the upper deck is a potential flow, the function $\Delta\phi(x_3, y_3) = -\Delta u^{(3,3)}(x_3, y_3) + i\Delta v^{(3,3)}(x_3, y_3)$ can be interpreted as an analytical function of the complex variable $z_3 = x_3 + iy_3$. Due to the matching condition with the main deck (4.21) and the linearized Bernoulli equation we have

$$\Delta u^{(3,3)}(x_3, 0) = -\Delta p^{(3,3)}(x_3) \; , \; \Delta v^{(3,3)}(x_3, 0) = -\Delta A'(x_3).$$

The pressure perturbation $\Delta p^{(3,3)}$ and the derivative of the displacement function $-\Delta A'(x_3)$ can be now interpreted as the real an imaginary part of the analytical function evaluated on the real axis. Using the equation for the pressure distribution in the main deck (4.21) we have

$$\Delta\phi(x_3, 0) = \Delta p^{(3,3)} - i\Delta A'(x_3) = \Delta p^{(3,5)} - \bar{A}(x_3) - i\Delta A'(x_3).$$

Now taking the asymptotic behavior of $\bar{A}(x_3)$ into account, we assume an asymptotic expansion of $\Delta\phi$ for $z \to \infty$ in the form: $\Delta\phi = \Delta\phi_0 + (a + ib)z^{\frac{1}{3}}$, where $\Delta\phi_0(z)$ is analytical at $z \to \infty$. The constants a and b are determined such that $\Delta A'(x_3) \to 0$ for $x_3 \to -\infty$ is valid. They turn out to be $a = -a_s$ and $b = \sqrt{3}a_s$.
Thus we obtain for the real and imaginary part of $\Delta\phi_0$ (cf. Appendix A.1):

$$\Re\Delta\phi_0 = \Delta p_1^{(3,5)}(x_3) - \bar{A}(x_3) - a_s|x_3|^{\frac{1}{3}}\left(1 + h(-x_3)\right),$$

$$\Im\Delta\phi_0 = -\Delta A'(x_3) + \sqrt{3}a_s x_3^{\frac{1}{3}} h(x_3),$$

where $h(x_3) = 1$ for $x > 0$ and $h(x_3) = 0$ for $x < 0$ is the Heaviside jump function.
Thus the asymptotic behavior of $\Delta p_1^{(3,5)}$ and $\Delta A'(x_3)$ is given as:

$$\Delta p_1^{(3,5)}(-x_3) \sim -2a_s|x_3|^{\frac{1}{3}} \; ; \quad \Delta A(x_3) \sim -\frac{3\sqrt{3}}{4}x_3^{\frac{4}{3}} \; ; \quad x_3 \to \infty$$

and the interaction law can be written in the form:

$$\Delta p_1^{(3,5)}(x_3) = \bar{A}(x_3) - 2a_s|x_3|^{\frac{1}{3}}\left(1 + h(x_3)\right) + \frac{1}{\pi}\int\limits_{-\infty}^{+\infty}\frac{\Delta A'(\zeta) + \sqrt{3}a_s\zeta^{\frac{1}{3}}h(\zeta)}{x_3 - \zeta}\,d\zeta. \qquad (4.38)$$

The interaction law formulated by equation (4.38) separates the singular parts and the integrand in the Hilbert integral decays sufficiently fast to zero for $x_3 \to \pm\infty$.

We point out the asymptotic behavior of $A(x_3) \sim x_3^{\frac{4}{3}}$, which has not been observed in the literature before.

In order to find the numerical solution, the asymptotic behavior (both in $x_3 \to \pm\infty$) of the pressure perturbation and the displacement function has to be known. This behavior is crucial, since the solution is very sensitive to any variation of boundary conditions.

4.4.3 Asymptotic behavior of the velocity profile for $x_3 \to -\infty$

Considering the asymptotic behavior of the pressure $\Delta p_1^{(3,5)}$ and the behavior of Stewartson's solution as $x_3 \to -\infty$, we conclude that flow in the lower deck is self-similar. Making the similarity ansatz (using the scaled stream function ΔH)

$$\Delta u_0^{(3,5)} = \Delta H'(\eta), \quad \text{with} \quad \eta = \frac{y_5}{|x_3|^{\frac{1}{3}}}, \qquad (4.39)$$

we obtain the similarity equation

$$\Delta H''' - F_B''(0)\frac{\eta^2}{3}\Delta H'' - \frac{F_B''(0)}{3}(\Delta H - \eta\Delta H') = \frac{2a_s}{3}, \qquad (4.40)$$

with boundary conditions $\Delta H(0) = \Delta H'(0) = 0$. The right hand-side of the equation (4.40) is due to the asymptotic behavior of the pressure perturbation $\Delta p_1^{(3,5)} \sim -2a_s|x_3|^{\frac{1}{3}}$.

The corresponding homogeneous equation has three linearly independent solutions, namely h_1, h_2, h_3, where we have: $h_1(\eta) \sim \eta\ln\eta$ for $\eta \to \infty, h_2(\eta) = \eta$.

$$\Delta H(\eta) = -\frac{2a_s}{F_B(0)} + C_1^{(3,5)}h_1(\eta) + C_2^{(3,5)}h_2(\eta) + C_3^{(3,5)}h_3(\eta) \qquad (4.41)$$

The third solution h_3 increases exponentially for $\eta \to \infty$ and in order to match the velocity profile with the main deck it has to be eliminated. Thus the asymptotic behavior of the $\Delta H(\eta)$ for $\eta \to \infty$ is given as

$$\Delta H(\eta) = -\frac{2a_s}{F_B(0)} + C_1^{(3,5)}\eta\ln\eta + C_2^{(3,5)}\eta \qquad (4.42)$$

and finally for the velocity profile we have:

$$\Delta H' = \Delta u_0^{(3,5)}(\eta) \sim C_1^{(3,5)}\ln\eta + C_2^{(3,5)}, \quad \eta \to \infty, \qquad (4.43)$$

$$\Delta u_0^{(3,5)}(x_3, y_5) \sim C_1^{(3,5)}\ln y_5 + \underbrace{C_2^{(3,5)} + \frac{C_1^{(3,5)}}{3}\ln x_3}_{\Delta A(x_3)}, \quad y_5 \to \infty. \qquad (4.44)$$

The constant terms with respect to y_5 can be identified as the asymptotic behavior of ΔA. The solution of the ODE (4.40) has a logarithmic term in the velocity profile.

The presence of the "ln"-terms has to be confirmed by matching with the boundary layer region (near the trailing edge), which will be done in next section.

In order to supplement the lower deck equation with correct asymptotic boundary condition for $y_5 \to \infty$, we need a condition which is satisfied by all linear combinations of the two admissible fundamental solutions, namely 1 (derivative of $h_2(\eta)$) and $\ln y_5$.

$$y_5 \Delta u_{0,y_5 y_5}^{(3,5)} + \Delta u_{0,y_5}^{(3,5)} = 0 \; ; \quad y_5 \to \infty \tag{4.45}$$

The asymptotic boundary condition (4.45) completes the formulation of lower deck equations system. The problem is well posed and the numerical calculation will be done in section 5.

4.5 Matching in trailing edge region

In order to complete the trailing edge problem, the detailed matching procedure for $x \to 0$ will be preformed. Special attention is paid to the appearance of the logarithmic terms and the presence of $x_3^{\frac{4}{3}}$-term in the displacement function ΔA. The matching procedure will confirm how different is the interaction mechanism of mixed convection case, than in all previously done investigations (inclinated plate Stewartson&Brown 1970, for instance). This strongly expressed non-symmetry is responsible for difficulties by numerical calculations (longer convergence process, "sensitivity" of numerical scheme in "zero region", etc...), which will be mentioned in section 5 (Numerics).

In the analysis particular attention will be given to the "genesis and resolution" of logarithm terms (equation 4.40), but also to the transition of the displacement function into the center wake line, which will enable correct implementation of triple deck concept to the global flow model with buoyancy parameter of order $\mathrm{Re}^{-\frac{1}{4}}$.

4.5.1 Triple deck structure

The existence of "ln-terms" (both in the longitudinal and perpendicular direction) was first observed in the lower deck region (for $x_3 \to -\infty$), so the matching procedure has to start here (inside of the lower deck).

Formulating the lower deck solution of velocity and temperature profiles in the main deck coordinates and applying the Van Dyke's matching principle, the behavior of $\Delta u, \Delta\theta, \Delta p$ inside of the main deck is obtained (details of matching routine are given in Appendix A.3)

Main deck (general solution):

$$\Delta u_0^{(3,4)}(x_3, y_4) \sim \Delta A(x_3) F_B''(y_4) + C_{B2}^{(3,4)} \ln \mathrm{Re} \; F_B''(y_4) + C_{B3}'(y_4) + ...,$$

$$\Delta \theta_0^{(3,4)}(x_3, y_4) \sim \Delta A(x_3) D_B'(y_4) + C_{D2}^{(3,4)} \ln \mathrm{Re} \; D_B'(y_4) + C_{D3}(y_4) + ...,$$

$$\Delta p_0^{(3,4)}(x_3, y_4) \sim \mathrm{Re}^{-\frac{1}{8}} C_{P1}^{(3,4)} x_3^{\frac{1}{3}} + ...,$$

where F_B, D_B are the Blasius similarity solution and temperature profile, respectively and the coefficients are given in Appendix A.3.

In contrast to equations (4.16 and 4.18) we have to add the terms $C_{B2}^{(3,4)} \ln \mathrm{Re}$ and $C_{D2}^{(3,4)} \ln \mathrm{Re}$. Matching the velocity with the lower deck (with similarity solution 4.40) we obtain:

$$\Delta A(x_3) \sim C_{\Delta A} \ln |x_3| \quad \text{for} \quad x_3 \to -\infty$$

and

$$C_{B3}'(y_4) \sim \ln y_4 \quad \text{for} \quad y_4 \to 0.$$

The same form is present by the temperature profile (the coefficients have to be adjusted).

Considering the profile of $\Delta u_0^{(3,4)}$ in $x_3 \to -\infty$ and rewritting it as:

$$\Delta u_0^{(3,4)}(x_3, y_4) \sim C_{\Delta A} \ln \underbrace{\frac{x_3}{\mathrm{Re}^{\frac{3}{8}}}}_{x_0} + C_{B3}'(y_4) + ...,$$

the matching procedure can be continued in the boundary layer. Terms obtained inside of the main deck have to be present in the boundary layer as well.

4.5.2 Boundary layer near trailing edge

Using the results obtained by the global flow (sub-section 3.3.2, the pressure perturbations), considerations in the main deck and combining them with governing equations (formulated as in A.2), the behavior in the vicinity of the trailing edge can be analyzed ($x_0 \to 0$, boundary-layer scale).

$$\triangle p_0^{(0,\,4)}(x_0, y_4) \sim C_{P1}^{(0,\,4)} |x_0|^{\frac{1}{3}} + \dots,$$

$$\triangle \psi_0^{(0,\,4)}(x_0, y_4) \sim \frac{C_1^{(3,\,5)}}{3 F_B''(0)} \ln |x_0| \; F_B'(y_4) + C_{B3}(y_4) + C_{B1}^{(0,\,4)} |x_0|^{\frac{1}{3}} + \dots,$$

$$\triangle \theta_0^{(0,\,4)}(x_0, y_4) \sim \frac{C_1^{(3,\,5)}}{3 F_B''(0)} \ln |x_0| \; D_B'(y_4) + C_{D3}(y_4) + C_{D1}^{(0,\,4)} |x_0|^{\frac{1}{3}} + \dots,$$

together with the symmetric terms (Ruban 1998):

$$\bar{\psi}^{(0,\,4)}(x_0, y_4) \sim F_B(y_4) + \frac{1}{2}\Big(F_B(y_4) - y_4 F_B'(y_4)\Big) x_0 + \dots,$$

$$\bar{\theta}^{(0,\,4)}(x_0, y_4) \sim D_B(y_4) - \frac{1}{2} x_0 D_B'(y_4) + \dots,$$

where F_B, D_B (and their derivatives) are similarity solutions at the plate (Blasius), $C_{B1}^{(0,\,4)}, C_{D1}^{(0,\,4)}$ are constants of less importance (next order terms) and $C_1^{(3,\,5)}$ is the value present in the equation (4.40), which has to be calculated numerically.

Functions $C_{B3}(y_4), C_{D3}(y_4) \sim y_4 \ln y_4$, $y_4 \to 0$ come from the matching procedure with viscid sub-layer and main deck.

All the coefficients are determined by the matching principle given in the appendix A.3 and A.4.

The terms present in the expansions for the stream function and temperature ($\triangle \psi_0^{(0,\,4)}, \triangle \theta_0^{(0,\,4)}$) arise as a consequence of sub-layer solution. The flow near $x_0 = 0$ can be decomposed into an inviscid and thin viscid sub-layer ($\sim x_0^{1/3}$), which has to fulfill the no-slip condition.

The sub-layer equations are solved in appendix A.4 and expanding the solutions for $\zeta \to \infty$ (similarity variable $\zeta = y_4/|x_0|^{\frac{1}{3}}$), the structure equivalent to the expansion of $\triangle \psi_0^{(0,\,4)}$ arises.

$$\triangle f^{(0,\,4)}(\zeta) \sim C_{f1}^{(0,\,4)} \zeta \ln \zeta + C_{f2}^{(0,\,4)} \zeta + C_{f3}^{(0,\,4)} + \dots;$$

$$\triangle f_\zeta^{(0,\,4)}(\zeta) \sim C_{f1}^{(0,\,4)} \ln \zeta + C_{f2}^{(0,\,4)} + \dots;$$

where $\triangle f^{(0,\,4)}$ is a scaled stream function.

The analogous solution exists for the temperature profile:

$$\triangle g^{(0,\,4)}(\zeta) \sim C_{f1}^{(0,\,4)} \ln \zeta + C_{d1}^{(0,\,4)} + \dots;$$

and now $\triangle g^{(0,\,4)}$ is a scaled temperature profile.

Using the Van Dyke's matching rule ($\zeta \to \infty$) the unknown coefficients inside of the sub-layer can be determined. For velocity holds:

$$\triangle f_\zeta^{(0,\,4)}(\zeta \to \infty) \sim \triangle u_0^{(0,\,4)}(x_0 \to 0, y_4 \to 0),$$

$$\Rightarrow \triangle \psi_{0,\zeta}^{(0,\,4)} = \triangle u_0^{(0,\,4)}(x_0 \to 0, y_4 \to 0) \sim C_{f1}^{(0,\,4)} \ln y_4 - \frac{C_{f1}^{(0,\,4)}}{3} \ln |x_0| + C_{f2}^{(0,\,4)} + \dots.$$

The final expansion is interesting since it delivers the coefficient $C_{f1}^{(0,\,4)} = f(C_1^{(3,\,5)})$ and also confirms the correct behavior of the functions C_{B3} and C_{D3}.

4.5.3 Matching the wake

The analysis presented in the previous sub-section can be applied in the near wake zone, but this procedure won't be given in details, since of greater importance is the transition of negative displacement function ΔA into the center wake line. However, the asymptotic behavior of all values will be shown in figure 4.4 . This transition should prove the correctness of matching the triple-deck structure and the global flow with the buoyancy parameter of order $\mathrm{Re}^{-\frac{1}{4}}$.

In order to make the transition "visable", the analysis has to start from the global flow (global coordinates), since the wake curvature has to be taken as well. For sake of convenience, the formulation of sums and difference won't be considered inside the main deck and the scaled distance from the center wake line will be introduced $(\bar{z})$.

$$\bar{z} = \mathrm{Re}^{\frac{1}{2}}(y_0 - y_{CW})$$

$$y_0 = y_{CW} + \bar{z}\,\mathrm{Re}^{-\frac{1}{2}}$$

$$y_4 = \bar{z} + \mathrm{Re}^{\frac{1}{4}}cx_0^{\frac{4}{3}}$$

$$y_{CW} \sim \mathrm{Re}^{-\frac{1}{4}}cx_0^{\frac{4}{3}}$$
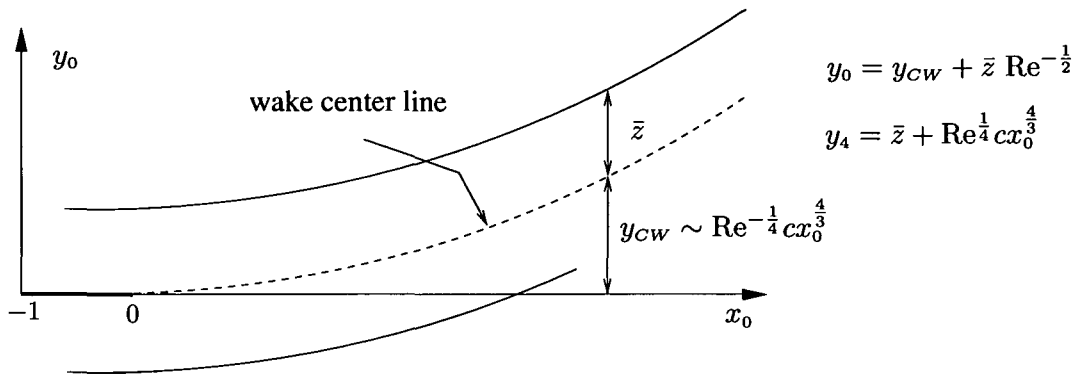
Figure 4.3 Scaled wake center line

The longitudinal velocity component will be reformulated in terms of the new coordinates $(x_0, \bar{z})$ and expanding it for $\mathrm{Re} \to \infty$ (applying Taylor two-parameter expansion), the following relationship is obtained:

$$u_W(x_0, \bar{z}) \sim u_W\left(x_0, y_4 - \mathrm{Re}^{\frac{1}{4}}\,c(\mathrm{Re}^{-\frac{3}{8}}\,x_3)^{\frac{4}{3}}\right),$$

$$\mathrm{Re} \to \infty \quad u_W(x_0, \bar{z}) \sim u_W(0, y_4) + u_{W,y_4}(0, y_4)\,\mathrm{Re}^{-\frac{1}{4}}\,x_3^{\frac{4}{3}} + \dots.$$

Finally, in the main deck we have:

$$u_+ - u_- = 2K\Delta u = 2\,\mathrm{Re}^{-\frac{1}{4}}(\Delta u_0 + \mathrm{Re}^{-\frac{1}{8}}\Delta u_1 + \dots) = 2\,\mathrm{Re}^{-\frac{1}{4}}\Delta A(x_0)\,F_B''(y_4) + \dots$$

$$\Rightarrow u_{W,y_4}(y_4)\,\mathrm{Re}^{-\frac{1}{4}}\,x_3^{\frac{4}{3}} = 2\,\mathrm{Re}^{-\frac{1}{4}}\,x_3^{\frac{4}{3}}\,C_{\Delta A1}\,F_B''(y_4)$$

$$\Rightarrow u_{W,y_4}(y_4) = 2\,C_{\Delta A1}\,F_B''(y_4) \;\; ; \;\; C_{\Delta A1}F_B''(0) = \frac{-3\sqrt{3}}{4} \quad \text{(cf. Sub-section 4.4.2)}$$

It is easy to note, that there is a smooth transition of the u-velocity componet from the main deck to the wake and the same can be said for temperature profile (by analogy). However, the attention will be restrected to velocities since they represent the stream function.

We conclude that, since the behavior of center wake line "agrees" with displacement function in the matching zone of main deck and the wake, the start assumption of implementation of the triple deck concepts into the global flow with the buoyancy parameter $K \sim O(\mathrm{Re}^{-\frac{1}{4}})$ is verified – "the assumption holds". Thus, the matching is completed.

In figures 4.4 and 4.5, the complete matching procedure is given.

y_0

Upper deck

Main deck

$x_3 = 0$

$$\Delta\psi^{(3,3)}(x_0, y_0) \sim C_{B0}^{(3,3)}(y_3) + C_{B1}^{(3,3)}(y_0) + Re^{-\frac{1}{8}} C_{B1}^{(3,3)}(y_0)|x_3|^{\frac{1}{3}} + \cdots$$

$$\Delta p^{(3,3)}(x_0, y_0) \sim C_{P0}^{(3,3)}(y_3) + Re^{-\frac{1}{8}} C_{P1}^{(3,3)}|x_3|^{\frac{1}{3}} + \cdots$$

$$\Delta u^{(3,4)}(x_3, y_4) \sim C_{\Delta A} \ln|x_3| F_B''(y_4) + C_{B2}^{(3,4)} \ln Re \, F_B''(y_4) + C_{B3}'(y_4) + \cdots$$

$$\Delta p^{(3,4)}(x_3, y_4) \sim Re^{-\frac{1}{8}} C_{P1}^{(3,4)} x_3^{\frac{1}{3}} + \cdots$$

$$\Delta\theta^{(3,4)}(x_3, y_4) \sim C_{\Delta A} \ln|x_3| D_B'(y_4) + C_{D2}^{(3,4)} \ln Re \, D_B'(y_4) + C_{D3}'(y_4) + \cdots$$

$y_4 \to 0$

$$\Delta u^{(3,5)} \sim C_1^{(3,5)} \ln y_4 - \frac{C_1^{(3,5)}}{3} \ln|x_3| - \frac{C_1^{(3,5)}}{8} \ln Re + C_2^{(3,5)} + \cdots$$

Lower deck

$y_5 \to \infty$

$$\Delta p^{(3,5)}(x_3, y_5) \sim -Re^{-\frac{3}{8}} 2a_s x_3^{\frac{5}{3}} + \cdots$$

$$\Delta u^{(3,5)}(x_3, y_5) \sim C_1^{(3,5)} \ln \frac{y_5}{|x_3|^{\frac{1}{3}}} + C_2^{(3,5)} + \cdots$$

$$\Delta\theta^{(3,5)}(x_3, y_5) \sim C_1^{(3,5)} \ln \frac{y_5}{|x_3|^{\frac{1}{3}}} + C_{d2}^{(3,5)} + \cdots$$

$x_3 \to -\infty$

$x_3 = Re^{\frac{3}{8}} x_0$

$x_3 \to -\infty$

Potential flow

Boundary layer

$x_0 \to 0^-$

$$\Delta\psi^{(0,0)}(x_0, y_0) \sim C_{B0}^{(0,0)}(y_0) + C_{B1}^{(0,0)}(y_0)|x_0|^{\frac{1}{3}} + \cdots$$

$$\Delta p^{(0,0)}(x_0, y_0) \sim C_{P0}^{(0,0)}(y_0) + C_{P1}^{(0,0)}|x_0|^{\frac{1}{3}} + \cdots$$

$$\Delta\psi^{(0,4)}(x_0, y_4) \sim \frac{C_1^{(3,5)}}{3F_B'(0)} \ln|x_0| F_B'(y_4) + C_{B3}(y_4) + \cdots$$

$$\Delta p^{(0,4)}(x_0, y_4) \sim C_{P1}^{(0,4)}|x_0|^{\frac{1}{3}} + \Delta p_0^{(0,4)}(0, y_4) + \cdots$$

$$\Delta\theta^{(0,4)}(x_0, y_4) \sim \frac{C_1^{(3,5)}}{3F_B''(0)} \ln|x_0| D_B'(y_4) + C_{D3}(y_4) + \cdots$$

$x_0 \to 0$

$y_4 \to 0$

$$\Delta u^{(0,4)} \sim C_{f1}^{(0,4)} \ln y_4 - \frac{C_{f1}^{(0,4)}}{3} \ln|x_0| + \cdots$$

$\zeta \to \infty$

$$\Delta p^{(0,4)}(x_3, y_5) \sim C_{P1}^{(0,4)} x_3^{\frac{1}{3}} + \cdots$$

$$\Delta f_\zeta^{(0,4)}(\zeta) \sim C_{f1}^{(0,4)} \ln\zeta + C_{f2}^{(0,4)} + \cdots$$

$$\Delta g^{(0,4)}(\zeta) \sim C_{f1}^{(0,4)} \ln\zeta + C_{d1}^{(0,4)} + \cdots$$

$y_4 = |x_0|^{\frac{1}{3}}\zeta$

Figure 4.4 Matching procedure in region $x_0 \to 0^-$ (schematic)
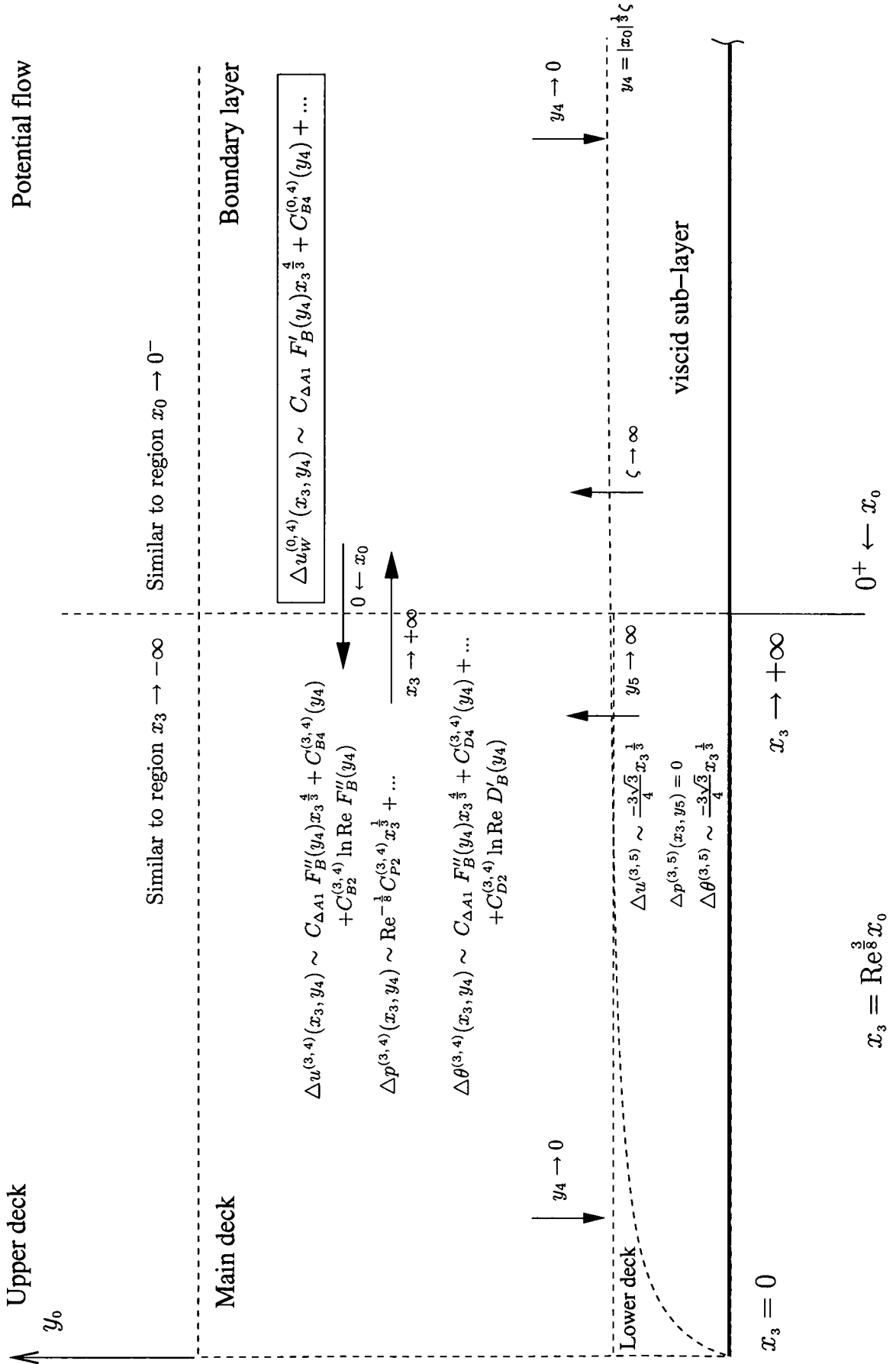
Figure 4.5 Matching procedure in region $x_0 \to 0^+$ (schematic)

5 Numerical results

5.1 Iteration scheme

The difficulties encounter by numerical methods for solving the boundary-layer equations in the vicinity of the trailing edge, or when the flow tends to separate from the body surface are well known. From 1969 (Stewartson) a number of methods for solving the interactive boundary-layer problems were developed and they have been categorized as direct, indirect or semi-inverse (Veldman 1981).

However, by all these methods (techniques with alternate treatment of viscous and inviscid region, cf. Veldman 1981), the numerical scheme provides a weak coupling of both areas. But near the trailing edges (also in separation zones), the interaction has a strong simultaneous character, i.e. there is no definitive solution-hierarchy between boundary layer and outer flow, usual for classical numerical schemes. The solution-hierarchy describes how the pressure distribution is calculated in the interactive boundary-layer problems. Following Veldman (1981) the hierarchy can be of direct and inverse type.

Thus in order to resolve the problem at the trailing edge, the numerical scheme has to be organized in a way to describe correctly the nature of the triple deck. In fact, the organization of the iteration technique appears to be crucial to its effectiveness.

Since the new (linear) triple deck problem is formulated at the trailing edge (equations 4.24-4.37), to avoid the numerical difficulties, it will be solved by so called "Quasi-simultaneous method" – developed by Veldman (1981).

This method prescribes a linear combination of the pressure and the displacement function (interaction law) as the boundary condition and then treats them as unknowns avoiding a fix numerical solution-hierarchy at the trailing edge. Namely, inside of triple deck the hierarchy changes its character form direct to inverse and again to direct. This change in hierarchy can be used to explain the convergence difficulties of direct and inverse methods. It is observed that numerical difficulties are present there, where numerical scheme differs from the asymptotic one.
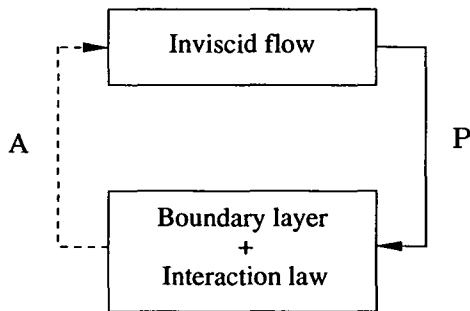
Quasi-simultaneous method

- no difficulties near separation points

- smooth transition between regions

- fast convergence process

- over-relaxation possible

Figure 5.1 Quasi-simultaneous method

In order to compute the solution of equation system (4.24-4.37), the iteration procedure shown in figure (5.1) will be slightly transformed, because of the peculiarities of the COLPAR code (Usher&Christiansen 1981). The iteration process is necessary since the problem has the elliptical/parabolic character and marching technique in this way can treat the triple deck problem.
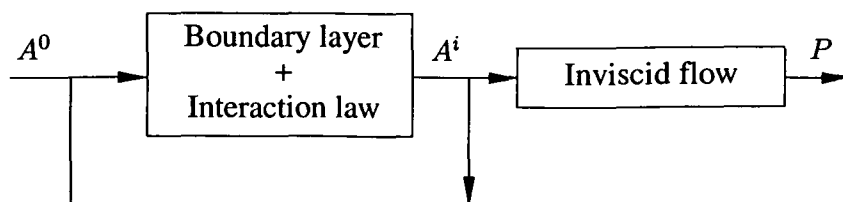

Figure 5.2 Scheme used by COLPAR

This numerical scheme prescribes the value of displacement function $A^{(0)}$, solves simultaneously boundary layer and interaction law and continues the iteration procedure until convergence is obtained. The pressure distribution will be calculated with final value of $A(x)$ using the interaction law.

The equations (44.24-4.37) are discretized in horizontal direction by a simple first order difference scheme. Thus at each grid point x_i a system of ordinary differential equations is obtained and solved by COLPAR.

5.2 Solution of lower deck equations

Using the argumentation given in chapter 4.4.3, the system (4.24-4.37) will be written in terms of stream functions and similarity variable:

$$(x_3^2 + 1)^{\frac{1}{3}} \bar\psi_1^{(3,5)}(x_3, \zeta), \quad (x_3^2 + 1)^{\frac{1}{6}} \triangle\psi_0^{(3,5)}(x_3, \zeta), \quad \zeta = \frac{y_5}{(x_3{}^2 + 1)^{\frac{1}{6}}}.$$

For further simplification of the calculation, the energy equation won't be considered, since the buoyancy influence is present in the interaction law. The momentum equation for the symmetric part is

$$\frac{1}{3}\frac{x_3}{\sqrt{x_3^2+1}} \ \bar\psi_{1,\zeta}^{(3,5)}\bar\psi_{1,\zeta}^{(3,5)} + \sqrt{x_3^2+1} \ \bar\psi_{1,\zeta}^{(3,5)}\bar\psi_{1,\zeta x_3}^{(3,5)} - \frac{2}{3}\frac{x_3}{\sqrt{x_3^2+1}} \ \bar\psi_{1}^{(3,5)}\bar\psi_{1,\zeta\zeta}^{(3,5)}$$

$$-\sqrt{x_3^2+1} \ \bar\psi_{1,x_3}^{(3,5)}\bar\psi_{1,\zeta\zeta}^{(3,5)} = -(x_3^2+1)^{\frac{1}{6}}\bar p_{1,x_3}^{(3,5)} + \bar\psi_{1,\zeta\zeta\zeta}^{(3,5)}. \tag{5.1}$$

For the anti-symmetric part we have:

$$\sqrt{x_3^2+1} \ \bar\psi_{1,\zeta}^{(3,5)}\triangle\psi_{0,\zeta x_3}^{(3,5)} + \frac{1}{3}\frac{x_3}{\sqrt{x_3^2+1}} \ \bar\psi_{1,\zeta}^{(3,5)}\triangle\psi_{0,\zeta}^{(3,5)} + \sqrt{x_3^2+1} \ \bar\psi_{1,\zeta x_3}^{(3,5)}\triangle\psi_{0,\zeta}^{(3,5)}$$

$$-\frac{2}{3}\frac{x_3}{\sqrt{x_3^2+1}} \ \bar\psi_{1}^{(3,5)}\triangle\psi_{0,\zeta\zeta}^{(3,5)} - \sqrt{x_3^2+1} \ \bar\psi_{1,x_3}^{(3,5)}\triangle\psi_{0,\zeta\zeta}^{(3,5)} - \frac{1}{3}\frac{x_3}{\sqrt{x_3^2+1}} \ \bar\psi_{1,\zeta\zeta}^{(3,5)}\triangle\psi_0^{(3,5)}$$

$$-\sqrt{x_3^2+1} \ \bar\psi_{1,\zeta\zeta}^{(3,5)}\triangle\psi_{0,x_3}^{(3,5)} = -(x_3^2+1)^{\frac{2}{6}}\triangle p_{1,x_3}^{(3,5)} + \triangle\psi_{0,\zeta\zeta\zeta}^{(3,5)}. \tag{5.2}$$

(The boundary conditions (4.36, 4.37) have to be written in a similar way)

Even though the system (5.1-5.2) seems more complicated than it use to be, this form is convenient to define the initial condition properly (region $x \to -\infty$). Using some simple algebra manipulation the similarity equation (4.40) can be obtained (Appendix A.5).

The problem is well posed and also reformulated in a way which will simplify the calculation, the solution of the lower deck equations are obtained and shown in following figures.
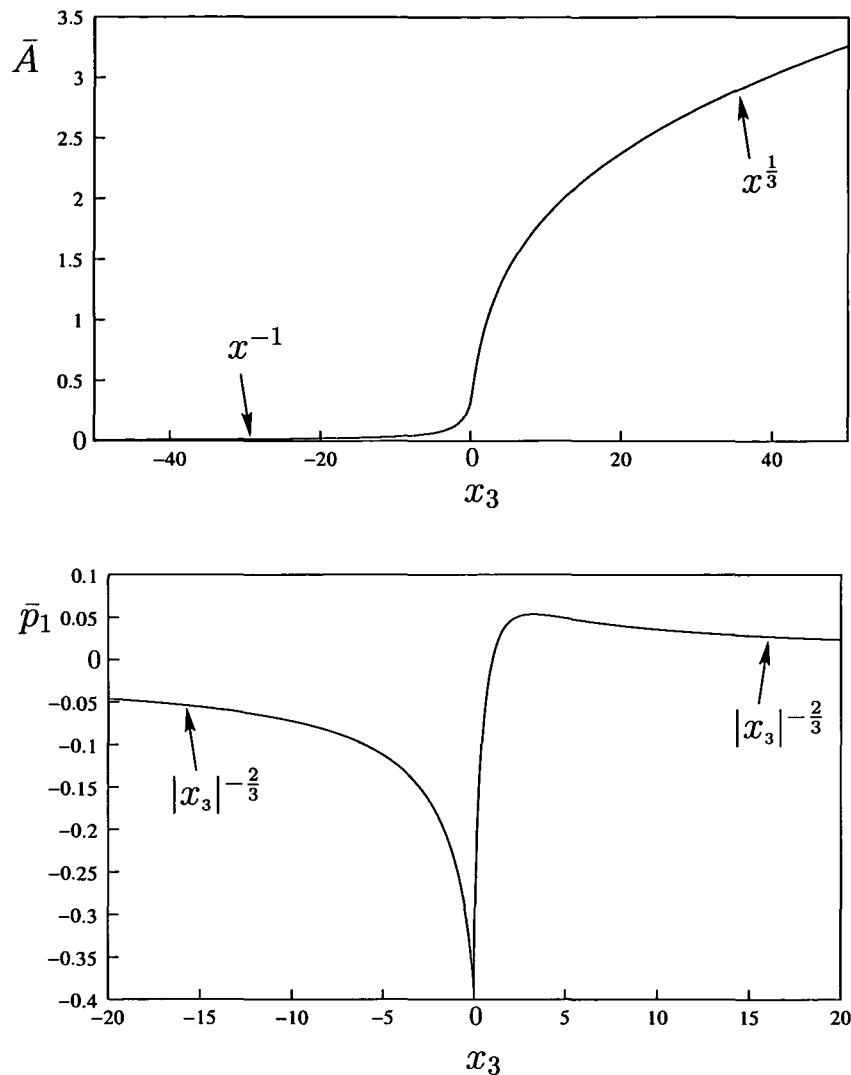
Figure 5.3 Stewartson solution of lower deck equations

The solutions in figure (5.3) concerning the symmetric problem, i.e. the Stewartson solution. The displacement function $\bar{A}(x_3)$ is growing slowly from zero in $x_3 \to -\infty$ region and the pressure is falling following the asymptotic behavior $\sim x_3^{-\frac{2}{3}}$. In the vicinity of the trailing edge the pressure reaches the finite negative value and the displacement function continues to grow. Then there is a region of the pressure recovery (and hence adverse pressure gradient) immediately after the trailing edge, before a pressure maximum is reached, after which pressure decreases to its asymptotic value (tends to zero). The displacement function reaches also its asymptotic behavior ($\sim x_3^{\frac{1}{3}}$).

The accuracy obtained by calculations is more than satisfying comparing with the solution of Melnik&Chow (1975).

On the other hand, solution of anti-symmetric case has several interesting properties predicted by section 4.4.
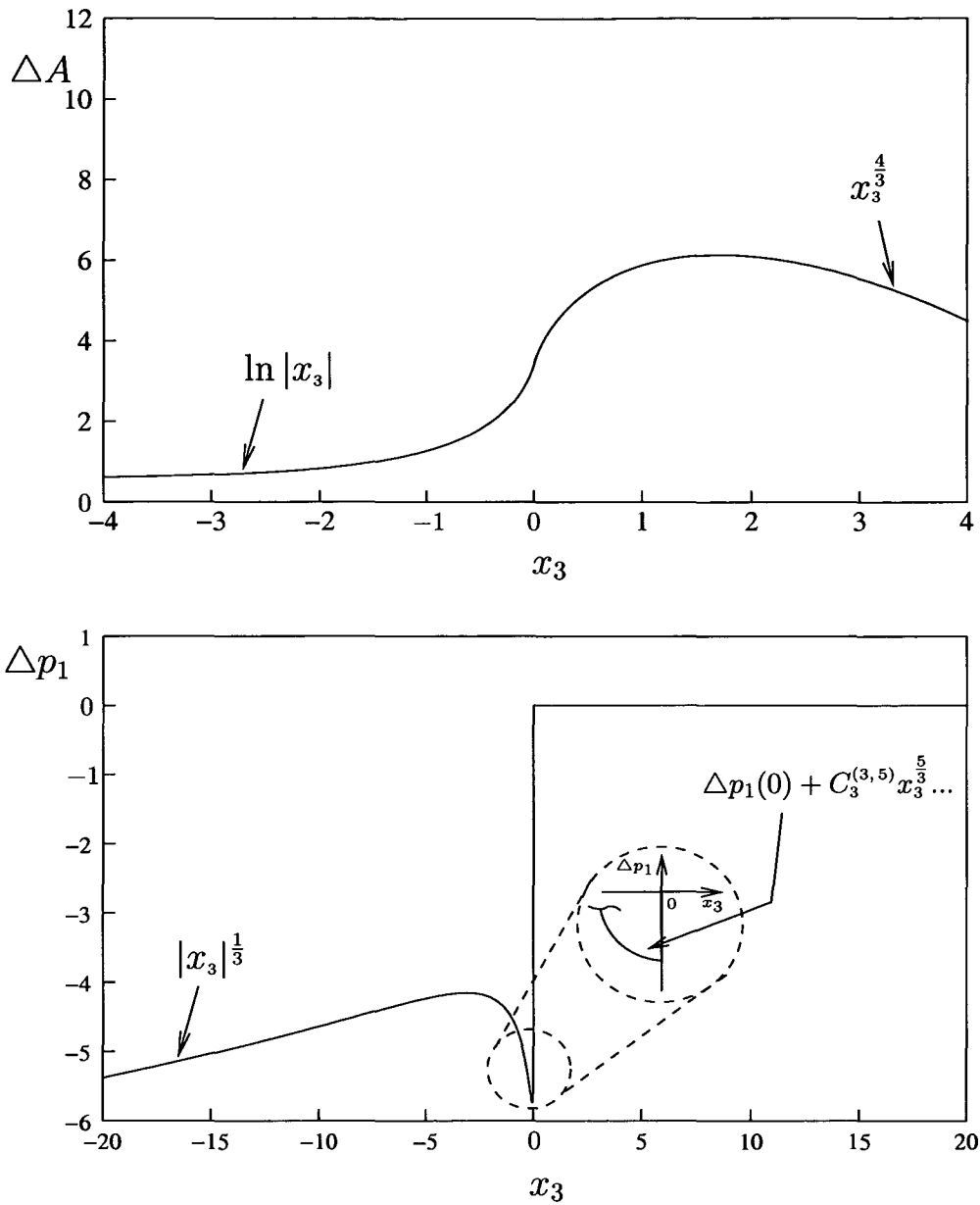
Figure 5.4 Solution of anti-symmetric problem
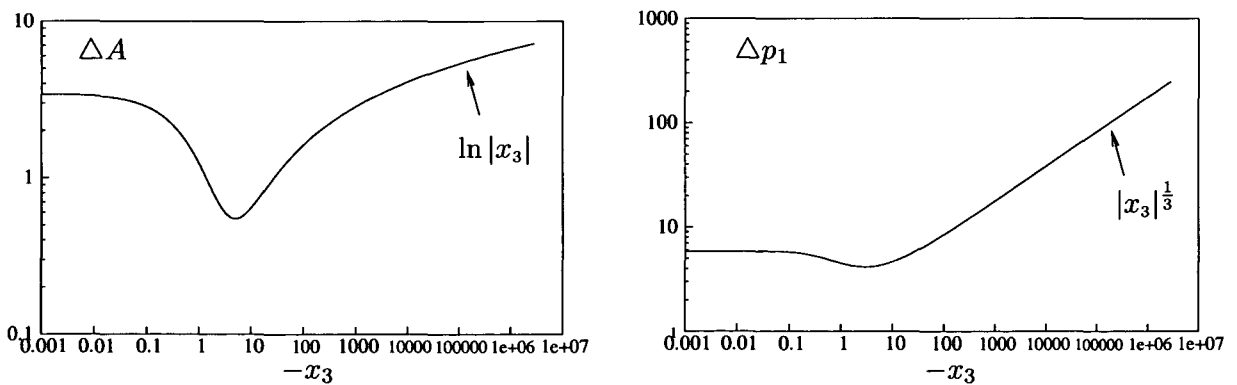
Figure 5.5 Solution of anti-symmetrical problem for $x_3 \to -\infty$

In figures 5.4 and 5.5 the values of the difference of the displacement functions and the pressure distribution are pointed out, namely as the values which directly characterize the in-

teraction mechanism. The velocity profiles are also calculated (the velocity differences in the longitudinal direction) and shown in figure 5.6.
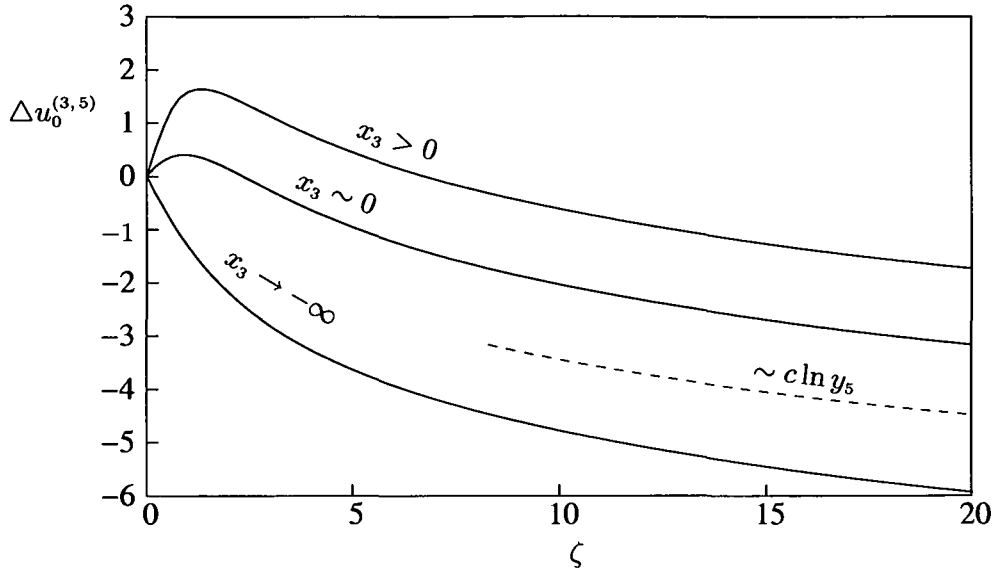
Figure 5.6 The velocity differences profiles

The solution of anti-symmetrical problem caused several numerical difficulties which will be briefly mentioned.

The problem is sensitive to any changes of the initial conditions (at $x_3 \to \pm\infty$), which made impact on the values near the trailing edge ($x_3 \to 0$). The non-uniform mesh was necessary "to reach" the correct asymptotic behavior, which could stable the solution in $x_3 \to 0$ region. The finite tangente is obtained by the pressure distribution at the trailing edge (figure 5.5).

The displacement function decreases from the infinity, since the asymptotic behavior is like $\sim \ln|x_3|$ (figure 5.6 shows this behavior in logarithmic scale for negative values of x_3).

In the vicinity of the trailing edge, it starts to grow, stays finite at the $x_3 = 0$ and finally it reaches the asymptotic value of $x_3^{4/3}$.

The shape of the displacement function in the $x_3 \approx 0$ region, i.e. the logarithmic singularity of displacement thickness derivative, signifies the peculiar "situation" at the trailing edge.

The pressure distribution causes this kind of behavior of ΔA, since it is discontinuous here. Far a way form the trailing edge, the pressure grows like $x_3^{\frac{1}{3}}$.

The figure 5.6 shows the velocity profiles in the vertical direction at specified x_3-values (at $x_3 \to -\infty$, $x_3 \sim 0$, $x_3 > 0$). It is important to note that the asymptotic behavior of solutions is like $\sim \ln y_4$, which confirms that the boundary condition (4.45) is satisfied. Recalling the analysis done in sub-section 4.4.3 the origin of the $\ln y_4$-term can be resolved. On the other hand, the boundary condition at the plate ($y_4 \to 0$) is also satisfied (4.36, 4.37).

We note to figures 5.4, 5.5 and 5.6 that boundray-layer flow is effected by buoyancy in a way that is here reported for the first time.

The pressure, in fact the pressure gradient, is adverse at the plate, it stays so up to trailing edge, where shortly obtains the favorable character. Note that we are dealing with pressure difference (difference between pressures at upper and lower side of the plate).

However, the pressure is discontinuous at $x_3 = 0$ and therefore the continuous transition in the wake is not possible on the length scale of lower deck. On the other hand, the displacement thickness is continuous at $x_3 = 0$

The appearance of the pressure discontinuity is not possible in the viscid flows, or in the Navier-Stokes equations at all. It is known that problems occurred by the pressure distribution

can be overcome by local analysis (vicinity of $x_3 = 0$). Introduction of new sub-layers will effect the equations in a sense that derivatives in x-direction will be of greater importance. Going further up to trailing edge, the equations will tend to complete Navier-Stokes (following Stewartson 1969., it is a region $O(\mathrm{Re}^{-\frac{6}{8}})$). Inside of this zone, all discontinuities have to be resolved, but analysis becomes to complicated. Thus, a try was done to find some other region which could overcome the problems by lower deck solution and still does not deal with complete Navier-Stokes equations.

In the present investigation two sub-layers will be introduced $O(\mathrm{Re}^{-\frac{4}{8}})$ and $O(\mathrm{Re}^{-\frac{5}{8}})$, which might be able to eliminate obtained discontinuity.

5.3 Local analysis of (3,5)-region near (0,0)-point

The numerical solution of the problem (5.1 and 5.2) pointed out that the pressure difference has a peculiar behavior at the trailing edge (the pressure is discontinues). This discontinuity from the lower deck exists in the main deck as well. However, in the upper deck $\Delta p_1^{(3,3)}$ is singular at $(0,0)$. Thus, using the analytic functions of a complex variable $z_3 = x_3 + iy_3$ we can guess the behavior of $\Delta p_1^{(3,3)}$. The complex velocity will be introduced:

$$w(z_3) = -u + iv = i \ln z_3$$

Now using the linearized Bernoulli equation $(\Delta p^{(3,3)}(x_3) = \Delta u^{(3,3)}(x_3, 0))$ the pressure can be interpreted as a real part of the analytical function $i \ln z_3$ evaluated on the real x-axis. Thus we have:

$$\Delta p_1^{(3,3)} = \Re\left\{ i(\ln|z_3| + i\arctan\frac{y_3}{x_3}) \right\}$$

After the evaluation, the pressure difference in the upper deck (close to zero) is given as:

$$\Delta p_1^{(3,3)}(0,0) = C_1^{(3,3)} \arctan\frac{y_3}{x_3} \tag{5.3}$$

The coefficient $C_1^{(3,3)}$ will be obtained after the matching procedure with main deck. In fact (5.3) will be used as a matching condition by the analysis of the additional sub-layers, where the pressure discontinuity might be resolved. This will be done in the next section.

On the other, in order to resolved the velocity field in the vicinity of the trailing edge the following strategy was performed.

Starting from the equations (4.32-4.35) and integrating the x-momentum equation (4.32) and continuity equation (4.34) in terms of x_3 we have:

$$\bar{u}_1^{(3,5)}\Delta u_{0,x_3}^{(3,5)} + \Delta v_0^{(3,5)}\bar{u}_{1,y_5}^{(3,5)} = -\Delta p_{1,x_3}^{(3,5)}, \quad \int\limits_{-\epsilon}^{+\epsilon} dx_3, \quad \epsilon \to 0$$

$$\Delta u_{0,x_3}^{(3,5)} + \Delta v_{0,y_5}^{(3,5)} = 0, \quad \int\limits_{-\epsilon}^{+\epsilon} dx_3,$$

$$\Rightarrow \bar{u}_1^{(3,5)}[\Delta u_0^{(3,5)}] + \Delta V \bar{u}_{1,y_5}^{(3,5)} = -[\Delta p_1^{(3,5)}], \tag{5.4}$$

$$[\Delta u_0^{(3,5)}] + \Delta V_{y_5} = 0, \tag{5.5}$$

where $\Delta V = \int\limits_{-\epsilon}^{+\epsilon} \Delta v_0^{(3,5)} dx_3$, $[\Delta u_0^{(3,5)}]$ is an integral over possible discontinuity (jump) in x-component of the velocity, $[\Delta p_1^{(3,5)}]$ is a pressure jump at the trailing edge.

Eliminating $[\Delta u_0^{(3,5)}]$ form the equation (5.4) using (5.5), the linear differential equation is derived

$$\Delta V_{1,y_5} - \frac{\bar{u}_{1,y_5}^{(3,5)}}{\bar{u}_1^{(3,5)}}\Delta V = \frac{1}{\bar{u}_1^{(3,5)}}[\Delta p_1^{(3,5)}], \tag{5.6}$$

with solution

$$\Delta V_1 = [\Delta p_1^{(3,5)}] \int\limits_{+\infty}^{y_5} \frac{\bar{u}_1^{(3,5)}(y_5)}{\bar{u}_1^{(3,5)}(\zeta)^2}d\zeta + \tilde{B}\bar{u}_1^{(3,5)}(y_5). \tag{5.7}$$

The coefficient $\tilde{B}$ has to be derived from the continuity equation (5.5) which yields:

$$[\Delta u_0^{(3,5)}] = -\Delta V_{1,y_5} = -\frac{\Delta p_1^{(3,5)}}{\bar{u}_1^{(3,5)}(y_5)} - \Big(\Delta p_1^{(3,5)} \int\limits_{+\infty}^{y_5} \frac{d\zeta}{\bar{u}_1^{(3,5)}(\zeta)^2} + \tilde{B}\Big)\bar{u}_{1,y_5}^{(3,5)}. \tag{5.8}$$

Considering the equation (5.8) in the limit of $y_5 \to \infty$ (matching with the main deck region), we conclude that $[\Delta u_0^{(3,5)}] = 0$. In fact, the horizontal velocity component does not have the discontinuity in the main deck, since the displacement function $\Delta A(x_3)$ is continues at the trailing edge. Following the main deck investigation $([\Delta u_0^{(3,5)}](x_3, y_4 \to 0) = \Delta A(x_3)F_B''(0) + ...)$ and keeping in mind that $\bar{u}_1^{(3,5)}(x_3, y_5 \to \infty) \sim y_5$, it turns out that $\tilde{B} = 0$. Thus we have

$$\Delta V_1 = [\Delta p_1^{(3,5)}] \int\limits_{+\infty}^{y_5} \frac{\bar{u}_1^{(3,5)}(y_5)}{\bar{u}_1^{(3,5)}(\zeta)^2}d\zeta \tag{5.9}$$

and

$$[\Delta u_0^{(3,5)}] = -\frac{\Delta p_1^{(3,5)}}{\bar{u}_1^{(3,5)}(y_5)} - \Big(\Delta p_1^{(3,5)} \int\limits_{+\infty}^{y_5} \frac{d\zeta}{\bar{u}_1^{(3,5)}(\zeta)^2}\Big)\bar{u}_{1,y_5}^{(3,5)}. \tag{5.10}$$

Further investigation of the $[\Delta u_0^{(3,5)}]$ in the vicinity of the trailing edge show again some interesting facts. Considering the $[\Delta u_0^{(3,5)}]$ in the limit of small vertical coordinate y_5 and using the integration by parts, we obtain a singularity in the velocity profile

$$[\Delta u_0^{(3,5)}](0) = -[\Delta p_1^{(3,5)}] \lim_{y_5 \to 0}\Big(\bar{u}_{1,y_5}^{(3,5)}(y_5) \int\limits_{+\infty}^{y_5} \frac{1}{\bar{u}_1^{(3,5)}(\zeta)} \frac{\bar{u}_{1,y_5,y_5}^{(3,5)}(\zeta)}{\bar{u}_{1,y_5}^{(3,5)}(\zeta)^2}\Big). \tag{5.11}$$

The singularity in the equation (5.11) was portended by the numerical solution of equations (5.1) and (5.2). The profile of the velocity differences in the vicinity of the trailing edge is given in figure 5.7.
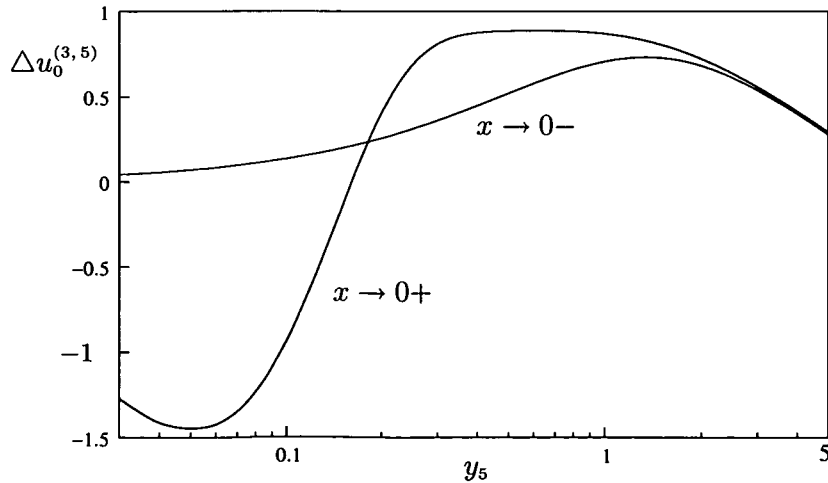
Figure 5.7 Velocity profile in the vicinity of the trailing edge

In the small region after the trailing edge the velocity has some "difficulties" to satisfy the boundary condition in the wake. This peculiar behavior indicates that a new sub-layer is needed in order to resolve the singularity obtained in (5.11). However these considerations are out of the scope of the present study. The disturbances shown in figure 5.7 vanish after a few calculation steps in the horizontal direction.

6 Additional sub-layers

The numerical results showed that $\Delta p_1^{(3,\,5)}$ has a discontinuity at $x_3 = 0$. Consequently the pressure perturbations in the main deck $\Delta p_1^{(3,\,4)}$ and in the upper deck $\Delta p_1^{(3,\,3)}$ are also discontinues. To resolve the discontinuity we will introduce additional sub-layers of the main and lower deck.
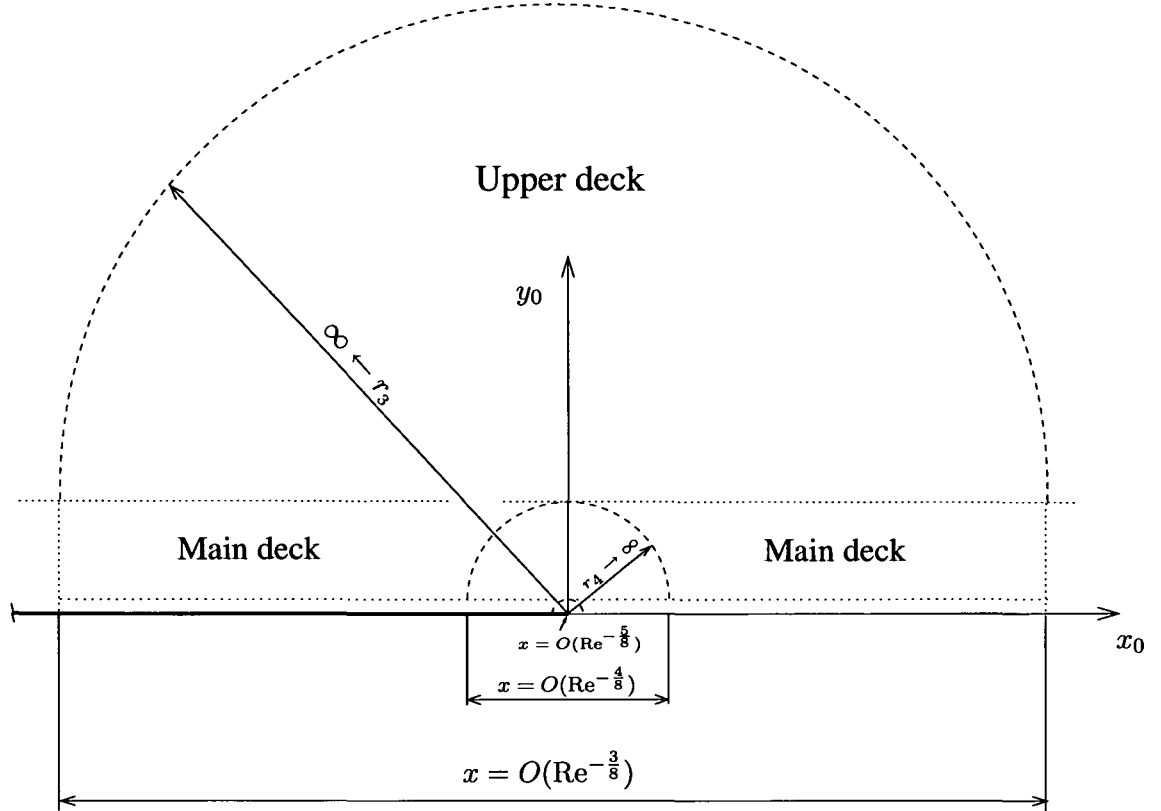
Figure 6.1 Additional layers

6.1 The (4,4)-region

It is well known that the solution of the "classical" trailing edge problem (Stewartson 1969, Messiter 1970) is continuous at the trailing edge. Thus the expansions of the symmetric part of the problem have the form:

$$\bar{u}^{(4,\,4)}(x_4, y_4) = \bar{u}_0^{(0,\,4)}(y_4) + \mathrm{Re}^{-\frac{1}{8}}\bar{u}_1^{(4,\,4)}(x_4, y_4) + ...,$$

$$\bar{v}^{(4,\,4)}(x_4, y_4) = \mathrm{Re}^{-\frac{2}{8}}\bar{v}_2^{(4,\,4)}(x_4, y_4) + ...,$$

$$\bar{p}^{(4,\,4)}(x_4, y_4) = \mathrm{Re}^{-\frac{2}{8}}\bar{p}_1^{(4,\,4)}(0) + \mathrm{Re}^{-\frac{3}{8}}\bar{p}_2^{(4,\,4)}(x_4, y_4) + ...,$$

$$\bar{\theta}^{(4,\,4)}(x_4, y_4) = \bar{\theta}_0^{(0,\,4)}(y_4) + \mathrm{Re}^{-\frac{1}{8}}\bar{\theta}_1^{(4,\,4)}(x_4, y_4) + ...$$

The leading order terms of the tangential component of the anti-symmetric part are also continues. The interaction pressure $\Delta p_1^{(3,\,4)}$ acts onto the first order terms, namely on $\Delta u_1^{(4,\,4)}$, $\Delta v_1^{(4,\,4)}$ and $\Delta \theta_1^{(4,\,4)}$. These effects have to be taken in to account, thus for the anti-symmetric part we have:

$$\Delta u^{(4,\,4)}(x_4, y_4) = \frac{C_1^{(3,\,5)}}{F_B''(0)}F_B''(y_4)\ln\mathrm{Re} + \Delta u_0^{(4,\,4)}(y_4) + \mathrm{Re}^{-\frac{1}{8}}\Delta u_1^{(4,\,4)}(x_4, y_4) + ...,$$

$$\Delta v^{(4,4)}(x_4, y_4) = \Delta v_0^{(4,4)}(y_4) + \mathrm{Re}^{-\frac{1}{8}} \Delta v_1^{(4,4)}(x_4, y_4) + ...,$$

$$\Delta p^{(4,4)}(x_4, y_4) = \Delta p_0^{(4,4)}(y_4) + \mathrm{Re}^{-\frac{1}{8}} \Delta p_1^{(4,4)}(x_4, y_4) + ...,$$

$$\Delta \theta^{(4,4)}(x_4, y_4) = \frac{C_1^{(3,5)}}{F_B''(0)} D_B'(y_4) \ln \mathrm{Re} + \Delta \theta_0^{(4,4)}(y_4) + \mathrm{Re}^{-\frac{1}{8}} \Delta \theta_1^{(4,4)}(x_4, y_4) + ...$$

Using these expansions the problem for the leading order terms is:

$$\bar{u}_0^{(0,4)}(y_4) \Delta u_{1,x_4}^{(4,4)} + \Delta v_1^{(4,4)} \bar{u}_{0,y_4}^{(0,4)} = -\Delta p_{1,x_4}^{(4,4)}, \tag{6.1}$$

$$\bar{u}_0^{(0,4)}(y_4) \Delta v_{1,x_4}^{(4,4)} = -\Delta p_{1,y_4}^{(4,4)} + \bar{\theta}_1^{(4,4)}, \tag{6.2}$$

$$\Delta u_{1,x_4}^{(4,4)} + \Delta v_{1,y_4}^{(4,4)} = 0, \tag{6.3}$$

$$\bar{u}_0^{(0,4)}(y_4) \Delta \theta_{1,x_4}^{(4,4)} + \Delta v_1^{(4,4)} \bar{\theta}_{0,y_4}^{(0,4)} = 0. \tag{6.4}$$

Subjected to the boundary conditions:

$$\Delta v_1^{(4,4)}(x_4, y_4 \to 0) = 0, \quad \Delta p_1^{(4,4)}(x_4, y_4 \to 0) = \Delta p_1^{(3,5)}(0-) \ ; \qquad x < 0, \tag{6.5}$$
$$\Delta \theta_1^{(4,4)}(x_4, y_4 \to 0) = 0$$

$$\Delta u_1^{(4,4)}(x_4, y_4 \to 0) = 0, \quad \Delta v_1^{(4,4)}(x_4, y_4 \to 0) = 0, \quad \Delta p_1^{(4,4)}(x_4, y_4 \to 0) = 0 \ ; \ x > 0. \tag{6.6}$$
$$\Delta \theta_1^{(4,4)}(x_4, y_4 \to 0) = 0.$$

The flow described by the equations (6.1-6.4) is inviscid, but in contrast to the main deck the y-momentum equation is not degenerate. Thus, the boundary conditions have some extra peculiarities which will be explained.

We note that boundary condition $\Delta p_1^{(4,4)} = \Delta p_1^{(3,5)}(0-)$ is all but trivial. Since $\Delta u_1^{(4,4)}$ in general will not satisfy the no-slip condition at the plate, a viscous sub-layer $(\mathrm{Re}^{\frac{4}{8}}, \mathrm{Re}^{\frac{6}{8}})$ is expected. The pressure in this viscous region is again determind by an interaction process. However, it turns out that this interaction process permits only the trivial solution $\Delta p_1^{(4,4)} = const = \Delta p_1^{(3,5)}(0-)$.

Matching the (4,4)-region with the upper deck (following results obtained in the sub-section 5.4) yields:

$$\lim_{r_4 \to \infty} \Delta p_1^{(4,4)}(r_4, \varphi) = \lim_{r_3 \to 0} \Delta p_1^{(3,3)}(r_3, \varphi) = \frac{\varphi}{\pi} \Delta p_1^{(3,5)}(0-), \tag{6.7}$$

where $r_4 = \sqrt{x_4^2 + y_4^2}$, $r_3 = \sqrt{x_3^2 + y_3^2}$, $\varphi = \arctan \frac{y}{x}$ and

$$[\Delta p] = \Delta p_1^{(3,5)}(0+) - \Delta p_1^{(3,5)}(0-) = -\Delta p_1^{(3,5)}(0-)$$

is a value of the pressure jump occurring in the lower deck. The matching zone will be illustrated in figure (6.2).
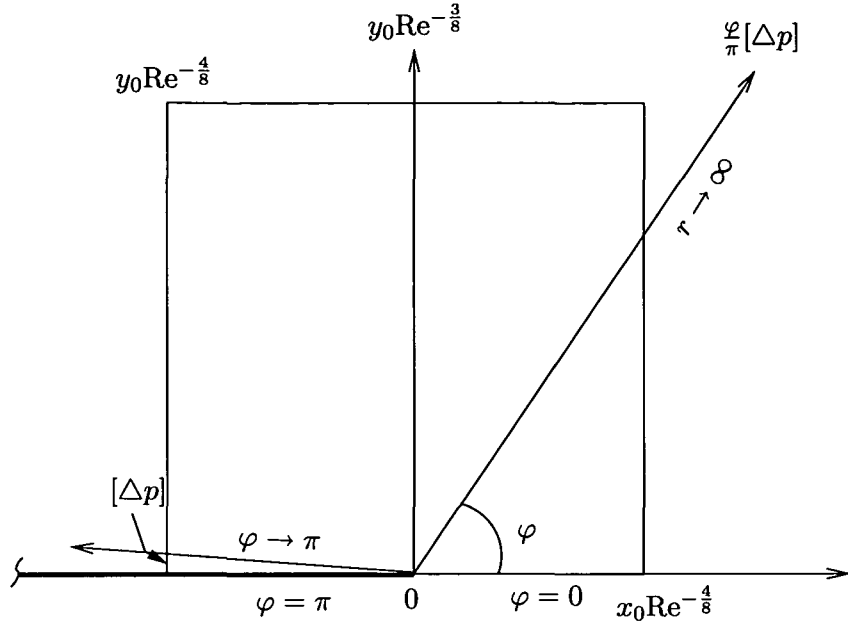
Figure 6.2 Matching of $O(\mathrm{Re}^{-\frac{4}{8}})$ zone

Taking the x-derivative of (6.1) and adding it to the y-derivative of (6.2) and using (6.2) to eliminate $\triangle v_1^{(4,\,4)}$, we obtain the pressure equation:

$$2\,\bar{u}_{0,y_4}^{(0,\,4)}\Big[\,\bar{\theta}_1^{(4,\,4)}(y_4) - \triangle p_{1,y_4}^{(4,\,4)}\Big] = \bar{u}_0^{(0,\,4)}(y_4)\Big[\bar{\theta}_{1,y_4}^{(4,\,4)} - \triangle p_{1,x_4x_4}^{(4,\,4)} - \triangle p_{1,y_4y_4}^{(4,\,4)}\Big] \tag{6.8}$$

It is an an elliptic equation and for $y_4 \to \infty$ (using: $\bar{u}_0^{(0,\,4)}(y_4 \to \infty) = 1$ and $\bar{\theta}_1^{(0,\,4)}(y_4 \to \infty) = 0$), it reduces to the potential equation (Laplace equation).

To analyze the local behavior at the $x_4 = y_4 = 0$ we use the polar coordinates (r, φ) and rewrite the equation (6.8) as

$$-2\Big(\bar{\theta}_1^{(4,\,4)}(y_4) - \triangle p_{1,r}^{(4,\,4)}\sin\varphi + \frac{\cos\varphi}{r}\triangle p_{1,\varphi}^{(4,\,4)}\Big) = -r\sin\varphi\Big(\triangle p_{1,rr}^{(4,\,4)} + \frac{1}{r}\triangle p_{1,r}^{(4,\,4)} + \frac{1}{r^2}\triangle p_{1,\varphi\varphi}^{(4,\,4)}\Big). \tag{6.9}$$

Considering that r is small, assuming that derivatives to the respect to r are uniformly bounded, we obtain the following ODE:

$$\sin\varphi\,\triangle p_{1,\varphi\varphi}^{(4,\,4)} - 2\cos\varphi\,\triangle p_{1,\varphi}^{(4,\,4)} = 0, \tag{6.10}$$

with the solution

$$\triangle p_1^{(4,\,4)}(r \to 0, \varphi) = -C_0^{(4,\,4)}\Big[\frac{1}{2}\varphi - \frac{1}{4}\sin 2\varphi\Big], \tag{6.11}$$

satisfying the boundary conditions (6.5) and (6.6).

The solution (6.11) shows again the discontinuous behavior of the pressure in the vicinity of the trailing edge.

Introduction of sub-layer (4,4) couldn't resolve the discontinues behavior of the pressure at $x_4, y_4 = 0$, but reduced it to a single point. Thus, the continuation of local investigation will be done in the region (5,5).

6.2 Numerical solution of (4,4)-region

The pressure equation (6.8) is rewritten as

$$\Delta p_{1,x_4 x_4}^{(4,4)} + \Delta p_{1,y_4 y_4}^{(4,4)} - 2\frac{\bar{u}_{0,y_4}^{(0,4)}}{\bar{u}_0^{(0,4)}}\Delta p_{1,y_4}^{(4,4)} = \bar{\theta}_{1,y_4}^{(4,4)} - 2\bar{\theta}_1^{(4,4)}. \tag{6.12}$$

We decompose the solution of the linear elliptic partial equation (6.12) into a particular solution and a solution of the homogenous problem:

$$\Delta p_1^{(4,4)}(x_4,y_4) = \underbrace{\bar{A}(0)\bar{\theta}_0^{(0,4)}(y_4)}_{\text{particular solut.}} + \underbrace{\hat{p}(x_4,y_4)}_{\text{homog. solut.}} , \tag{6.13}$$

$$\Rightarrow \hat{p}_{x_4 x_4} + \hat{p}_{y_4 y_4} - 2\frac{\bar{u}_{0,y_4}^{(0,4)}}{\bar{u}_0^{(0,4)}}\hat{p}_{y_4} = 0 \tag{6.14}$$

With some small corrections due to transformation (6.13), the boundary conditions (6.5) and (6.6) are also valid for equation (6.14):

$$\hat{p}(x_4,0) = -\bar{A}(0)\bar{\theta}_0^{(0,4)}(0) ; \quad x_4 > 0, \tag{6.15}$$

$$\hat{p}(x_4,0) = \Delta p_1^{(3,5)}(0-) - \bar{A}(0)\bar{\theta}_0^{(0,4)}(0) ; \quad x_4 < 0. \tag{6.16}$$

Following the transformation (6.13), the matching condition (according to equation (6.7)) has the form

$$\hat{p}(r \to \infty, \varphi) = \frac{\Delta p_1^{(3,5)}(0-)}{\pi} - \bar{A}(0)\bar{\theta}_0^{(0,4)}(0) , \quad \varphi \in [0,\pi]. \tag{6.17}$$
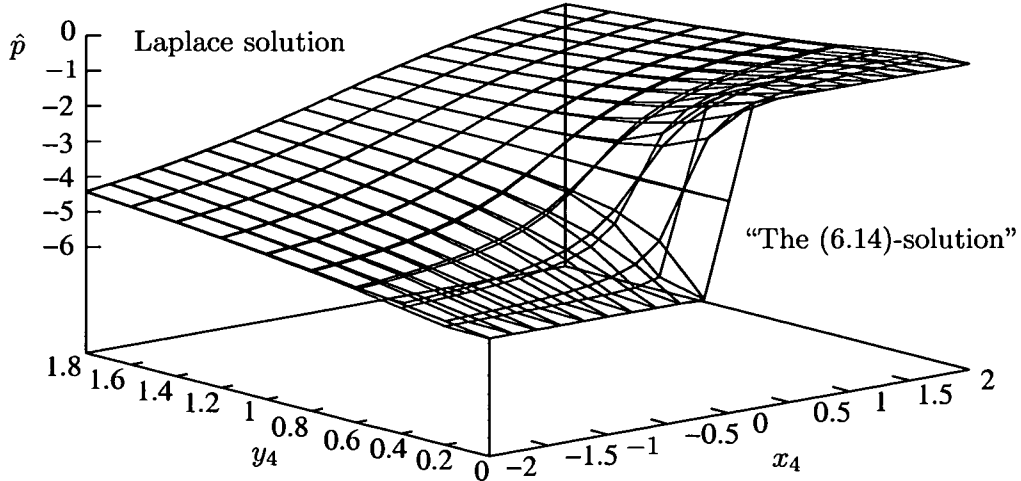
Figure 6.3 The pressure distribution

The solution of equation (6.14) is shown in figure 6.3 and compared with the Laplace equation, which serves as asymptote for $r \to \infty$ of equation (6.14).

Near the trailing edge $(x_4, y_4 \sim 0)$ the difference between the (6.14)-solution and the Laplace solution is expressed. In the region of "infinity" $(x_4, y_4 \to \infty)$ the "transition" to the Laplace solution occurs.

6.3 The (5,5)-region

The local analysis of (5,5)-region follows the same lines as the previous analysis of the (4,4)-region, thus for the symmetric part there are:

$$\bar{u}^{(5,5)}(x_5, y_5) = \mathrm{Re}^{-\frac{1}{8}} \bar{u}_1^{(5,5)}(y_5) + ...,$$

$$\bar{v}^{(5,5)}(x_5, y_5) = \mathrm{Re}^{-\frac{3}{8}} \bar{v}_2^{(5,5)}(x_5, y_5) + ...,$$

$$\bar{p}^{(5,5)}(x_5, y_5) = \mathrm{Re}^{-\frac{2}{8}} \bar{p}_1^{(5,5)}(0) + ...,$$

$$\bar{\theta}^{(5,5)}(x_5, y_5) = \bar{\theta}_1^{(5,5)}(y_5) + ...$$

and for the anti-symmetric part:

$$\triangle u^{(5,5)}(x_5, y_5) = \triangle u_0^{(5,5)}(x_5, y_5) + \mathrm{Re}^{-\frac{1}{8}} \triangle u_1^{(5,5)}(x_5, y_5) + ...,$$

$$\triangle v^{(5,5)}(x_5, y_5) = \triangle v_0^{(5,5)}(x_5, y_5) + \mathrm{Re}^{-\frac{1}{8}} \triangle v_1^{(5,5)}(x_5, y_5) + ...,$$

$$\triangle p^{(5,5)}(x_5, y_5) = \triangle p_0^{(5,5)}(0) + \mathrm{Re}^{-\frac{1}{8}} \triangle p_1^{(5,5)}(x_5, y_5) + ...,$$

$$\triangle \theta^{(5,5)}(x_5, y_5) = \triangle \theta_0^{(5,5)}(x_5, y_5) + \mathrm{Re}^{-\frac{1}{8}} \triangle \theta_1^{(5,5)}(x_5, y_5) + ...$$

Using these expansions the problem can be formulated as:

$$\bar{u}_1^{(5,5)}(y_5)\triangle u_{0,x_5}^{(5,5)} + \triangle v_0^{(5,5)}\bar{u}_{1,y_5}^{(5,5)} = -\triangle p_{1,x_5}^{(5,5)}, \tag{6.18}$$

$$\bar{u}_1^{(5,5)}(y_5)\triangle v_{0,x_5}^{(5,5)} = -\triangle p_{1,y_5}^{(5,5)}, \tag{6.19}$$

$$\triangle u_{0,x_5}^{(5,5)} + \triangle v_{0,y_5}^{(5,5)} = 0, \tag{6.20}$$

$$\bar{u}_1^{(5,5)}(y_5)\triangle \theta_{0,x_5}^{(5,5)} + \triangle v_0^{(5,5)}\bar{\theta}_{1,y_5}^{(5,5)} = 0, \tag{6.21}$$

subjected to the boundary conditions:

$$\triangle v_0^{(5,5)}(x_5, 0) = 0, \quad \triangle \theta_0^{(5,5)}(x_5, 0) = 0, \quad \triangle p_1^{(5,5)}(x_5, 0) = \triangle p_1^{(4,4)}(0-) \quad ; x < 0, \tag{6.22}$$

$$\triangle u_0^{(5,5)}(x_5, 0) = 0, \quad \triangle v_0^{(5,5)}(x_5, 0) = 0, \quad \triangle p_1^{(5,5)}(x_5, 0) = 0 \quad ; \qquad x > 0, \tag{6.23}$$

$$\triangle \theta_0^{(5,5)}(x_5, 0) = 0.$$

As in sub-section 6.1 we obtained an inviscid flow with the same boundary condition at $y = 0$. These conditions have to be supplemented by the matching condition to the (4,4)-region. Applying the same arguments as in sub-section 6.1 the condition $\triangle p_1^{(5,5)}(x_5, 0) = \triangle p_1^{(4,4)}(0-) = const$ can be derived. Thus the matching condition to (4,4)-region is given by the equation (6.10) and it is illustrated in figure 6.4.
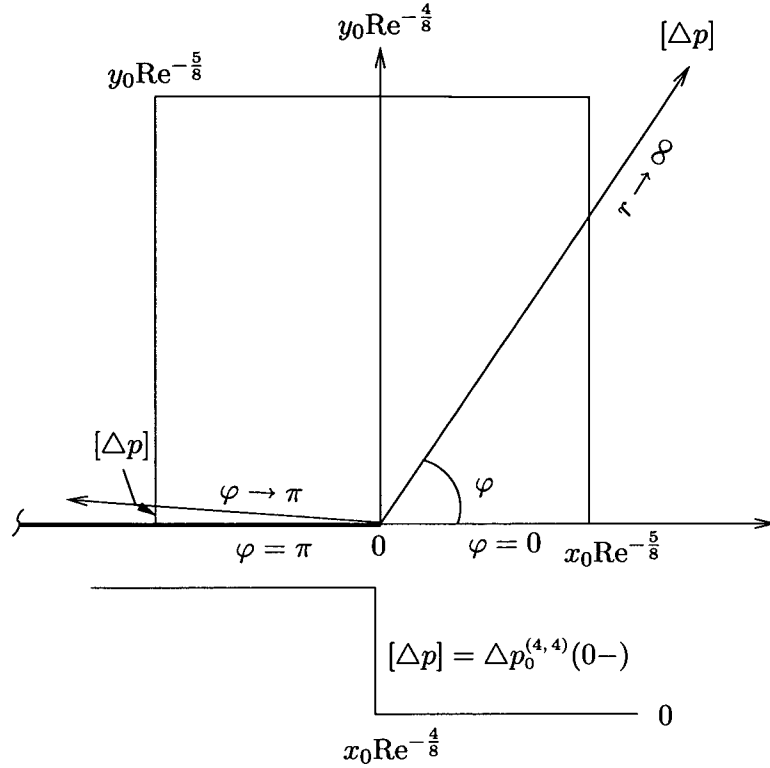
Figure 6.4 Matching condition for zone $O(\mathrm{Re}^{-\frac{5}{8}})$

Taking the x-derivative of equation (6.17) and y-derivative of (6.18) and manipulating them (cf. sub-section 6.2), the form suitable for numerical calculation is obtained:

$$2\ \bar{u}^{(5,5)}_{1,y_5}\Delta p^{(5,5)}_{1,y_5} = \bar{u}^{(5,5)}_1(y_5)\left[\Delta p^{(5,5)}_{0,x_5x_5} + \Delta p^{(5,5)}_{0,y_5y_5}\right].\tag{6.24}$$

Similar to the region (4,4), the equation (6.24) can be further transformed using the polar coordinates (r,φ), keeping in mind now that $\bar{u}^{(5,5)}_1$ is the Stewartson solution (evaluated at $x = 0-$)

$$\sin\varphi\ \Delta p^{(5,5)}_{1,\varphi\varphi} - 2\cos\varphi\ \Delta p^{(5,5)}_{1,\varphi} = 0.\tag{6.25}$$

The local behavior is given by

$$\Delta p^{(5,5)}_1(r\to 0,\varphi) = -C^{(4,4)}_0\left[\frac{1}{2}\varphi - \frac{1}{4}\sin 2\varphi\right].\tag{6.26}$$

As it was expected, the pressure discontinuity is reduced to a single point.

The equation (6.24) won't be numerical analyzed (solution of the equation 6.13 is available), however the matching of the (5,5)-region is preformed.

6.4 Matching the velocity components

To conclude the analysis we discuss the matching of the velocity components. Special care is taken of the logarithmic terms. We remark that the vertical velocity component $\Delta v^{(3,4)}_0$ (approaching $x_3 \to 0$) has a logarithmic singularity.

6.4.1 Matching of (3,4),(4,4)-regions

The considerations start from (3,4)-region, namely form the main deck (cf. sub-sections 4.3 and 4.4.2), where the vertical velocity component is written as

$$\triangle v^{(3,\,4)} = \mathrm{Re}^{-\frac{1}{8}} \, \triangle A'(x_3) \, F'_B(y_4) + \dots = \mathrm{Re}^{-\frac{1}{8}} \, \ln x_3 \, F'_B(y_4) + \dots.$$

Applying the Van Dyke's matching principle, i.e. matching the main deck solution with (4,4)-region, we conclude that the logarithmic terms present in the main deck expansions "appear" in the (4,4)-region just as next order terms ($\sim O(\mathrm{Re}^{-\frac{1}{8}})$):

$$\triangle v^{(3,\,4)}(x_3 \to 0, y_4) = \triangle v^{(4,\,4)}(x_4 \to \infty, y_4),$$

$$\triangle v^{(3,\,4)}(x_4 \mathrm{Re}^{-\frac{1}{8}}, y_4) = \mathrm{Re}^{-\frac{1}{8}} \left(-\frac{1}{8} \ln \mathrm{Re} + \ln x_4 \right) F'_B(y_4) + \dots.$$

In the (4,4)-region we have

$$\triangle v^{(4,\,4)}(x_4 \to \infty, y_4) = \triangle v_0^{(4,\,4)}(y_4) + \mathrm{Re}^{-\frac{1}{8}} \left(b_1^{(4,\,4)} \ln \mathrm{Re} + b_2^{(4,\,4)} \ln x_4 \right) + \dots.$$

thus it is obvious that $\triangle v_0^{(4,\,4)}$ is not affected by the ln-terms.

6.4.2 Matching of (4,4),(5,5)-regions

Recalling the asymptotic expansions of the velocity in the (5,5)-region and considering the limit $y_4 \to 0$ and $y_5 \to \infty$ (matching the (4,4) and (5,5)-region now) we can conclude again, that the singular (ln)-terms do not influence the leading order terms of the velocity ($\triangle v_0^{(5,\,5)}$).

$$\triangle v^{(5,\,5)}(x_5, y_5 \to \infty) = \triangle v_0^{(5,\,5)}(x_5, y_5 \to \infty) + \mathrm{Re}^{-\frac{1}{8}} \triangle v_1^{(5,\,5)}(x_5, y_5 \to \infty) + \dots,$$

$$\triangle v^{(4,\,4)}(x_4, y_4 \to 0) = \triangle v_0^{(4,\,4)}(y_4 \to 0) + \mathrm{Re}^{-\frac{1}{8}} \left(b_1^{(4,\,4)} \ln \mathrm{Re} + b_2^{(4,\,4)} \ln x_4 \right) + \dots.$$

The further investigations of (5,5)-region are out of the scope of the present study.

7   Conclusions

The present work describes the steady, laminar flow around a heated finite plate for large Reynolds numbers and weak buoyancy effects. Eventhough the problem of the flow around a finite plate (with or without temperature difference) has been an interesting theme for a long time (starting with Stewartson 1969), this study is one of few reported investigations dealing with a complete flow field analysis. The flow field was originally decomposed into a four regions, namely potential flow, boundary layer at the plate, wake and trailing edge. However at the trailing edge additional zones (sub-layers) had to be involved as well. All these regions and sub-regions have been analyzed in detail.

The resolving of the mixed convection flow past a horizontal plate has brought several interesting facts, concerning the global flow (potential flow and boundary layer in the wake and at the plate) and the trailing edge properties as well. In contrast to all previous studies (Stewartson&Brown 1970, Melnik&Chow 1975, Schneider 2005, etc...), the present problem is characterized by a strong flow unsymmetry, resulting as a consequence of the buoyancy-acting on one hand and the inclination angle of the free stream on an other.

Their influence on the global flow has been considered in terms of limit $K \to 0$, $\mathrm{Re} \to \infty$, $\phi \to 0$. The investigation showed that the buoyancy parameter K and the inclination angle of the free stream ϕ have to be of comparable size $K \sim \phi \sim O(\mathrm{Re}^{-\frac{1}{4}})$, in order to obtain an meaningfull solution for the global flow. For the analysis of the flow near the trailing edge the tripe deck concept (Stewartson 1969, Messiter 1970) can be applied and the local solution can be matched to the outer flow without any difficulties.

The most interesting new feature concerning the global flow is the interaction mechanism between the wake and the outer (potential) flow. Thus we are dealing with a coupled problem, which affects the boundary-layer flow at the plate as well.

Two coupling parameters, namely λ and κ (reduced inclination parameter and reduced buoyancy parameter, respectively), have been defined to characterize the global flow field. The first one is a measure for the velocity overshoot in the far wake region and the second one, measures the influence of the hydrostatic pressure perturbations onto the potential flow around the plate. We note that solution have been found only for $\lambda > 0$ and κ less than a critical value (depending on λ, here $\lambda = 1$).

The critical value of κ is near 0.915 and all values larger than the critical one cause the breakdown of proposed numerical solution scheme. The reason for the difficulties by the marching technique (which we are using by the boundary-layer equation solution), remains an "open question".

- Is it a small region of reversed flow (indicated by the longitudinal velocity componet at the center line of the wake)?
  The marching technique does not work in this case!

- Is it a bifurcation point?

- Are there locally multiple solutions?

On the other hand for $\kappa > 0$ the buoyancy effects are not limited to the boundary layer and the wake only, where it leads to the velocity overshoot. The potential flow is then markedly influenced by buoyancy.

The potential flow correction (induced by the hydrostatic pressure difference across the wake) was determined by the vortex strength distribution in the wake and at the plate. The difficulties with unbounded velocities induced by the vortex sheet are circumvented by the positive reduced inclination parameter ($\lambda > 0$). It guarantees that the vortex strength will decay for $x \to \infty$. As we already remarked, Schneider (2005) used a different concept to handle the matter (he

neglected the inclination of the center line of the wake and introduced the horizontal walls parallel to the plate).

Further, the buoyancy-induced potential flow influences the lift forces and in the present case it reduces them and for sufficiently large values of κ it reverses them. The same phenomenon was reported in Schneider (2005).

The local analysis of the trailing edge region also pointed out several interesting facts.

The order of the magnitude of the buoyancy parameter $K \sim Re^{-\frac{1}{4}}$ is one of the major results, since by all recent investigations (Lagree (1999) and Steinrück (2001)) the value $K \sim Re^{-\frac{1}{8}}$ was named as a necessary factor for applicability of the triple deck concept.

Since the unsymmetric flow was considered, for the sake of convenience the flow near the trailing edge was decomposed into the symmetric and anti-symmetric part. The symmetric one was described in terms of the classical triple deck concept (Stewartson 1969), while for anti-symmetric part the new (linear) triple deck problem was formulated.

Solution of the linear triple deck problem brought several interesting features concerning the displacement function and the pressure distribution (new asymptotic behaviors are derived, *ln*-terms by the matching procedure, etc...).

It turns out that on the triple deck scale the pressure is discontinuous at the trailing edge. Note that on the scale of the global flow, the pressure is continues satisfying the Kutta condition.

In order to resolve the discontinuity new sub-layers of order $(Re^{\frac{4}{8}}, Re^{\frac{4}{8}})$ and $(Re^{\frac{5}{8}}, Re^{\frac{5}{8}})$ are introduced. However, these sub-layers reduced the discontinuity to a single point.

It seems that the complete resolution of the singular behavior of the pressure is only possible in the $Re^{\frac{6}{8}}$-scale, where the flow is described by the full Navier-Stokes equations.

Beside analysing the linearized full Navier-Stokes equations, the further investigations might concern the three dimensional flow around the horizontal surface.

A Appendix

A.1 Interaction law for anti-symmetric part of solution

Applying the potential theory and analytic functions and combining them with Stewartson solution, the interaction law of the anti-symmetric problem will be formulated.

Using the known pressure distribution in the main deck (equation 4.23), the analytic function $\triangle\phi(x_3, y_3)$ at the real axis (close to zero) can be written as

$$\triangle\phi(x_3) = \triangle p(x_3) - \bar{A}(x_3) - i\triangle A'(x_3).$$

Taking the asymptotic behavior of $\bar{A}(x_3)$ into account, the asymptotic expansion for $\triangle\phi(z)$ can be assumed as:

$$\triangle\phi(z) = \triangle\phi_0 + (a + bi)z^{\frac{1}{3}} \; ; \; z \to \infty, \tag{A.1}$$

where $\triangle\phi_0$ is analytic at $z \to \infty$.

Similar holds for the displacement function (derivative of the displacement function)

$$\triangle A'(x_3) = B'(x_3) - bx_3^{\frac{1}{3}}h(x_3), \tag{A.2}$$

where $h(x_3)$ is jump function and $B'(x_3)$ finite part of the integral.
Then at the real axis there are:

$$\varphi = 0, \quad \triangle A'(x_3) \sim -bx_3^{\frac{1}{3}},$$

$$\triangle p - \bar{A} \sim ax_3^{\frac{1}{3}},$$

$$\varphi = \pi, \quad \triangle p - \bar{A} \sim \Re\left\{(a + bi)|x|^{\frac{1}{3}}(\cos\frac{\pi}{3} + i\sin\frac{\pi}{3}\right\} = (\frac{a_s}{2} - \frac{\sqrt{3}b}{2})|x|^{\frac{1}{3}},$$

$$\triangle A' \sim -\Im\left\{(a + bi)|x|^{\frac{1}{3}}(\cos\frac{\pi}{3} + i\sin\frac{\pi}{3}\right\} = -(\frac{b}{2} + \frac{\sqrt{3}a_s}{2})|x|^{\frac{1}{3}}.$$

At the plate the derivative of displacement function has to fulfill the condition

$$\triangle A' \to 0, \quad \text{for} \quad x \to -\infty$$

and as the consequence, the coefficients a and b are obtained: $a = -a_s$, $b = -\sqrt{3}a = \sqrt{3}a_s$.
Then the real and imaginary part of function $\triangle\phi_0(z)$ are:

$$\Re\triangle\phi_0 = \triangle p - \bar{A}(x) - a_s|x|^{\frac{1}{3}}[1 + h(-x)], \tag{A.3}$$

$$\Im\triangle\phi_0 = -\triangle A'(x) + \sqrt{3}a_s|x|^{\frac{1}{3}}h(x) \tag{A.4}$$

and using

$$\Re\triangle\phi_0 = \underbrace{\frac{1}{\pi}\int_{-\infty}^{+\infty}\frac{\bar{B}'(\zeta)}{x_3 - \zeta}\,d\zeta}_{\text{finite part of integral}}, \tag{A.5}$$

the interaction law in the form of equation (4.38) is obtained.

$$\triangle p_1^{(3,5)}(x_3) = \bar{A}(x_3) - 2a_s|x_3|^{\frac{1}{3}}\left(1 + h(x_3)\right) + \frac{1}{\pi}\int_{-\infty}^{+\infty}\frac{\triangle A'(\zeta) + \sqrt{3}a_s\zeta^{\frac{1}{3}}h(\zeta)}{x_3 - \zeta}\,d\zeta. \tag{A.6}$$

A.2 Scaling of governing equations

The governing equations are the complete Navier-Stokes equations (systems 4.1, 4.2) combined to the continuity and energy equations. However for convenience, they will be reformulated inside of each mentioned regions, to point out the different flow and physical characteristics. Similar to systems (4.1, 4.2), again the sums and differences will be distinguish.

A.2.1 Boundary layer scale

The anti-symmetric part:

$$\bar{u}^{(0,4)}\triangle u_{x_0}^{(0,4)} + \triangle u^{(0,4)}\bar{u}_{x_0}^{(0,4)} + \bar{v}^{(0,4)}\triangle u_{y_4}^{(0,4)} + \triangle v^{(0,4)}\bar{u}_{y_4}^{(0,4)} = -\triangle p_{x_0}^{(0,4)} + \frac{1}{\mathrm{Re}}(\triangle u_{x_0x_0}^{(0,4)} + \mathrm{Re}\triangle u_{y_4y_4}^{(0,4)}),$$

$$\frac{1}{\mathrm{Re}}(\bar{u}^{(0,4)}\triangle v_{x_0}^{(0,4)} + \triangle u^{(0,4)}\bar{v}_{x_0}^{(0,4)} + \bar{v}^{(0,4)}\triangle v_{y_4}^{(0,4)} + \triangle v^{(0,4)}\bar{v}_{y_4}^{(0,4)}) = -\triangle p_{y_4}^{(0,4)} + \frac{\mathrm{Gr}}{\mathrm{Re}^{\frac{5}{2}}K}\bar{\theta}^{(0,4)} +$$
$$\frac{1}{\mathrm{Re}^{\frac{3}{2}}}(\mathrm{Re}^{-\frac{1}{2}}\triangle v_{x_0x_0}^{(0,4)} + \mathrm{Re}^{\frac{1}{2}}\triangle v_{y_4y_4}^{(0,4)}),$$

$$\triangle u_{x_0}^{(0,4)} + \triangle v_{y_4}^{(0,4)} = 0,$$

$$\bar{u}^{(0,4)}\triangle \theta_{x_0}^{(0,4)} + \triangle u^{(0,4)}\bar{\theta}_{x_0}^{(0,4)} + \bar{v}^{(0,4)}\triangle \theta_{y_4}^{(0,4)} + \triangle v^{(0,4)}\bar{\theta}_{y_4}^{(0,4)} = \frac{1}{\mathrm{RePr}}(\triangle \theta_{x_0x_0}^{(0,4)} + \mathrm{Re}\triangle \theta_{y_4y_4}^{(0,4)}).$$

The symmetric part:

$$\bar{u}^{(0,4)}\bar{u}_{x_0}^{(0,4)} + \bar{v}^{(0,4)}\bar{u}_{y_4}^{(0,4)} + K^2(\triangle u^{(0,4)}\triangle u_{x_0}^{(0,4)} + \triangle v^{(0,4)}\triangle u_{y_4}^{(0,4)}) = -\bar{p}_{x_0}^{(0,4)} + \frac{1}{\mathrm{Re}}(\bar{u}_{x_0x_0}^{(0,4)} + \mathrm{Re}\bar{u}_{y_4y_4}^{(0,4)}),$$

$$\frac{1}{\mathrm{Re}}\left(\bar{u}^{(0,4)}\bar{v}_{x_0}^{(0,4)} + \bar{v}^{(0,4)}\bar{v}_{y_4}^{(0,4)} + K^2(\triangle u^{(0,4)}\triangle v_{x_0}^{(0,4)} + \triangle v^{(0,4)}\triangle v_{y_4}^{(0,4)})\right) = -\bar{p}_{y_4}^{(0,4)} + \frac{\mathrm{Gr}}{\mathrm{Re}^{\frac{5}{2}}}K\triangle \theta^{(0,4)} +$$
$$\frac{1}{\mathrm{Re}^{\frac{3}{2}}}(\mathrm{Re}^{-\frac{1}{2}}\bar{v}_{x_0x_0}^{(0,4)} + \mathrm{Re}^{\frac{1}{2}}\bar{v}_{y_4y_4}^{(0,4)}),$$

$$\bar{u}_{x_0}^{(0,4)} + \bar{v}_{y_4}^{(0,4)} = 0,$$

$$\bar{u}^{(0,4)}\bar{\theta}_{x_0}^{(0,4)} + \bar{v}^{(0,4)}\bar{\theta}_{y_4}^{(0,4)} + K^2(\triangle u^{(0,4)}\triangle \theta_{x_0}^{(0,4)} + \triangle v^{(0,4)}\triangle \theta_{y_4}^{(0,4)}) = \frac{1}{\mathrm{RePr}}(\bar{\theta}_{x_0x_0}^{(0,4)} + \mathrm{Re}\bar{\theta}_{y_4y_4}^{(0,4)}).$$

A.2.2 Main deck scale

The anti-symmetric part:

$$\bar{u}^{(3,4)}\triangle u_{x_3}^{(3,4)} + \triangle u^{(3,4)}\bar{u}_{x_3}^{(3,4)} + \bar{v}^{(3,4)}\triangle u_{y_4}^{(3,4)} + \triangle v^{(3,4)}\bar{u}_{y_4}^{(3,4)} = -\triangle p_{x_3}^{(3,4)}$$
$$+ \frac{1}{\mathrm{Re}}(\mathrm{Re}^{\frac{3}{8}}\triangle u_{x_3x_3}^{(3,4)} + \mathrm{Re}^{\frac{5}{8}}\triangle u_{y_4y_4}^{(3,4)}),$$

$$\frac{1}{\mathrm{Re}}(\mathrm{Re}^{\frac{6}{8}}\bar{u}^{(3,4)}\triangle v_{x_3}^{(3,4)} + \mathrm{Re}^{\frac{6}{8}}\triangle u^{(3,4)}\bar{v}_{x_3}^{(3,4)} + \mathrm{Re}^{\frac{3}{8}}\bar{v}^{(3,4)}\triangle v_{y_4}^{(3,4)} + \mathrm{Re}^{\frac{3}{8}}\triangle v^{(3,4)}\bar{v}_{y_4}^{(3,4)}) = -\triangle p_{y_4}^{(3,4)}$$
$$+ \frac{\mathrm{Gr}}{\mathrm{Re}^{\frac{5}{2}}K}\bar{\theta}^{(3,4)} + \frac{1}{\mathrm{Re}^{\frac{3}{2}}}(\mathrm{Re}^{\frac{5}{8}}\triangle v_{x_3x_3}^{(3,4)} + \mathrm{Re}^{\frac{7}{8}}\triangle v_{y_4y_4}^{(3,4)}),$$

$$\triangle u_{x_3}^{(3,4)} + \triangle v_{y_4}^{(3,4)} = 0,$$

$$\bar{u}^{(3,4)}\triangle\theta_{x_3}^{(3,4)} + \triangle u^{(3,4)}\bar{\theta}_{x_3}^{(3,4)} + \bar{v}^{(3,4)}\triangle\theta_{y_4}^{(3,4)} + \triangle v^{(3,4)}\bar{\theta}_{y_4}^{(3,4)} =$$
$$+\frac{1}{\mathrm{Re}\,\mathrm{Pr}}(\mathrm{Re}^{\frac{3}{8}}\triangle\theta_{x_3 x_3}^{(3,4)} + \mathrm{Re}^{\frac{5}{8}}\triangle\theta_{y_4 y_4}^{(3,4)}).$$

The symmetric part:

$$\bar{u}^{(3,4)}\bar{u}_{x_3}^{(3,4)} + \bar{v}^{(3,4)}\bar{u}_{y_4}^{(3,4)} + K^2(\triangle u^{(3,4)}\triangle u_{x_3}^{(3,4)} + \triangle v^{(3,4)}\triangle u_{y_4}^{(3,4)}) = -\bar{p}_{x_3}^{(3,4)} + \frac{1}{\mathrm{Re}}(\mathrm{Re}^{\frac{3}{8}}\bar{u}_{x_3 x_3}^{(3,4)} + \mathrm{Re}^{\frac{5}{8}}\bar{u}_{y_4 y_4}^{(3,4)}),$$

$$\frac{1}{\mathrm{Re}}\left(\mathrm{Re}^{\frac{6}{8}}\bar{u}^{(3,4)}\bar{v}_{x_3}^{(3,4)} + \mathrm{Re}^{\frac{6}{8}}\bar{v}^{(3,4)}\bar{v}_{y_4}^{(3,4)} + K^2(\mathrm{Re}^{\frac{6}{8}}\triangle u^{(3,4)}\triangle v_{x_3}^{(3,4)} + \mathrm{Re}^{\frac{6}{8}}\triangle v^{(3,4)}\triangle v_{y_4}^{(3,4)})\right) = -\bar{p}_{y_4}^{(3,4)} +$$
$$\frac{\mathrm{Gr}}{\mathrm{Re}^{\frac{5}{2}}}K\triangle\theta^{(3,4)} + \frac{1}{\mathrm{Re}^{\frac{3}{2}}}(\mathrm{Re}^{\frac{5}{8}}\bar{v}_{x_3 x_3}^{(3,4)} + \mathrm{Re}^{\frac{7}{8}}\bar{v}_{y_4 y_4}^{(3,4)}),$$

$$\bar{u}_{x_3}^{(3,4)} + \bar{v}_{y_4}^{(3,4)} = 0,$$

$$\bar{u}^{(3,4)}\bar{\theta}_{x_3}^{(3,4)} + \bar{v}^{(3,4)}\bar{\theta}_{y_4}^{(3,4)} + K^2(\triangle u^{(3,4)}\triangle\theta_{x_3}^{(3,4)} + \triangle v^{(3,4)}\triangle\theta_{y_4}^{(3,4)}) = \frac{1}{\mathrm{RePr}}(\mathrm{Re}^{\frac{3}{8}}\bar{\theta}_{x_3 x_3}^{(3,4)} + \mathrm{Re}^{\frac{5}{8}}\bar{\theta}_{y_4 y_4}^{(3,4)}).$$

A.2.3 Lower deck scale

The anti-symmetric part:

$$\bar{u}^{(3,5)}\triangle u_{x_3}^{(3,5)} + \triangle u^{(3,5)}\bar{u}_{x_3}^{(3,5)} + \bar{v}^{(3,5)}\triangle u_{y_5}^{(3,5)} + \triangle v^{(3,5)}\bar{u}_{y_5}^{(3,5)} = -\triangle p_{x_3}^{(3,5)}$$
$$+\frac{1}{\mathrm{Re}}(\mathrm{Re}^{\frac{3}{8}}\triangle u_{x_3 x_3}^{(3,5)} + \mathrm{Re}^{\frac{7}{8}}\triangle u_{y_5 y_5}^{(3,5)}),$$

$$\frac{1}{\mathrm{Re}}(\mathrm{Re}^{\frac{5}{8}}\bar{u}^{(3,5)}\triangle v_{x_3}^{(3,5)} + \mathrm{Re}^{\frac{5}{8}}\triangle u^{(3,5)}\bar{v}_{x_3}^{(3,5)} + \mathrm{Re}^{\frac{3}{8}}\bar{v}^{(3,5)}\triangle v_{y_5}^{(3,5)} + \mathrm{Re}^{\frac{3}{8}}\triangle v^{(3,5)}\bar{v}_{y_5}^{(3,5)}) = -\mathrm{Re}^{\frac{1}{8}}\triangle p_{y_5}^{(3,5)}$$
$$+\frac{\mathrm{Gr}}{\mathrm{Re}^{\frac{5}{2}}K}\bar{\theta}^{(3,5)} + \frac{1}{\mathrm{Re}^{\frac{3}{2}}}(\mathrm{Re}^{\frac{4}{8}}\triangle v_{x_3 x_3}^{(3,5)} + \mathrm{Re}\triangle v_{y_5 y_5}^{(3,5)}),$$

$$\triangle u_{x_3}^{(3,5)} + \triangle v_{y_5}^{(3,5)} = 0,$$

$$\bar{u}^{(3,5)}\triangle\theta_{x_3}^{(3,5)} + \triangle u^{(3,5)}\bar{\theta}_{x_3}^{(3,5)} + \bar{v}^{(3,5)}\triangle\theta_{y_5}^{(3,5)} + \triangle v^{(3,5)}\bar{\theta}_{y_5}^{(3,5)} =$$
$$+\frac{1}{\mathrm{Re}\,\mathrm{Pr}}(\mathrm{Re}^{\frac{3}{8}}\triangle\theta_{x_3 x_3}^{(3,5)} + \mathrm{Re}^{\frac{7}{8}}\triangle\theta_{y_5 y_5}^{(3,5)}).$$

The symmetric part:

$$\bar{u}^{(3,5)}\bar{u}_{x_3}^{(3,5)} + \bar{v}^{(3,5)}\bar{u}_{y_5}^{(3,5)} + K^2(\triangle u^{(3,5)}\triangle u_{x_3}^{(3,5)} + \triangle v^{(3,5)}\triangle u_{y_5}^{(3,5)}) = -\bar{p}_{x_3}^{(3,5)} + \frac{1}{\mathrm{Re}}(\mathrm{Re}^{\frac{3}{8}}\bar{u}_{x_3 x_3}^{(3,5)} + \mathrm{Re}^{\frac{7}{8}}\bar{u}_{y_5 y_5}^{(3,5)}),$$

$$\frac{1}{\mathrm{Re}}\left(\mathrm{Re}^{\frac{5}{8}}\bar{u}^{(3,5)}\bar{v}_{x_3}^{(3,5)} + \mathrm{Re}^{\frac{5}{8}}\bar{v}^{(3,5)}\bar{v}_{y_5}^{(3,5)} + K^2(\mathrm{Re}^{\frac{5}{8}}\triangle u^{(3,5)}\triangle v_{x_3}^{(3,5)} + \mathrm{Re}^{\frac{5}{8}}\triangle v^{(3,5)}\triangle v_{y_5}^{(3,5)})\right) = -\mathrm{Re}^{\frac{1}{8}}\bar{p}_{y_5}^{(3,5)} +$$
$$\frac{\mathrm{Gr}}{\mathrm{Re}^{\frac{5}{2}}}K\triangle\theta^{(3,5)} + \frac{1}{\mathrm{Re}^{\frac{3}{2}}}(\mathrm{Re}^{\frac{4}{8}}\bar{v}_{x_3 x_3}^{(3,5)} + \mathrm{Re}\,\bar{v}_{y_5 y_5}^{(3,5)}),$$

$$\bar{u}_{x_3}^{(3,5)} + \bar{v}_{y_5}^{(3,5)} = 0,$$

$$\bar{u}^{(3,5)}\bar{\theta}_{x_3}^{(3,5)} + \bar{v}^{(3,5)}\bar{\theta}_{y_5}^{(3,5)} + K^2(\triangle u^{(3,5)}\triangle\theta_{x_3}^{(3,5)} + \triangle v^{(3,5)}\triangle\theta_{y_5}^{(3,5)}) = \frac{1}{\mathrm{RePr}}(\mathrm{Re}^{\frac{3}{8}}\bar{\theta}_{x_3 x_3}^{(3,5)} + \mathrm{Re}^{\frac{7}{8}}\bar{\theta}_{y_5 y_5}^{(3,5)}).$$

A.2.4 Wake equations

The anti-symmetric part:

$$\bar{u}_w^{(0,4)} \triangle u_{w,x_0}^{(0,4)} + \triangle u_w^{(0,4)} \bar{u}_{w,x_0}^{(0,4)} + \bar{v}_w^{(0,4)} \triangle u_{w,y_4}^{(0,4)} + \triangle v_w^{(0,4)} \bar{u}_{w,y_4}^{(0,4)} = \lambda\, \bar{y}_w' \bar{\theta}_w +$$

$$\frac{1}{\mathrm{Re}} (\triangle u_{w,x_0 x_0}^{(0,4)} + \mathrm{Re}\triangle u_{w,y_4 y_4}^{(0,4)}),$$

$$\frac{1}{\mathrm{Re}} (\bar{u}_w^{(0,4)} \triangle v_{w,x_0}^{(0,4)} + \triangle u_w^{(0,4)} \bar{v}_{w,x_0}^{(0,4)} + \bar{v}_w^{(0,4)} \triangle v_{w,y_4}^{(0,4)} + \triangle v_w^{(0,4)} \bar{v}_{w,y_4}^{(0,4)}) = -\triangle p_{w,y_4}^{(0,4)} + \frac{\mathrm{Gr}}{\mathrm{Re}^{\frac{5}{2}} K} \bar{\theta}_w^{(0,4)} +$$

$$\frac{1}{\mathrm{Re}^{\frac{3}{2}}} (\mathrm{Re}^{-\frac{1}{2}} \triangle v_{w,x_0 x_0}^{(0,4)} + \mathrm{Re}^{\frac{1}{2}} \triangle v_{w,y_4 y_4}^{(0,4)}),$$

$$\triangle u_{w,x_0}^{(0,4)} + \triangle v_{w,y_4}^{(0,4)} = 0,$$

$$\bar{u}_w^{(0,4)} \triangle \theta_{w,x_0}^{(0,4)} + \triangle u_w^{(0,4)} \bar{\theta}_{w,x_0}^{(0,4)} + \bar{v}_w^{(0,4)} \triangle \theta_{w,y_4}^{(0,4)} + \triangle v_w^{(0,4)} \bar{\theta}_{w,y_4}^{(0,4)} = \frac{1}{\mathrm{RePr}} (\triangle \theta_{w,x_0 x_0}^{(0,4)} + \mathrm{Re}\triangle \theta_{w,y_4 y_4}^{(0,4)}).$$

The symmetric part:

$$\bar{u}_w^{(0,4)} \bar{u}_{w,x_0}^{(0,4)} + \bar{v}_w^{(0,4)} \bar{u}_{w,y_4}^{(0,4)} + K^2 (\triangle u_w^{(0,4)} \triangle u_{w,x_0}^{(0,4)} + \triangle v_w^{(0,4)} \triangle u_{w,y_4}^{(0,4)}) = -\bar{p}_{w,x_0}^{(0,4)} + K\lambda \bar{y}_w' \triangle \theta_w$$

$$\frac{1}{\mathrm{Re}} (\bar{u}_{w,x_0 x_0}^{(0,4)} + \mathrm{Re}\bar{u}_{w,y_4 y_4}^{(0,4)}),$$

$$\frac{1}{\mathrm{Re}} \left(\bar{u}_w^{(0,4)} \bar{v}_{w,x_0}^{(0,4)} + \bar{v}_w^{(0,4)} \bar{v}_{w,y_4}^{(0,4)} + K^2 (\triangle u_w^{(0,4)} \triangle v_{w,x_0}^{(0,4)} + \triangle v_w^{(0,4)} \triangle v_{w,y_4}^{(0,4)}) \right) = -\bar{p}_{w,y_4}^{(0,4)} + \frac{\mathrm{Gr}}{\mathrm{Re}^{\frac{5}{2}}} K\triangle \theta_w^{(0,4)} +$$

$$\frac{1}{\mathrm{Re}^{\frac{3}{2}}} (\mathrm{Re}^{-\frac{1}{2}} \bar{v}_{w,x_0 x_0}^{(0,4)} + \mathrm{Re}^{\frac{1}{2}} \bar{v}_{w,y_4 y_4}^{(0,4)}),$$

$$\bar{u}_{w,x_0}^{(0,4)} + \bar{v}_{w,y_4}^{(0,4)} = 0,$$

$$\bar{u}_w^{(0,4)} \bar{\theta}_{w,x_0}^{(0,4)} + \bar{v}_w^{(0,4)} \bar{\theta}_{w,y_4}^{(0,4)} + K^2 (\triangle u_w^{(0,4)} \triangle \theta_{w,x_0}^{(0,4)} + \triangle v_w^{(0,4)} \triangle \theta_{w,y_4}^{(0,4)}) = \frac{1}{\mathrm{RePr}} (\bar{\theta}_{w,x_0 x_0}^{(0,4)} + \mathrm{Re}\bar{\theta}_{w,y_4 y_4}^{(0,4)}).$$

A.3 Matching main - lower deck

Using the similarity solution of equation (4.40) and applying Van Dyke's matching principle (1975) we have

$$\Delta u_0^{(3,5)}(x_3, y_5) \sim C_1^{(3,5)} \ln \frac{y_5}{|x_3|^{\frac{1}{3}}} + C_2^{(3,5)} + \dots.$$

Rewriting the expansion for $\Delta u_0^{(3,5)}$ in terms of $x_3 \to -\infty, y_5 \to \infty$ (inner variable)

$$\Delta u_0^{(3,5)}(x_3, y_4 \, \mathrm{Re}^{-\frac{1}{8}}) \sim C_1^{(3,5)} \ln y_4 - \frac{C_1^{(3,5)}}{3} \ln|x_3| - \frac{C_1^{(3,5)}}{8} \ln \mathrm{Re} + C_2^{(3,5)} + \dots$$

and doing the same by outer variable ($y_4 \to 0$)

$$\Delta u_0^{(3,4)}(x_3, 0) \sim C_{\Delta A} \ln |x_3| F_B''(0) + C_{B2}^{(3,4)} \ln \mathrm{Re} \; F_B''(0) + \dots \quad \dots (\text{sub-section } 4.5.1),$$

$$\Rightarrow \Delta u_0^{(3,4)}(x_3, y_4 \to 0) = \Delta u_0^{(3,5)}(x_3, y_5 \to \infty) \quad \dots (\text{matching principle}),$$

thus, finally we have:

$$C_{\Delta A} = \frac{C_1^{(3,5)}}{3 F_B''(0)} \;, \quad C_{B2}^{(3,4)} = -\frac{C_1^{(3,5)}}{8 F_B''(0)}.$$

Similar is valid for temperature profile:

$$\Delta \theta_0^{(3,5)}(x_3, y_5 \to \infty) \sim C_{f1}^{(3,5)} \ln y_5 - \frac{C_{f1}^{(3,5)}}{3} \ln |x_3| + C_{f2}^{(3,5)} + \dots,$$

$$\Delta \theta_0^{(3,4)}(x_3, 0) \sim C_{\Delta A} \ln |x_0| \; D_B'(0) + C_{D2}^{(3,4)} \ln \mathrm{Re} \; D_B'(0) + \dots; \quad \dots (\text{sub-section } 4.5.1),$$

$$\Rightarrow \Delta \theta_0^{(3,4)}(x_3, y_4 \to 0) = \Delta \theta_0^{(3,5)}(x_3, y_5 \to \infty) \quad \dots (\text{matching principle}),$$

$$\Rightarrow C_{f1}^{(3,5)}, C_{f2}^{(3,5)} = f(C_{\Delta A}, \dots).$$

A.4 Boundary layer solution in region $x_0 \to 0$

Using the governing system (appendix A.2) and the expansions proposed in section 4.5.2 (for $\Delta \psi_0^{(0,4)}$ and $\Delta \theta_0^{(0,4)}$), the obtained boundary equations (close to the trailing edge) are inviscid, so the viscid sub-layer intoduction is necessary.

The highest order terms:

$$\bar{\psi}_{0,y_4}^{(0,4)} \, C_{B2,y_4}^{(0,4)} - \bar{\psi}_{0,y_4 y_4}^{(0,4)} C_{B2}^{(0,4)} = 0 \; \Rightarrow C_{B2}^{(0,4)}(y_4) = a_{B2}^{(0,4)} \; \bar{\psi}_{0,y_4}^{(0,4)} = \frac{C_1^{(3,5)}}{3 F_B''(0)} \, F_B'(y_4), \qquad (A.7)$$

$$\bar{\psi}_{0,y_4}^{(0,4)} \, C_{D2,y_4}^{(0,4)} - \bar{\theta}_{0,y_4}^{(0,4)} C_{B2}^{(0,4)} = 0 \; \Rightarrow C_{D2}^{(0,4)}(y_4) = a_{B2}^{(0,4)} \; \bar{\theta}_{0,y_4}^{(0,4)} = \frac{C_1^{(3,5)}}{3 F_B''(0)} D_B'(y_4), \qquad (A.8)$$

where F_B, D_B come from boundary-layer solution at the plate (Blasius).

Other perturbations (coefficients) can be determined as next order terms, but these investigations are beyond the scope of the present work.

The sub-layer has to fulfill the no-slip condition, where the similarity solution exists (similarity variable $\zeta = y_4/|x_0|^{\frac{1}{3}}$):

$$\Delta f_{\zeta\zeta\zeta}^{(0,4)} - \frac{F_B''(0)}{3} \zeta^2 \, \Delta f_{\zeta\zeta}^{(0,4)} + \frac{F_B''(0)}{3} \zeta \, \Delta f_{\zeta}^{(0,4)} - \frac{F_B''(0)}{3} \, \Delta f^{(0,4)} = -\frac{c_{P1}^{(3,4)}}{3}, \qquad (A.9)$$

$$\Delta g_{\zeta\zeta}^{(0,4)} - \frac{F_B''(0)\mathrm{Pr}}{3} \zeta^2 \, \Delta g_{\zeta}^{(0,4)} - \frac{D_B'(0)\mathrm{Pr}}{3} \zeta \, \Delta f_{\zeta}^{(0,4)} + \frac{D_B'(0)\mathrm{Pr}}{3} \, \Delta f^{(0,4)} = 0, \qquad (A.10)$$

with $f^{(0,4)}(\zeta), g^{(0,4)}(\zeta)$ as scaled stream function and scaled temperature profile, respectively.

Considrations done by the equation (4.40) can be applied here as well (there are analytical solutions for both profiles):

$$\triangle f^{(0,4)}(\zeta \to \infty) \sim C_{f1}^{(0,4)}\zeta \ln\zeta + C_{f2}^{(0,4)}\zeta + C_{f3}^{(0,4)} + ...,$$

$$\triangle f_{\zeta}^{(0,4)}(\zeta \to \infty) \sim C_{f1}^{(0,4)}\ln\zeta + C_{f2}^{(0,4)} + ...,$$

$$\triangle g^{(0,4)}(\zeta \to \infty) \sim C_{f1}^{(0,4)}\ln\zeta + C_{d1}^{(0,4)} + ...$$

The obtained solutions have to be matched to the inviscid solution, in order to calculate the unknown coefficients.

A.5 Asymptotic conditions at $x \to -\infty$

The reformulation of lower deck equations in system (5.1-5.2) was done in order to simplify the numerical procedure, since the asymptotic behavior in $x \to -\infty$ region is defined by ODE (4.40). In order to derive the form of equation (4.40) starting with the system of equations (5.1,5.2), we use the classical interaction problem i.e. the asymptotic behavior of the Stewartson solution (sub-section 4.4.1). At $x \to -\infty$ the following relations hold:

$$\bar{\psi}_1^{(3,\,5)} \sim \frac{1}{2}\zeta^2,$$

then following derivatives vanish

$$\bar{\psi}_{1,x_3}^{(3,\,5)} = 0 \,, \quad \bar{\psi}_{1,\zeta,x_3}^{(3,\,5)} = 0$$

and knowing that

$$\triangle p_1^{(3,\,5)} = -2a_s|x_3|^{\frac{1}{3}} \,, \quad \frac{x_3}{\sqrt{x_3{}^2 + 1}} \approx -1,$$

the equation (5.2) is transformed to

$$\triangle \psi_{0,\zeta\zeta\zeta}^{(3,5)} - \frac{\zeta^2}{3}\triangle \psi_{0,\zeta\zeta}^{(3,5)} - \frac{1}{3}\left(\triangle \psi_0^{(3,5)} - \zeta\triangle \psi_{0,\zeta}^{(3,5)} \right) = \frac{2a_s}{3}. \tag{A.11}$$

References

Daniels, P. G. 1992 *A singularity in thermal boundary layer flow on a horizontal surface*, J. Fluid Mech. **242**, 419-440.

Denier, J.P., Duck, P.W., Li, J. 2005 *On the growth (and suppression) of very short-scale disturbances in mixed forced-free convection boundary layers*, J. Fluid Mech. **526**, 147 - 170.

Goldstein, S. 1930 *Concerning some solutions of the boundary layer equations in hydrodynamics*, Proc. Camb. Phil. Soc., **26**, 1-30.

Hadamard, J. 1932 *Le Problème de Cauchy et les Èquations aux Dèrivèes Partielles Linèaires Hyperboliques*, Hermann.

Kluwick, A. 1998 *Recent advances in boundary layer theory*, CISM Courses and lectures, **390**, 231-319.

Lagree, P. -Y. 1999 *Thermal mixed convection induced locally by a step change in surface temperature in a Poiseuille flow in the framework of triple deck theory*, Int. J. Heat and Mass Transfer, **42**, 2509-2524.

Lagree, P. -Y. 2001 *Removing the marching breakdown of the boundary-layer equations for mixed convection above a horizontal plate*, Intl J. Heat Mass Transfer, **44**, 3359-3372.

Leal, L. G. 1992 *Laminar Flow and Convective Transport Process*, Butterworth-Heinemann.

Melnik, R. E. & Chow, R 1975 *Asymptotic Theory of Two-Dimensional Trailing-Edge Flows*, NASA SP-347.

Merkin, J. H. & Ingham, D. B. 1987 *Mixed convection similarity solutions on a horizontal surface*, J. Appl. Math. Phys. (ZAMP), **38**, 102-116.

Messiter, A. F. 1970 *Boundary-layer flow near the trailing edge of a flat plate*, SIAM J. Appl. Math., **18**(1), 241-257.

Neiland, V. 1969 *Theory of laminar boundary layers separation in supersonic flow*, Izvestiia Akademii Nauk SSSR Mekhanika Zhidkosti i Gaza 4, 53-57.

Robertson, G. E., Seinfeld, J. H. & Leal, L. G. 1973 *Combined forced and free convection flow past a horizontal flat plate*, AIChE J., **19**, 998-1008.

Savić, Lj. & Steinrück, H. 2005 *Mixed convection flow past a horizontal plate*, Theoret. Appl. Mech., **32, no 1**, 1-19.

Schlichting, H. & Gersten, K. 2000 *Boundary-layer theory*, Springer.

Schneider, W. 1978 *Mathematische Methoden der Strömungsmechanik*, Vieweg.

Schneider, W. 1979 *A similarity solution for combined forced and free convection flow over a horizontal plate* , Int. J. Heat Mass Transfer **22**, 1401-1406.

Schneider, W. & Wasel, M. G. 1985 *Beakdown of the boundary-layer approximation for mixed convection above a horizontal plate* , Int. J. Heat Mass Transfer **28**, 2307-2313.

Schneider, W. 2000 *Mixed convection at a finite plate*, in Third European Thermal Sciences Conference.

Schneider, W. 2001 *Peculiarities of boundary-layer flows over horizontal plates*, in Applicable Mathematics – Its Perspectives and Challenges (ed. J. C. Misra), pp. 118-123. Narosa. New Delhi

Schneider, W. 2005 *Lift, thrust and heat transfer due to mixed convection flow past a horizontal plate of finite length*, J. Fluid Mech. **529**, 51-69.

Sobey, I. J. 2000 *Introduction to Interactive Boundary Layer Theory*, Oxford University Press.

Steinrück, H. 1994 *Mixed convection over a cooled horizontal plate: non-uniqueness and numerical instabilities of the boundary layer equations*, J. Fluid Mech. **278**, 251-265.

Steinrück, H. 1995 *Mixed convection over a horizontal plate self-similar and connecting boundary layer flows*, Fluid Dyn. Res. **15**, 113-127.

Steinrück, H. 2001 *A review of the mixed convection boundary-layer flow over a horizontal cooled plate*, GAMM-Mitteilungen, **2**, 1277-158.

Stewartson, K. 1969 *On the flow near the trailing edge of a flat plate*, Mathematica **16**(1), 106-121.

Stewartson, K. & Williams, P. 1969 *Self induced separation*, Proceedings of Royal Society **A 312**, 181-206.

Stewartson, K. & Brown, N. S. 1970 *Trailing-edge stall*, J. Fluid Mech. **42**, part 3, 181-206.

Sychev, V. V., Ruban, A. I., Sychev, V. V., & Korolev, G. L. 1998 *Asymptotic theory of separated flows*, Cambridge University Press.

Usher, U., Christiansen, J., Russel, R. D. 1981 *Collocation software for boundary value ODEs*, ACM Trans. Math. Software **7**, 209-222.

Van Dyke, M. 1975 *Perturbations Methods in Fluid Mechanics*, Parabolic Press.

Veldman, A. E. P. 1981 *New, Quasi-simultaneous Method to Calculate Interacting Boundary Layers*, AIAA Journal **19** NO.1, 79-85 106-121.

Wickern, G. 1991 *Mixed convection from arbitrarily inclined semi-infinite flat plate - I. The influence of the inclination angle*, Int. J. Heat Mass Transfer **34**, No.8, 1935-1945.

Curriculum Vitae

Personal details

Name:	Ljubomir Savić
Date of birth:	23. February 1977
Place of birth:	Belgrade, Serbia
Nationality:	Serbian
Father:	DI Radoje Savić
Mother:	Mag. Mirjana Savić
Sister:	DI Aleksandra Savić
Address:	Trappelgasse 3/1/2, 1040 Wien, AU
Email:	lsavic@mail.tuwien.ac.at

Education:

1984. - 1992.	Primary school "Branko Ćopić", Belgrade
1992. - 1996.	High school "Sveti Sava", Belgrade
1996. - 2001.	Faculty of Mechanical Engineering University of Belgrade
12.07.2001.	Graduation degree "Dipl.Ing" Master's Thesis: "The contribution to the characterization of the flying ash of the block A6 of "Nikola Tesla" steam power plant - Obrenovac, Serbia".
01.04.2002.	Research assistant at the Institute of Fluid Mechanics and Heat Transfer, Vienna University of Technology, Austria. PhD Thesis: "Mixed Convection Boundary-Layer Flow over a Horizontal Plate"

Work experience:

01.04.2002. - present	Research assistant at the TU Vienna
10.2001. - 01.2002	Research assistant at the Faculty of Mechanical Engineering University of Belgrade, Department of Combustion